To the Graduate Council:

I am submitting herewith a thesis written by David C. King entitled "Interpretation of Stable Isotope Compositions of Pedogenic Carbonate in Late Silurian to Late Devonian Paleosols, Appalachian Basin." I have examined the final copy of this thesis for form and content and recommend that it be accepted in partial fulfillment of the requirements for the degree of Master of Science, with a major in Geology.

Dr. Claudia I. Mora, Major Professor

We have read this thesis
and recommend its acceptance:

Dr. Steven G. Driese

Dr. Kenneth R. Walker

Accepted for the Council:

Associate Vice Chancellor and
Dean of The Graduate School

INTERPRETATION OF STABLE ISOTOPE COMPOSITIONS OF PEDOGENIC CARBONATE IN LATE SILURIAN TO LATE DEVONIAN PALEOSOLS, APPALACHIAN BASIN

A Thesis
presented for the
Master of Science Degree
The University of Tennessee, Knoxville

David C. King
December 1998

DEDICATION

To my family

Don King
Carolyn Sutera King
Gina King Knapp
and Jeffery King

for making me all that I am and
for being a silent inspiration always

ACKNOWLEDGEMENTS

I would like to offer my thanks and appreciation to all who contributed to the completion of this thesis and my experiences throughout my college career. First and foremost, my major advisor, Dr. Claudia I. Mora has contributed an amazing amount of support with regards to field work, revisions, and encouragement. Also contributing directly to the quality and my understanding of this thesis were my thesis committee members, Drs. Stephen G. Driese and Kenneth R. Walker. I appreciate their careful editing and suggestions, especially due to the restricted timetable.

For the more hands-on aspects of my thesis, I'd like to begin by thanking Dr. Marvin I. Bennett for the computer technical support and advice. I could not have completed the thesis by the summer if it were not for him. The Paleopedology Research Group was also a constant source of reference and great ideas. In particular, thank you Zhensheng Chen, for keeping the mass spectrometer running at peak efficiency; Janee Ansley for showing the way, and Jennifer Elick for leading by example.

Before my arrival to Knoxville, there were those people who have greatly contributed to the quality of my character and were instrumental in my commitment and enthusiasm towards my success. My love and thanks go out to my mom, dad, sister, brothers, niece and nephew for making me who I am. Then, as an undergraduate a completely new group of people began to add texture. Leading the way would be Tim Kuhn, for whom I've shared a brain with for many years. Academically, Dr. Boger and Janie were just an incredible team and often times saw potential within me that I was unaware of at the time.

Upon my first arrival at Knoxville, there were an instrumental group of people who made graduate school a much nicer place. First of all, I'd like to thank Pete Nester for numerous road trips, for showing me how to take everything to extremes, Space Ghost, and all those other things that we dare not mention. Next in line is Clark Cropper and his lovely wife, Cheri, for being outstanding role models, for offering me an escape from Knoxville, and for keeping me grounded. For being so sprightly and precious, Elizabeth Humbert and Janee Ansley offered a refreshing change of pace as well. Near the completion of my thesis, my officemates and summer buddies had to put up with a lot as I slowly turned into a stress ball. This group of remarkable people include Dee Dee Haun, Janna Peevler, Clint Penfield and Dave Remley. I'd also like to thank my Sylvan buddies and kids. Knowing in advance that I'll have to leave many people out who deserve thanks, I resolve this by saying you know who you are and you have my thanks.

Support for my research was funded by the University of Tennessee, Knoxville, the National Science Foundation, the Pennsylvania Department of Conservation and Research, and Southeastern Geological Society of America.

ABSTRACT

Stable isotope (carbon and oxygen) compositions of pedogenic carbonate in Late Silurian (Bloomsburg Formation) and Late Devonian (Catskill Formation) paleosols from central and eastern Pennsylvania and southeastern New York were evaluated for their utility in constraining paleoatmospheric pCO_2 using Cerling's (1991) soil carbonate paleobarometer. The utility of soil carbonate isotopic compositions in paleoenvironmental studies is dependent upon an understanding of (a) the local stratigraphic and geologic history of the paleosol and (b) soil physics controlling CO_2 diffusion and carbonate precipitation. Isotopic reequilibration of ancient soil carbonate can occur in three contrasting environments: (1) pedogenic, (2) early and burial diagenetic, and (3) in a burial environment dominated by hot, tectonically driven fluid.

Significant isotopic re-equilibration is recorded in five of six Silurian and one of three Devonian paleosols analyzed. Pedogenic carbonate in Late Silurian Bloomsburg Formation paleosols at Wurtsboro (NY), Port Jervis (NY) and Harrisburg (PA) were dolomitized and reequilibrated in a post-pedogenic environment and in the presence of a ^{13}C-depleted source of carbon ($\delta^{13}C < -10.0‰$ PDB). Dolomite oxygen compositions reflect equilibration at temperatures less than those paleosols which have calcite as the principal carbonate ($\delta^{18}O > -10.0‰$ PDB). Paleosol localities at Lehigh Gap (PA) and Port Jervis (NY) are located very near the Blue Mountain Structural Front and record exchange with very hot, ^{13}C- and ^{18}O-depleted, migrating tectonic fluids ($\delta^{13}C < -8.0‰$ PDB, $\delta^{18}O < -15.0‰$ PDB). Only the Bloomsburg Formation locality at Danville (PA) offers convincing evidence for retention of a pedogenic carbon isotope composition and

exhibits $\delta^{13}C$ variation within the outcrop sequence. From the Danville carbonate $\delta^{13}C$ values, paleoatmospheric CO_2 levels can be interpreted using the soil carbonate paleobarometer and in light of sedimentological controls on CO_2 diffusion.

Isotopic composition of pedogenic carbonate in Late Devonian paleosols are less disturbed. Paleosol carbonate at the Newport (PA) locality exhibits the most negative average $\delta^{13}C$ value (~9.5‰ PDB), presumably due to its location near the Blue Mountain Structural Front. The Liverpool paleosol yielded only one carbonate sample. Paleosol localities at Powys (PA) and Trout Run (PA) were least buried relative to the other localities studied and retain the least altered pedogenic carbon isotope compositions for Late Devonian paleobarometric estimates.

Estimates of paleoatmospheric CO_2 levels for the Late Silurian and Late Devonian were made using carbonate carbon isotope compositions of pedogenic micrite from Danville (PA; Bloomsburg Formation, $\delta^{13}C$ = -6.0‰ PDB), calcite-micrite from Powys (PA; Catskill Formation; Sherman Creek Member, $\delta^{13}C$ = -7.2‰) and micrite and microspar from Trout Run (PA; Catskill Formation; Duncannon Member, -7.7‰). The Late Silurian atmospheric pCO_2 is estimated to be from 2,400 to 4,500 ppmV. Between formation of the Sherman Creek Member paleosols at the Powys locality and formation of the Duncannon Member at the Trout Run Locality, the atmospheric pCO_2 is estimated to have dropped 100 to 400 ppmV (from 2,300-4,000 to 1,900-3,900 ppmV). By modeling pCO_2 from pedogenic carbonate found within paleosols, a better understanding of the development of the Earth's atmosphere through time and its relationship to terrestrial biota can be gained.

TABLE OF CONTENTS

CHAPTER		PAGE
I.	**Introduction**	1
II.	**The Soil Carbonate CO_2 Paleobarometer and Carbonate Isotopes**	6
	ISOTOPIC CONSTRAINTS FOR THE PALEOBAROMETER	9
	Isotopic composition of atmospheric CO_2	9
	Isotopic composition of plant organic matter	9
	Microbial respiration	9
	Controls on diffusion through soils	10
	Soil carbonate precipitation	11
	THEORETICAL DEPTH PROFILES	11
III.	**Paleosol-Bearing Lithologies**	15
	BLOOMSBURG FORMATION	17
	CATSKILL FORMATION	24
IV.	**Methods**	26
V.	**Results**	30
	BLOOMSBURG FORMATION	35
	Wurtsboro and Port Jervis	35
	Harrisburg	43
	Lehigh Gap	45
	Port Clinton	47
	Danville	55
	CATSKILL FORMATION	57
	Powys (Sherman Creek Member)	57
	Trout Run (Duncannon Member)	70
	Newport and Liverpool (Duncannon Member)	77
VI.	**Discussion**	83
	PEDOGENIC CARBONATE	83
	EARLY DIAGENETIC CARBONATE	84
	LATE DIAGENETIC CARBONATE	86
VII.	**Interpretation**	88
	BLOOMSBURG FORMATION	88
	Wurtsboro, Port Jervis, and Harrisburg	88
	Port Clinton and Lehigh Gap	90
	Danville	91
	LATE DEVONIAN PALEOSOLS	93

Powys 93
Trout Run 94
Liverpool and Newport 95
ESTIMATIONS OF LATE SILURIAN TO LATE DEVONIAN pCO_2 95

VIII. **Conclusions** 101

LITERATURE CITED 103

APPENDICES 115
A: LOCATION OF PALEOSOL OUTCROPS 116
B: CARBON ISOTOPE ANALYSES 118

VITA 123

LIST OF FIGURES

FIGURE PAGE

1. Estimates of Paleozoic atmospheric pCO_2 from pedogenic carbonate in vertic paleosols compared to Berner's (1994) carbon cycle model..... 2

2. Fractionation pathway of carbon through (a) biosynthesis of CO_2 into organic plant matter and oxidation of soil organic matter, (b) CO_2 diffusion through soil matrix, and (c) precipitation in pedogenic environment..... 7

3. Theoretical $\delta^{13}C$ values vs. depth for pedogenic carbonate calculated from Cerling's (1991) paleobarometer..... 12

4. Theoretical $\delta^{13}C$ values for pedogenic carbonate calculated from Cerling's (1991) paleobarometer assuming an exponential decrease in permeability (ε) and porosity (ρ) with depth. 14

5. Idealized meandering-stream, fining upward sequence of the Catskill alluvial plain, typical of the (a) alluvial-deltaic plain (Sherman Creek Member) and (b) alluvial plain (Duncannon Member)..... 16

6. General location map for both Bloomsburg and Catskill Formation outcrops 18

7. General stratigraphy for the Bloomsburg Formation from Wurtsboro, NY to Lewistown, PA including approximate paleosol location..... 19

8. General stratigraphy for the Catskill Formation from Reading, PA to the New York state boarder..... 20

9. Map of Pennsylvania, illustrating Bloomsburg Formation paleosol localities with respect to structural features and burial depths..... 21

10. Map of Pennsylvania, illustrating Catskill Formation paleosol localities with respect to structural features and burial depths..... 22

11. Map of Pennsylvania, illustrating paleosol localities and occurrence of the Bloomsburg Formation outcrop belt..... 23

12. Map of Pennsylvania, illustrating paleosol localities and occurrence of the Devonian Formation outcrop belt..... 25

13. Bloomsburg (Late Silurian) Formation stable isotope compositions from various localities in Pennsylvania and New York..... 31

LIST OF FIGURES (continued) PAGE

14. Catskill (Late Devonian) Formation stable isotope compositions from various localities in Pennsylvania 32

15. Schematic profile of the Wurtsboro, NY outcrop including the location of two carbonate-bearing paleosols 37

16. Schematic profile of the Wurtsboro, NY paleosol 6 including sample locations 38

17 Schematic profile of the Wurtsboro, NY paleosol 1 including sample locations 39

18. Photomicrographs of Wurtsboro, NY, Port Jervis, NY, and Harrisburg, PA paleosols carbonate morphologies 40

19. Schematic profile of the carbonate-bearing Port Jervis, NY paleosol including sample locations 42

20. Schematic profile of the carbonate-bearing Harrisburg, PA paleosol including sample location 44

21. Schematic profile of the carbonate-bearing Lehigh Gap (PA) paleosol including sample locations 46

22. Photomicrographs of Lehigh Gap, PA paleosol carbonate morphologies 48

23. Schematic profile of the Port Clinton, PA outcrop exposed along approximately one mile of highway 49

24. Schematic profile of the Port Clinton, PA paleosols 1 and 2 including sample locations 51

25. Schematic profile of the carbonate-bearing Port Clinton paleosol 4 including sample location 52

26. Photomicrographs of Port Clinton, PA and Danville, PA paleosols carbonate morphologies 53

27. Schematic profile of the carbonate-bearing Danville, PA paleosol including sample locations 56

LIST OF FIGURES (continued) PAGE

28. Danville paleosol $\delta^{13}C$ values with respect to stratigraphic position relative to the Mifflintown Formation contact (from Driese et al., 1992) 58

29. Schematic sketch of the Powys, PA outcrops including the location of five carbonate-bearing paleosols..... 59

30. Schematic profile of the carbonate-bearing Powys, PA paleosols 1 and 4 including sample locations..... 61

31. Schematic profile of the carbonate-bearing Powys, PA paleosols 5 and 8 including sample locations..... 62

32. Schematic profile of the carbonate-bearing Powys, PA paleosol Pow3 including sample location..... 63

33. Photomicrographs of Powys, PA paleosols (1st suite) carbonate morphologies..... 64

34. Photomicrographs of Powys, PA paleosols (2nd suite) carbonate morphologies..... 66

35. Photomicrographs of Powys, PA paleosols (3rd suite) carbonate morphologies..... 68

36. Powys paleosol carbonate isotope compositions..... 71

37. Schematic profile of the carbonate-bearing Trout Run, PA outcrop including sample locations..... 72

38. Photomicrographs of Trout Run, PA paleosol (1st suite) carbonate morphologies..... 74

39. Photomicrographs of Trout Run, PA paleosol (2nd suite) carbonate morphologies..... 76

40. Trout Run paleosol carbonate isotope compositions with respect to carbonate morphology..... 78

41. Schematic profile of the Newport, PA) paleosol (from Driese and Mora, 1993)..... 80

42. Schematic profile of the carbonate-bearing Liverpool, PA paleosol including sample locations..... 82

43. Estimate of Late Silurian atmospheric pCO_2 (Bloomsburg Formation)..... 96

44. Estimate of Late Devonian atmospheric pCO_2 (Catskill Formation, Sherman Creek Member)..... 97

45. Estimate of Late Devonian atmospheric pCO_2 (Catskill Formation, Duncannon Member)..... 98

46. Estimates of Paleozoic atmospheric pCO_2 from pedogenic carbonate in vertic paleosols (Mora et al., 1996) and Berner's (1994) carbon cycle model compared to estimates from this study..... 100

I. Introduction

Paleosols represent the composite product of physical and biological processes of ancient soil ecosystems. The chemistry of paleosols has been used as an indicator of climate, vegetation, and atmospheric composition (Cerling, 1984, 1991, 1992; Holland, 1984; Wright, 1986; Feakes and Retallack, 1988; Cerling et al., 1989; Quade et al., 1989, 1995; Retallack, 1990; Goldstein, 1991; Joeckel, 1991; Mora et al., 1991, 1996; Driese and Mora, 1993; Cerling and Quade, 1993; Elick et al., 1998). Soils, which form in contact with the atmosphere, may provide especially useful climate proxies, as compared to oceanic systems that are subject to the processes of aqueous diffusion (Robinson, 1991). Stable carbon isotope analysis of pedogenic carbonate has already proven to be effective in determining paleoatmospheric pCO_2 levels using the soil carbonate CO_2 paleobarometer of Cerling (1991) (Cerling, 1991, 1992: Mora et al., 1991, 1993, 1996; Driese and Mora, 1993; Ghosh et al., 1995). Isotopic studies of Paleozoic paleosols indicate elevated pCO_2 levels (up to 15 times modern day; Fig. 1) during the Late Silurian, dropping to near modern day levels by the Early Permian (Mora et al., 1996). The steepest drop in atmospheric CO_2 levels appears roughly coincident with the time interval during which terrestrial vascular plants evolved and diversified (Beerbower, 1985; Niklas et al., 1985; Gensel and Andrews, 1987). Soil colonization by vascular plants may have been associated with enhanced rates of weathering, sedimentation, and organic carbon burial (Kump and Garrels, 1986; Berner and Canfield, 1989; Robinson, 1991; Berner, 1993, 1994; Algeo et al., 1992), and contributed to a steep drop in atmospheric pCO_2.

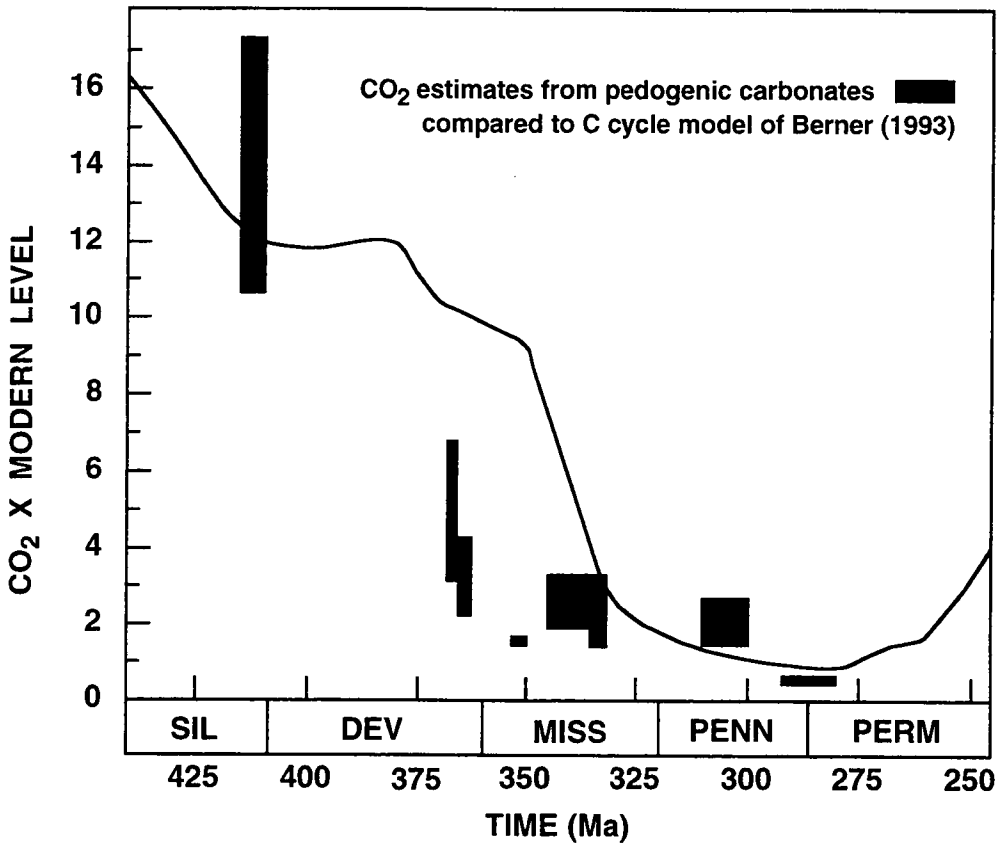

Figure 1. Estimates of Paleozoic atmospheric pCO_2 from pedogenic carbonate in vertic paleosols compared to Berner's (1994) carbon cycle model line curve. The steepest drop of CO_2 occurs during the evolution and diversification of the terrestrial ecosystems (from Mora et al., 1996).

The origin and initial radiation of terrestrial vascular plants was a major evolutionary event with important consequences for atmospheric compositions (Edwards, 1996). Biosynthesis of lignin and cambium aided in the development of larger, more complex plants with large tap roots, better water efficiency and preservation potential (Kenrick and Crane, 1997, Driese and Mora, in press). In turn, there was an increase in refractory biopolymers and slower recycling time in litter and soil (Edwards, 1996). Thus, the emergence and radiation of terrestrial vascular plants during the Siluro-Devonian may have initiated a time of substantial increase in burial rates of terrestrial organic carbon. Middle to Late Paleozoic disturbances of atmospheric O_2 and CO_2 (Kump, 1989) are hypothesized to be caused by "bottlenecks" in the cycling of lignin and other compounds synthesized by land plants (Robinson, 1991). Burial of refractory organic material would have had a dramatic effect on the Earth's carbon budget. A simplified organic mass balance equation that demonstrates this is:

$$CH_2O \text{ (organic matter)} + O_2 \leftrightarrow CO_2 + H_2O$$

Carbon sequestration in soils/sediments led to a shift of mass balance in the global carbon cycle, including drawdown of atmospheric CO_2. Thus, modeling pCO_2 from pedogenic carbonate, found within Middle to Late Paleozoic paleosols, can lead to a better understanding of the development of the Earth's atmosphere through time and the relationship of atmosphere to the terrestrial biota.

Previous studies which utilized the soil carbonate paleobarometer have focused on paleosols younger than Late Devonian, when the environment of soil carbonate precipitation was reasonably analogous to present conditions. Based on evidence of the

type, size, and occurrence of flora, post-Devonian paleosols most likely had similar soil respiration rates and depths of soil-respired CO_2 production compared to their modern counterparts. The relative influences of physical and biological processes on carbon isotopes and CO_2 diffusion in paleosols from the Late Silurian to the Late Devonian, however, may not have been analogous to modern soils (Amundson et al., 1988; Quade et al., 1989) for which soil-CO_2 diffusion models are defined. For example, the primary variable affecting the soil carbonate (i.e., soil-CO_2) carbon isotope profile for modern soils in arid environments is the soil respiration rate, which is related to the density of vegetation cover (Amundson et al., 1988; Quade et al., 1989; Cerling, 1991). When plant communities are sparse or have shallow roots, the influence of isotopically-heavy atmospheric CO_2 on soil-CO_2 compositions may be significant, especially toward the top of the soil profile. Paleosols exhibiting the first evidence of terrestrial vascular plants (in the form of rhizomes or rhizoliths) occur in Late Silurian rocks (Driese et al., 1992; Beerbower, 1985; Niklas et al., 1985). Late Silurian paleosols exhibit root-like features dominated by sparse, mat-like morphologies (Driese et al., 1992; 1993a), suggesting relatively shallow mean depths of CO_2 production ($<<$ 5 cm) by plant respiration or decay. Diversification of plant assemblages in the Early to Middle Devonian period introduced more robust and deeply rooting plant assemblages (Gensel and Andrews, 1987; Elick et al., 1998), presumably resulting in greater and deeper production of soil-respired CO_2.

The purpose of the present study is to examine Late Silurian to Late Devonian paleosols occurring within the Appalachian Basin in Pennsylvania and New York in

order to: (1) characterize the petrographic and stable isotopic characteristics of pedogenic carbonate within the paleosols; (2) evaluate the relationships between isotopic composition and (a) carbonate morphology, (b) depth in paleosol, and (c) gross paleosol morphology in the context of the soil-carbonate paleobarometer; (3) evaluate possible diagenetic alteration of the pedogenic carbonate, and; (4) where possible, use the carbon isotope compositions to constrain atmospheric levels of CO_2 during this time period of rapid evolutionary change in terrestrial ecosystems.

II. The Soil Carbonate CO_2 Paleobarometer and Carbonate Isotopes

The origin of soil carbonate and its carbon isotope composition is summarized in Figure 2 and is discussed below. Isotopic fractionation of CO_2 is a stepwise process representing: (1) origin of CO_2 by oxidation of organic matter, and microbial respiration, with some contribution of atmospheric CO_2, (2) diffusion through the soil matrix, and (3) bicarbonate formation and precipitation of pedogenic carbonate. Studies of modern and geologically young soils have established a correlation between: (a) the production and diffusion of CO_2 in soil, (b) atmospheric levels of CO_2, and (c) the isotopic compositions of pedogenic carbonates, resulting in the development of a CO_2 paleobarometer (Cerling, 1984; 1991; Quade et al., 1989).

The concentration of CO_2 in soil is described by:

$$\partial C^*_s / \partial t = D^*_s(\partial^2 C^*_s / \partial z^2) + \phi^* s(z)$$

where:

$\phi^*_s(z)$ is the CO_2 production rate as a function of depth

z is the depth of CO_2 production

D^*_s is the coefficient of bulk diffusion of CO_2 through the soil

C^*_s is the concentration of CO_2 in the soil.

Measurements of CO_2 in modern soils suggest that CO_2 exhibits an exponential decrease with depth (Cerling, 1991). For this particular production function, the specific solution to the above equation is:

$$S(z) = (\phi^*_s(0)\ \bar{z}^2 / D^*_s)\ (1 - e^{-z/\bar{z}})$$

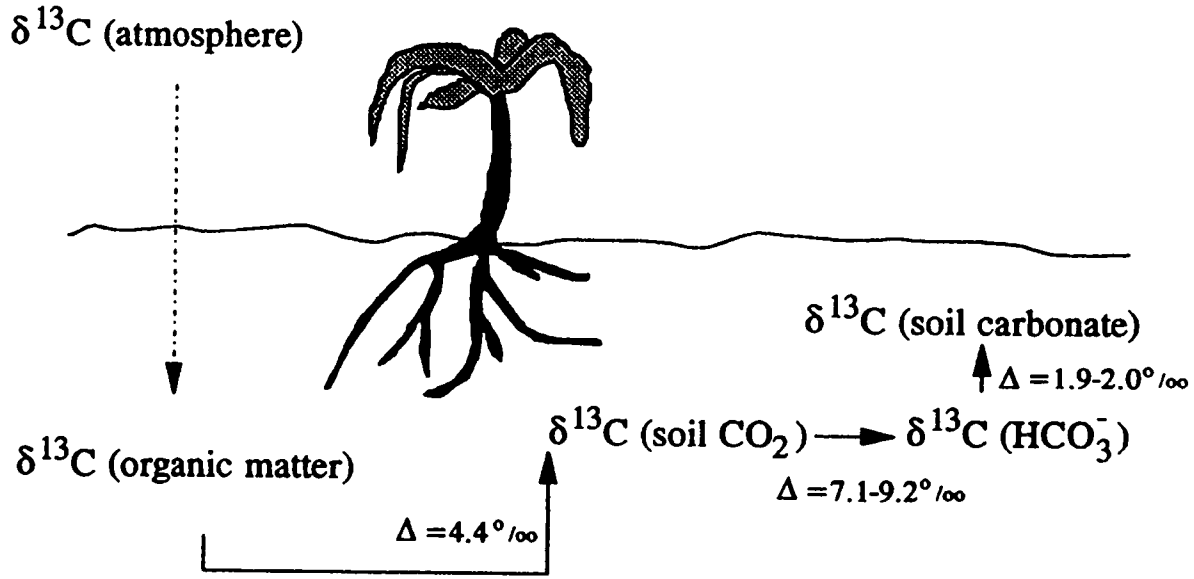

Figure 2. Fractionation pathway of carbon through: (a) biosynthesis of CO_2 into organic plant matter and oxidation of soil organic matter, (b) CO_2 diffusion through the soil matrix, and (c) carbonate precipitation in pedogenic environment. Dashed arrow indicates variable input of atmospheric CO_2.

where:

S(z) is the concentration of soil-CO_2 (minus atmospheric CO_2)

$\bar{z}$ is the characteristic (average) depth of CO_2 production.

Substituting isotope-specific diffusion coefficients and using delta notation, the equation can be written:

$$\delta_s(z) = ({}^1/R_{PDB}[([S(z)({}^{D^*s}/D^{13}{}_s)\hat{\delta}_\phi] + C^*{}_a\hat{\delta}_a) / (S(z)(1 - ({}^{D^*s}/D^{13}{}_s)\hat{\delta}_\phi) + C^*{}_a(1 - \hat{\delta}_a))]-1) \times 1000$$

where:

$\delta_s(z)$ is the isotopic value of soil-CO_2

R_{PDB} is the absolute ratio of ^{13}C to ^{12}C for the standard PDB

$D^{13}{}_s$ is the diffusion coefficient of $^{13}CO_2$ through the soil

$C^*{}_a$ is the concentration of CO_2 in the atmosphere

and:

$$\hat{\delta}_i = [R_{PDB}(\delta_i/1000 + 1)] \ / \ [1 + R_{PDB}(\delta_i/1000 + 1)]$$

where:

δ_s is carbon isotopic composition of soil-CO_2

δ_a is carbon isotopic composition of atmospheric CO_2

δ_ϕ is carbon isotopic composition of soil-respired CO_2

$R_{PDB} = 0.011237$

Thus, the final isotope composition recorded in the pedogenic calcite will correspond to the relative proportion of soil-respired and atmospheric CO_2 in the soil-CO_2 reservoir,

regulated by factors influencing CO_2 diffusion in soil. Numerous variables such as $\bar{z}$, D^*_s, δ_a and δ_ϕ must be known or reasonably constrained in order for the paleobarometer to be useful.

ISOTOPIC CONSTRAINTS FOR THE PALEOBAROMETER

Isotopic composition of atmospheric CO_2

The first variable that must be constrained is the atmospheric $\delta^{13}C$ value. This value that can calculated based on marine inorganic carbon carbonate for which there are numerous sources (e.g. Popp et al., 1986; Veizer et al., 1986), assuming equilibrium of atmospheric CO_2 with the marine reservoir.

Isotopic composition of plant organic matter

Modern plants utilize several different photosynthetic pathways to convert CO_2 into plant matter. The incorporation of CO_2 via the C3, C4, or CAM pathways yields different isotope compositions (-20 to -35‰, -10 to -14‰, -10 to 22‰ respectively; Deines et al., 1974; Hoefs, 1987; Ehleringer, 1988). The absence of any evidence for pre-Miocene plants which utilized the C4 (and, by default, CAM) pathway during photosynthesis allows us to assume that all Siluro-Devonian vascular plants utilized the C3 pathway (Thomasson et al., 1988; Mora et al., 1993).

Microbial respiration

Microbial degradation and oxidation of soil organic matter (SOM) is the primary source of soil-CO_2. Although the concentration of bulk-SOM is variable with depth, the

roots have a very stable carbon isotope composition (Boutton et al., 1993). The initial decay of soil litter is associated with minor alteration of bulk isotopic compositions of soil carbon. However, this is not expected to significantly influence soil carbonate compositions because soil carbonate precipitation occurs on a scale several orders of magnitude slower than rapid bacterial alteration of SOM (10^2-10^3 vs. 10^0-10^1 yrs; Mora et al., 1996). Another concern is that a significant portion of SOM may be animal in origin. We can assume that the impact on bulk SOM $\delta^{13}C$ is likely to be small (< 2‰) because these animals largely consume and metabolize soil vegetation. A previous study suggests that animal-based organic matter does not significantly affect the isotopic composition of bulk SOM (Mora et al., 1996).

Controls on diffusion through soils

Diffusion of CO_2 through the soil matrix and mixing of atmospheric with soil-respired CO_2 is regulated by the physical characteristics of the soil. Soils developed in humid to sub-humid conditions show little atmospheric influence on soil-CO_2 (Cerling, 1984; Cerling and Hay, 1986), even with low respiration rates. Some Ordovician soils are thought to have been just as CO_2-rich as modern temporal forests, with the source of CO_2 primarily derived from the decomposition of non-vascular plants (Yapp and Poths, 1994). High soil-CO_2 concentrations can also be a result of slow CO_2 diffusion out of the soil (Keller and Wood, 1993), limited by a high degree of water saturation.

Unfortunately, physical soil characteristics that regulate the diffusion rate of gasses through a soil profile, such as permeability (ε) and porosity (ρ), are not preserved during burial diagenesis and lithification. By limiting our studies to paleosols which

share as many sedimentologic and pedogenic characteristics as possible, variations in soil isotopic profiles imposed by these factors are minimized.

Soil carbonate precipitation

CO_2 solution into soil water and precipitation of carbonate are controlled by the temperature dependent isotopic fractionations between CO_2 and HCO_3^- and HCO_3^- and calcite (Friedman and O'Neil, 1977). Paleoclimate reconstructions provide reasonable estimates of surface temperature. Although these estimates predict a seasonal effect on the carbon isotope composition, soil carbonate precipitation occurs at rates (10^{-7} to 10^{-9} moles/cm^2/yr) of several orders of magnitude less than that of CO_2 respiration flux (10^{-3} to 10^{-5} moles/cm^2/yr) (Cerling and Quade, 1993). Thus dissolution/reprecipitation of the soil carbonate may occur, recording a time average of soil-CO_2 isotope compositions (Amundson et al., 1989; Mora et al., 1993, 1996).

THEORETICAL DEPTH PROFILES

Carbonate precipitated in equilibrium with end-member reservoirs of atmospheric ($\delta^{13}C_{atm}$ = -6.5‰) and soil-respired CO_2 ($\delta^{13}C_{SOM}$ = -26‰) would have $\delta^{13}C$ of approximately +3‰ PDB and -12‰ PDB, respectively. Depth profiles of soil-CO_2 $\delta^{13}C$ values have been calculated to reflect: (a) changing atmospheric pCO_2, and (b) variable soil respiration rate (Fig. 3). These calculations indicate that by increasing atmospheric pCO_2, pedogenic carbonate will have more positive carbon-isotope compositions. Conversely, increasing soil pCO_2 by increasing soil respiration rate results in more negative carbonate $\delta^{13}C$ values. The curves shown in Figure 3 indicate that soil carbonate

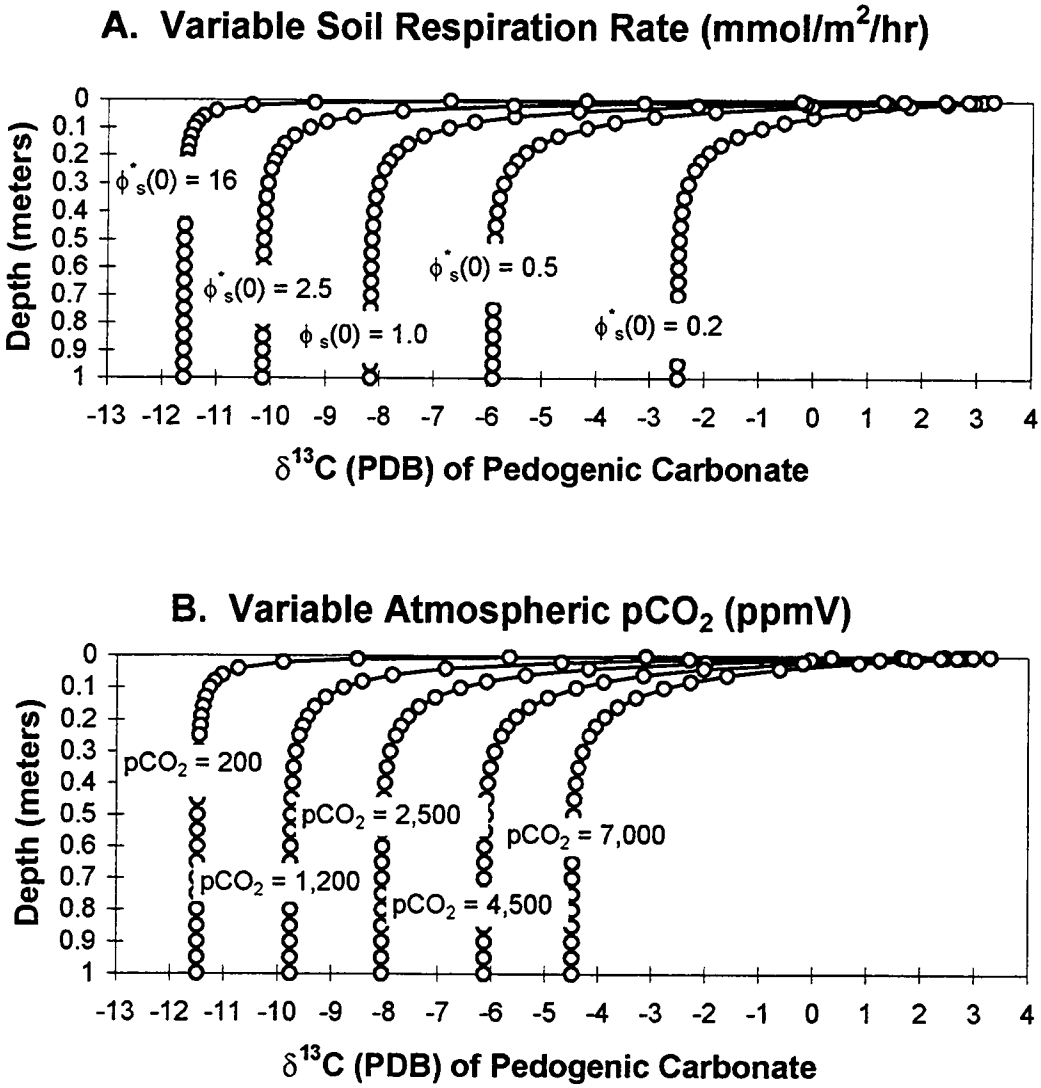

Figure 3. Theoretical $\delta^{13}C$ values vs. depth for pedogenic carbonate calculated from Cerling's (1991) paleobarometer. Varying (A) soil respiration rate and (B) atmospheric pCO_2 will regulate the mixture between the two reservoirs in the soil matrix, thereby dictating the shape of the curve and, ultimately, the isotopic composition of pedogenic calcite.

$\delta^{13}C$ values tend to approach a constant value, which will yield the best minimum estimate of atmospheric pCO_2. Lower respiration rates or high atmospheric pCO_2 tend to flatten the shape of the pedogenic $\delta^{13}C$ profile. Because low respiration rates were likely the case during the Siluro-Devonian, pedogenic carbonate in Late Silurian paleosols is more likely to retain a wide range of $\delta^{13}C$ values. This increases the likelihood that atmospheric pCO_2 will be overestimated for these paleosols.

Slight differences in clay content or layering (relict bedding) that is present in many cumulative soils, may alter soil-CO_2 concentration and isotope profiles by preserving diffusion barriers within the soil profile. Cumulative soils are composed of numerous superposed soil profiles deposited during long-term aggradation. A low permeability layer may alter fluid flow through a soil, creating a perched water table or a locally wetter environment, that can affect CO_2 diffusion in soil. Theoretical depth-soil carbonate (i.e. soil-CO_2) relationships have been calculated, assuming exponentially decreasing porosity (ε) and permeability (ρ) with depth (Fig. 4). This results in variable $\delta^{13}C$ values with depth, rather than isotope compositions which approach a constant value (Fig. 3). Over time, an average isotope composition is recorded and will most likely result in less distinct isotopic profiles than calculated here. However,understanding these diffusion-related parameters may aid in the interpretation of the Late Silurian cumulative paleosols formed in a frequently inundated coastal setting.

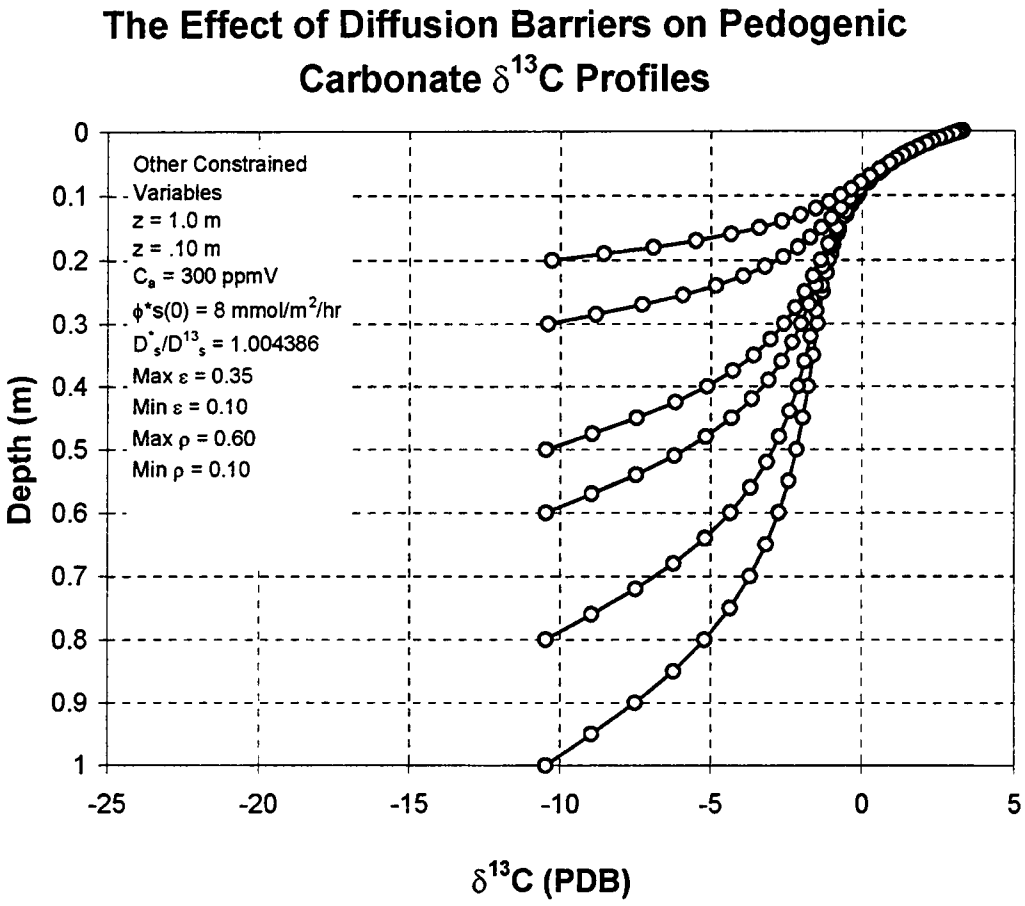

Figure 4. Theoretical $\delta^{13}C$ values for pedogenic carbonate calculated from Cerling's (1991) paleobarometer assuming an exponential decrease in permeability (ε) and porosity (ρ) with depth. Each curve terminates at an impermeable, horizontal boundary that passes through the deepest calculated data point.

III. Paleosol-bearing Lithologies

Within the Appalachian Basin, paleosols occur in the upper, clay-rich parts of fining-upward sequences in Paleozoic red-bed successions ranging from Ordovician to Permian age. Local horizons that are bioturbated by roots, exhibit blocky fractures, are mottled, and have slickensided clay linings and pseudoanticlines are interpreted as paleosols (Bridge and Nickelsen 1985; Blodgett 1985; Retallack, 1985).

Paleosols are found in both delta-plain (marginal-marine) and alluvial-plain sequences. Sevon (1985) described end-member examples of these paleosols in the Catskill Formation (Fig. 5), which are representative of the paleosols examined in this study. Both the alluvial-plain and delta-plain sequences are fining-upward successions deposited in association with channel migration and flooding events, and the majority of pedogenic carbonate is found within the upper portion of the fine-grained package. The alluvial-plain (more inland) paleosol contains less pedogenic carbonate than the delta-plain paleosol. Each sequence typically consists of a basal coarse sandstone or conglomerate unit that contains small rounded pebbles. The sequences then typically grade into a coarse siltstone, and can continue into a fine-grained mudstone. Within these packages there will often be more coarse thin interlayers, which represent crevasse-splay flooding events during paleosol development.

The paleosols targeted in this study are typically clay-rich red-beds exhibiting morphological features analogous to those of modern Vertisols. Vertisols typically form in marginal-marine or alluvial-plain environments and display shrink/swell features, weak horizontation, and sepic fabrics and peds surrounded by stress cutans (Soil Survey

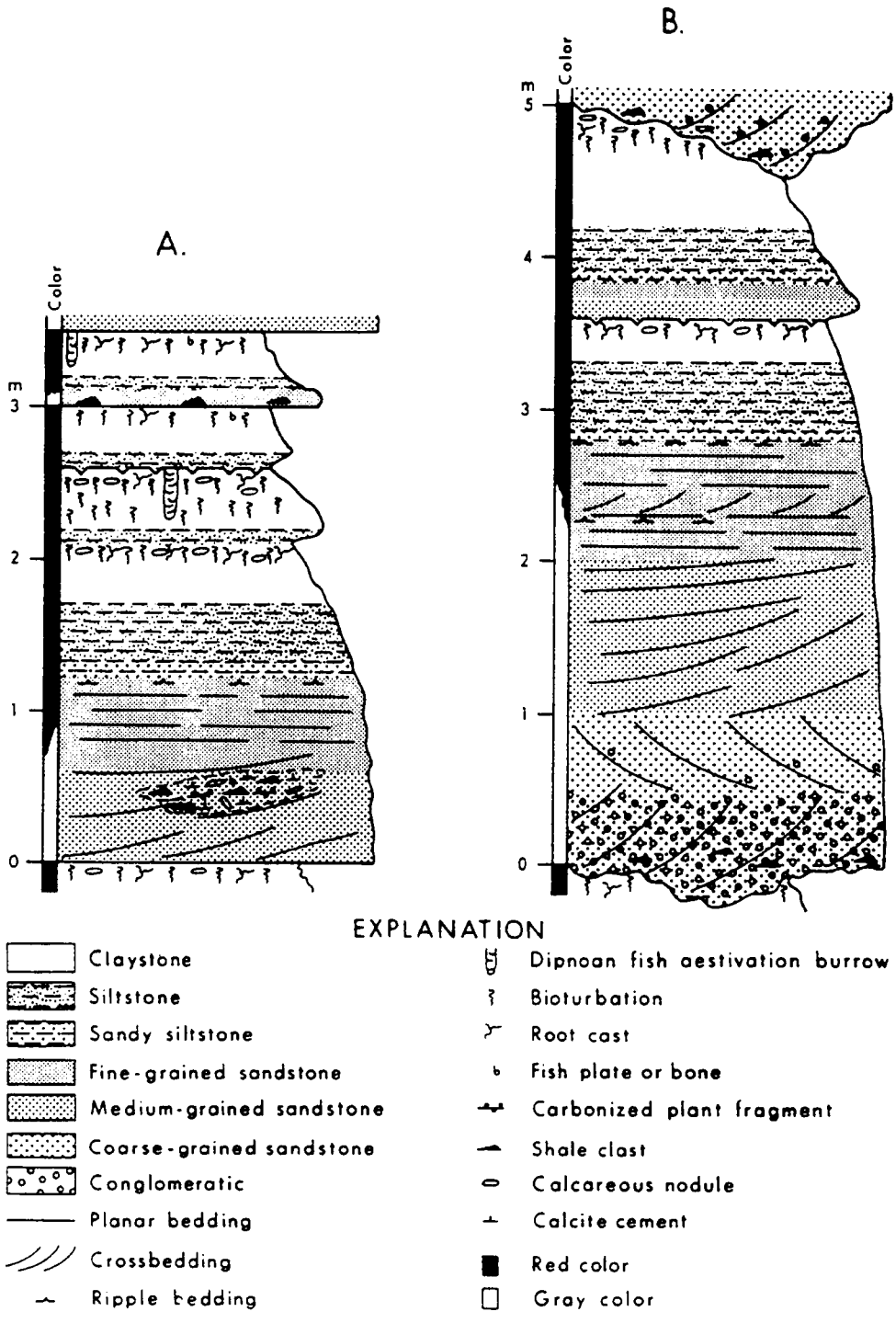

Figure 5. Idealized meandering-stream, fining-upward sequence of the Catskill alluvial plain, typical of the: (a) alluvial-deltaic plain (Sherman Creek Member) and (b) alluvial plain (Duncannon Member) (from Sevon, 1985).

Staff, 1994). Dudal and Eswaran (1988) and Coulombe et al. (1996) have compiled more complete summaries of the morphological properties. Vertisols typically form in tropical to warm-temperate climates where there are 4-8 months of dry conditions, when most pedogenic carbonate is precipitated.

The paleosols examined in this study occur within the Upper Silurian Bloomsburg and Upper Devonian Catskill Formations, located in western New York and Pennsylvania (Fig. 6). The stratigraphic relationship of each paleosol to its respective formation is presented in Figures 7 and 8. Depths of burial, along with the location of the Allegheny and Blue Mountain Structural Front, are shown relative to the location of the paleosols in Figures 9 and 10 (Levine, 1986; Beaumont et al., 1987; Nickelsen, 1988).

BLOOMSBURG FORMATION

The Bloomsburg Formation is upper Ludlovian to lower Pridolian in age, conformably overlying the Mifflintown Formation (Hoskins, 1961; Patchen et al., 1985; Cotter, 1993). In central Pennsylvania (Danville, Port Clinton, and Harrisburg localities), the depositional setting was one of a low-energy, delta-plain system that experienced episodic subaerial conditions (Fig. 11). In eastern Pennsylvania and southeastern New York (Wurtsboro, Port Jervis, and Lehigh Gap locations) the stratigraphy indicates siliciclastic-rich, terrestrial sequences at more inland localities (Hoskins, 1961; Rickard, 1969; Driese et al., 1992). The source of terrigenous, clastic sediment was the Taconic Mountains to the east, paleogeographically located

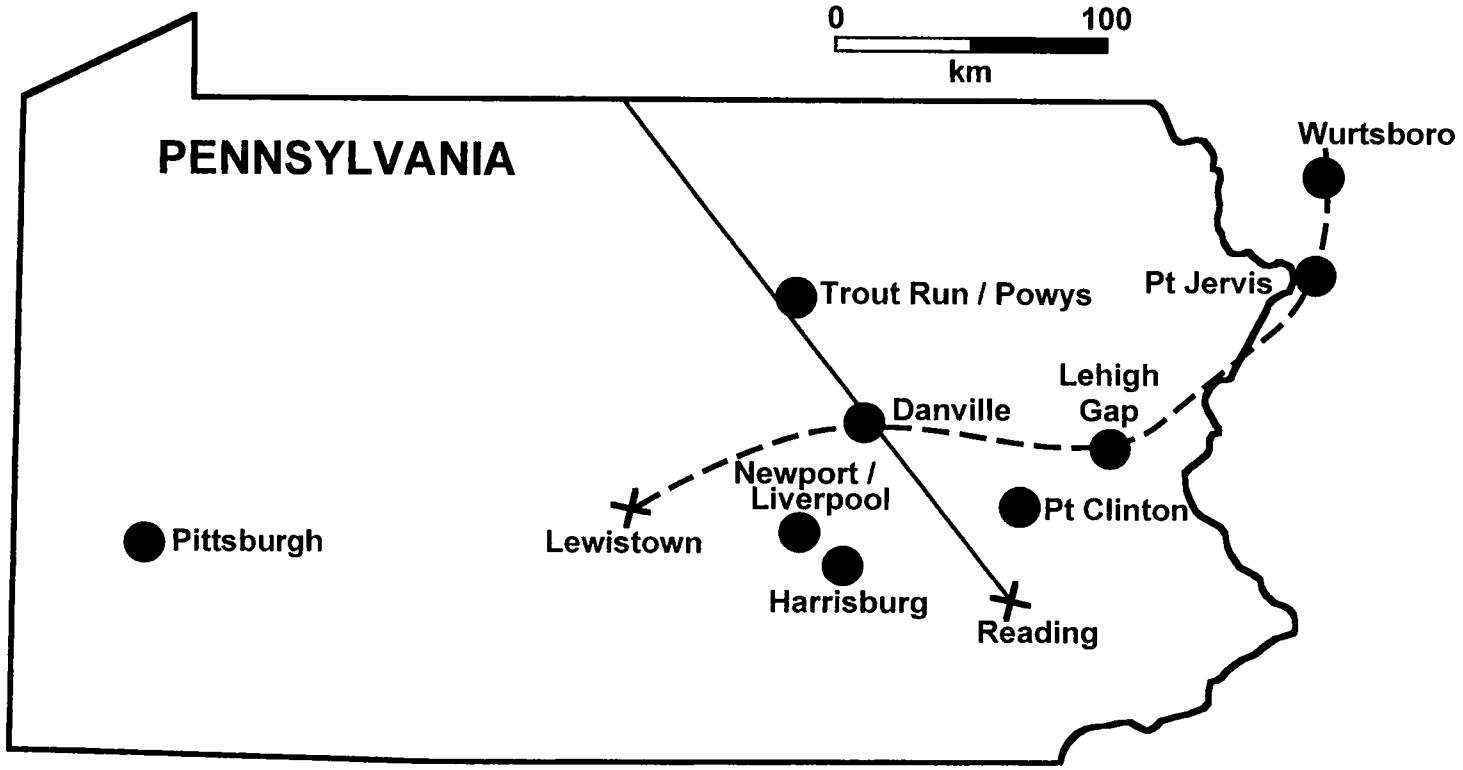

Figure 6. General location map for both Bloomsburg and Catskill Formation outcrops. Dashed line indicates position of generalized stratigraphic section for the Bloomsburg Formation (see Figure 7) and solid line indicates position of generalized stratigraphic section for the Catskill Formation (see Figure 8).

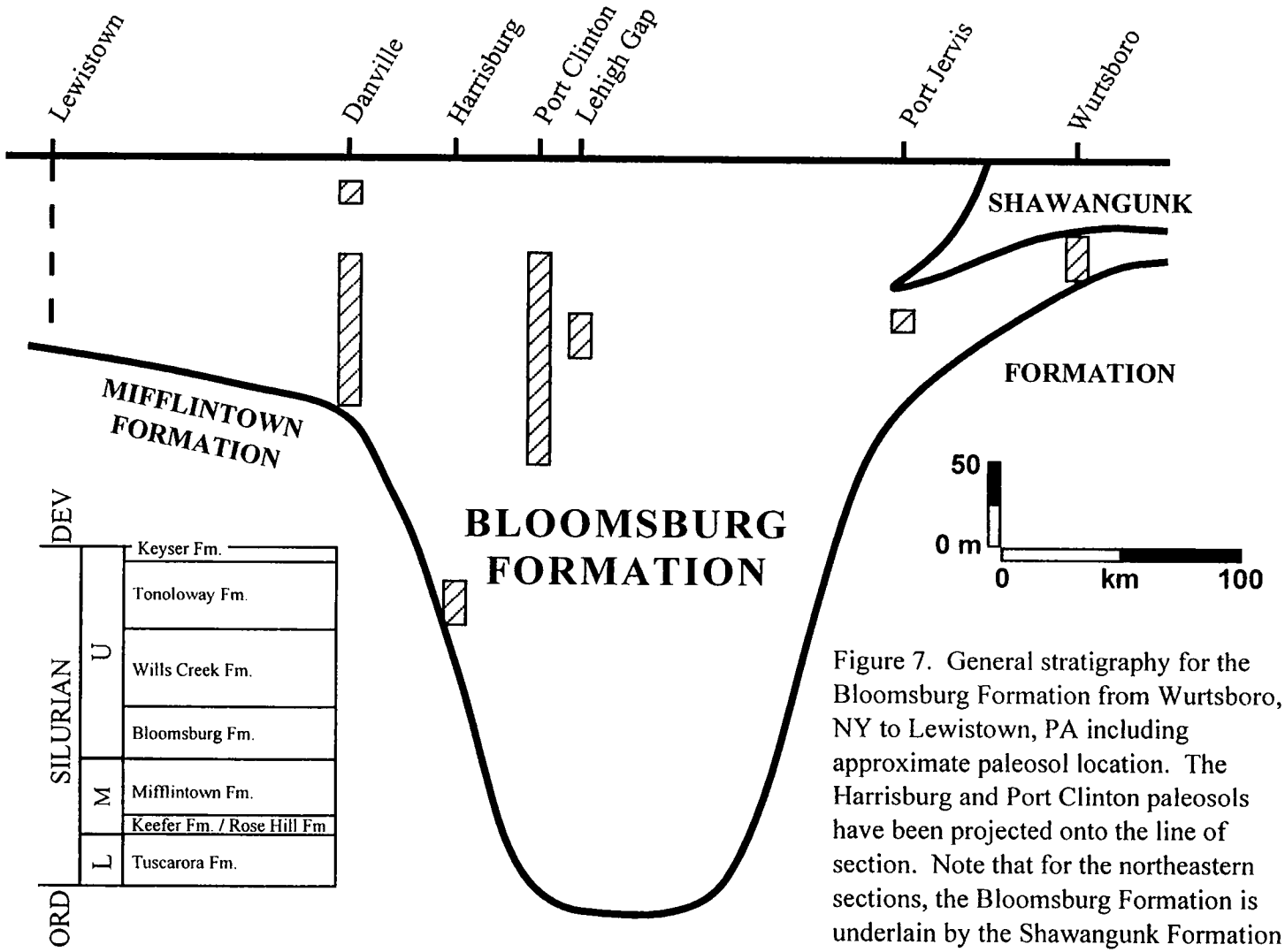

Figure 7. General stratigraphy for the Bloomsburg Formation from Wurtsboro, NY to Lewistown, PA including approximate paleosol location. The Harrisburg and Port Clinton paleosols have been projected onto the line of section. Note that for the northeastern sections, the Bloomsburg Formation is underlain by the Shawangunk Formation (from Hoskins, 1961 and Epstein, 1993).

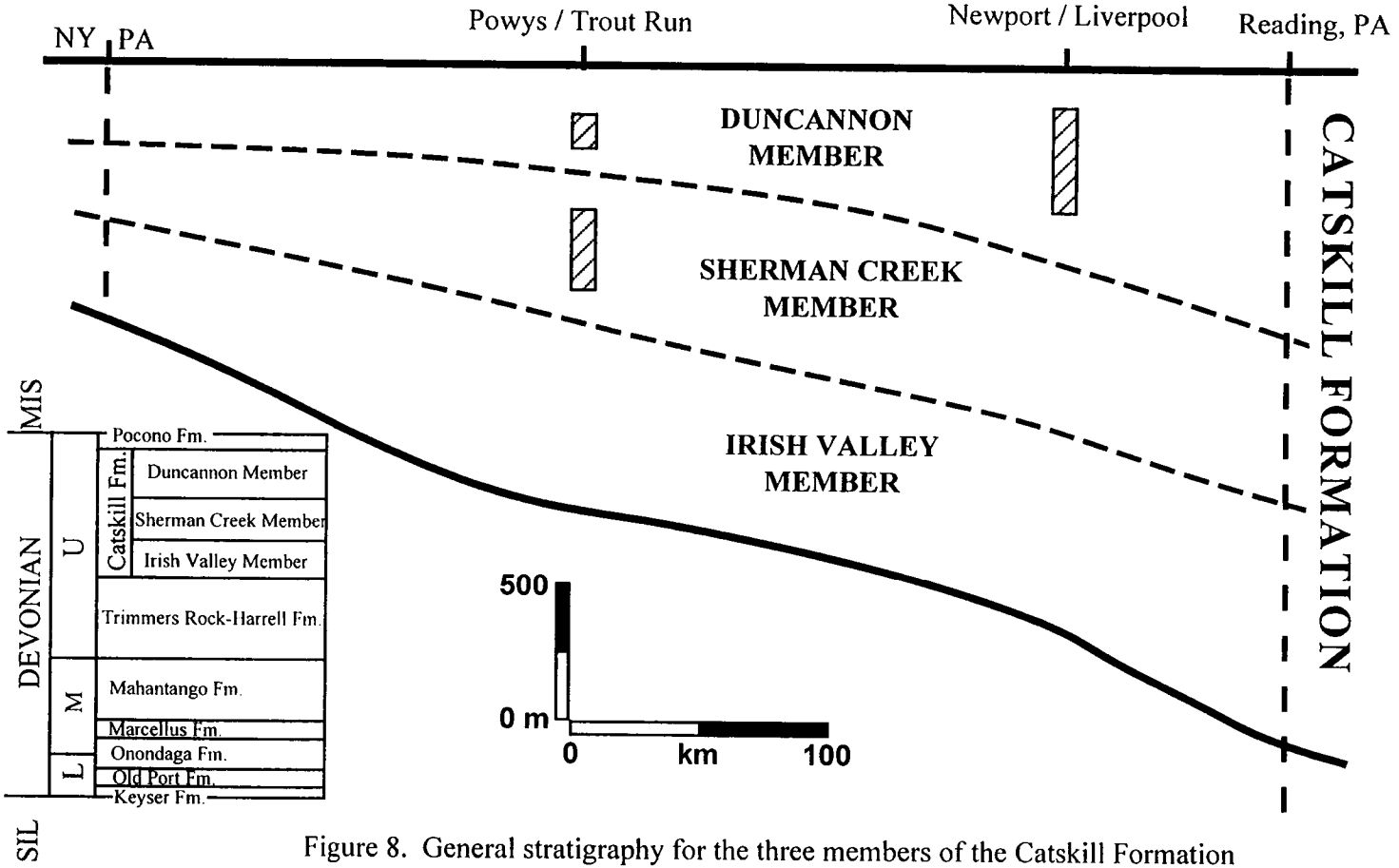

Figure 8. General stratigraphy for the three members of the Catskill Formation from Reading, PA to the New York border. The Newport and Liverpool are projected onto the line of section (after Ayrton, 1963).

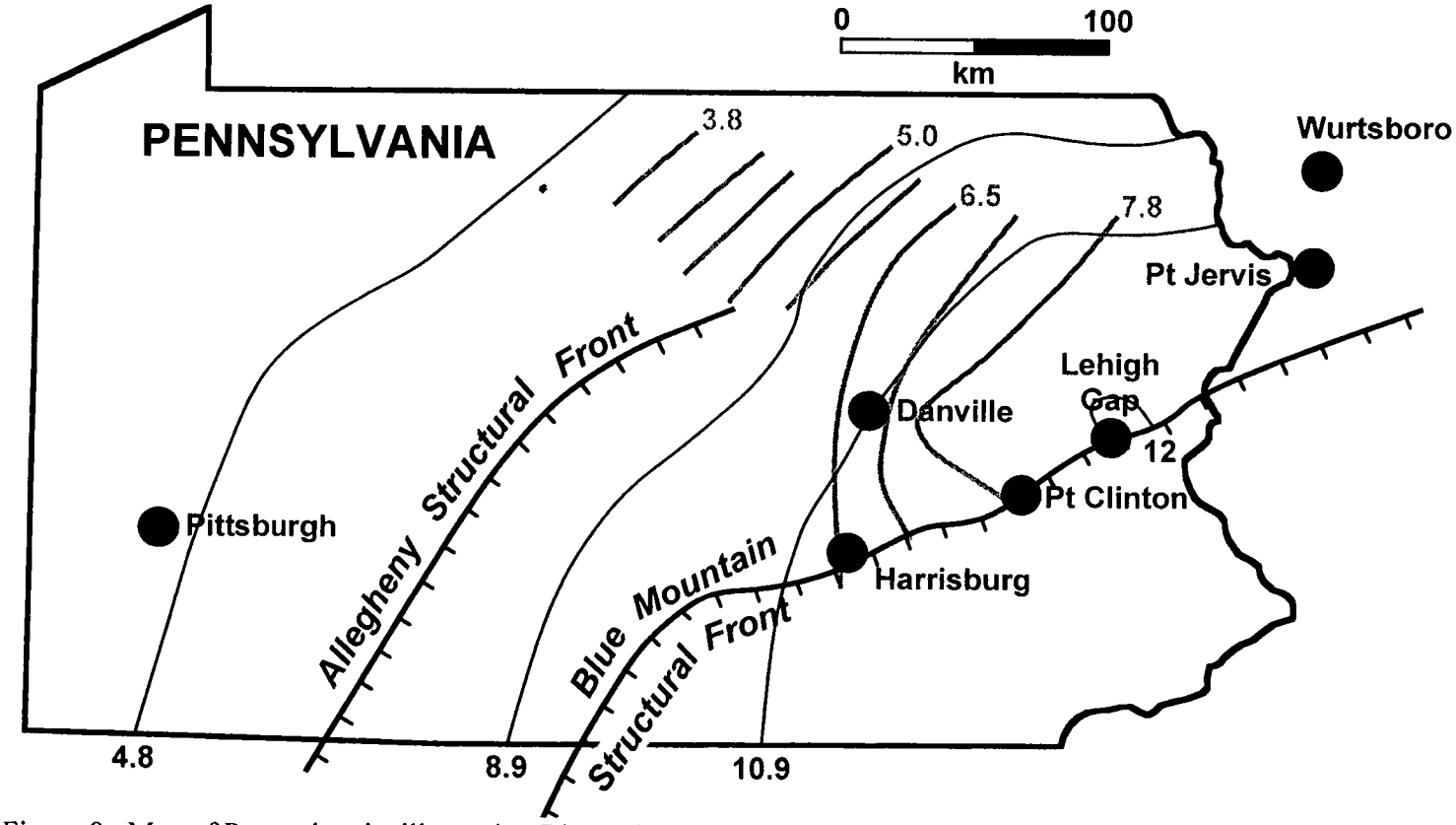

Figure 9. Map of Pennsylvania, illustrating Bloomsburg Formation paleosol localities with respect to stuctural features and burial depths. Hatched lines represent the two major thrust faults that cross-cut through Paleozoic formations (after Nickelson, 1988). Thick, dashed lines represent the mean burial depths to the base of the Mississippian Formation estimated from coal rank (after Levine, 1986). Black lines represent minimum estimates for maximum burial depths to the top of the Silurian (after Beaumont et al., 1987 and Ayrton, 1963). Note that there is a fourth burial isopach located near the Lehigh Gap locality.

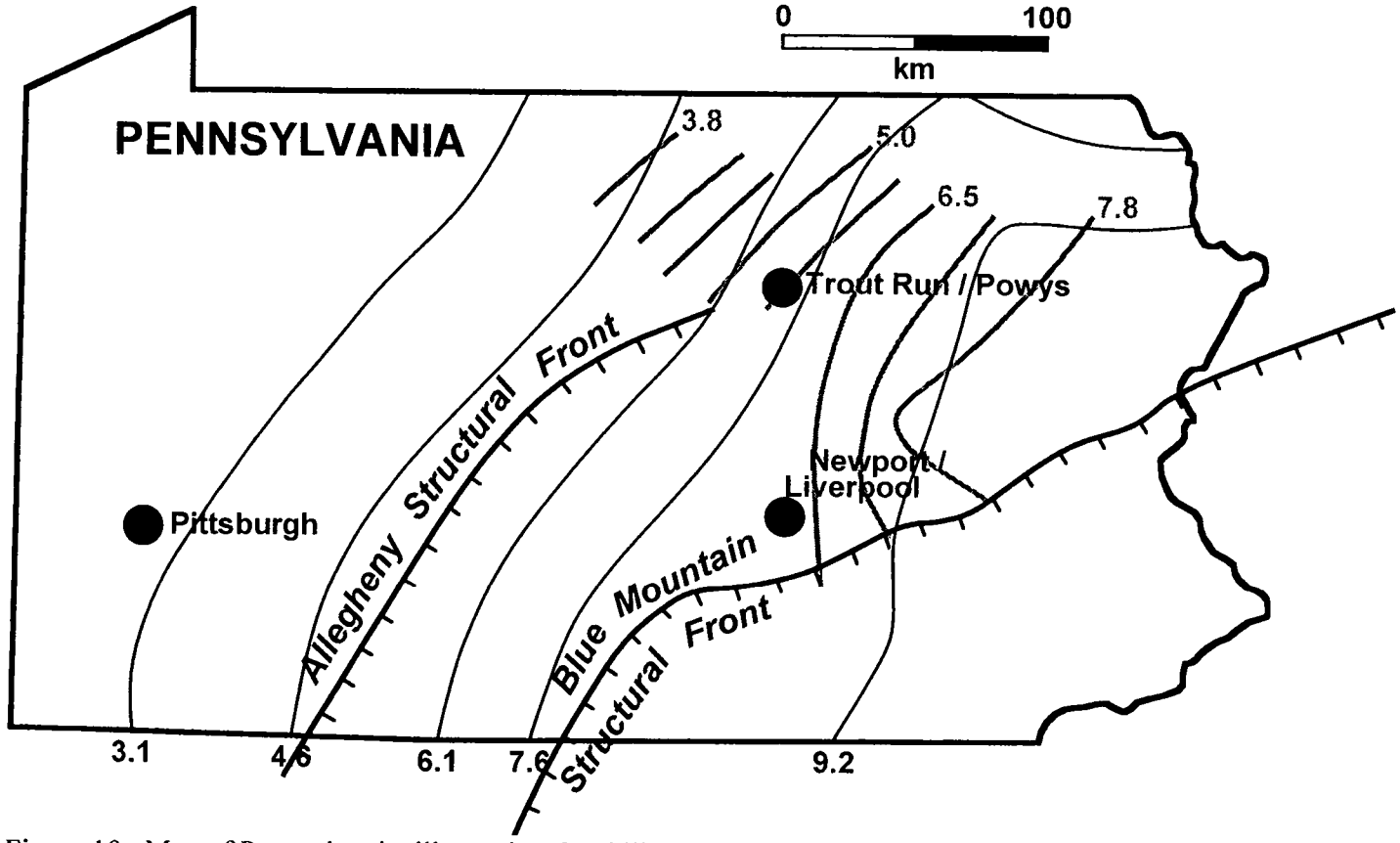

Figure 10. Map of Pennsylvania, illustrating Catskill Formation paleosol localities with respect to stuctural features and burial depths. Hatched lines represent the two major thrust faults that cross-cut through Paleozoic formations (after Nickelson, 1988). Thick, dashed lines represent the mean burial depths to the base of the Mississippian Formation estimated from coal rank (after Levine, 1986). Black lines represent minimum estimates for maximum burial depths to the top of the Devonian (after Beaumont et al., 1987).

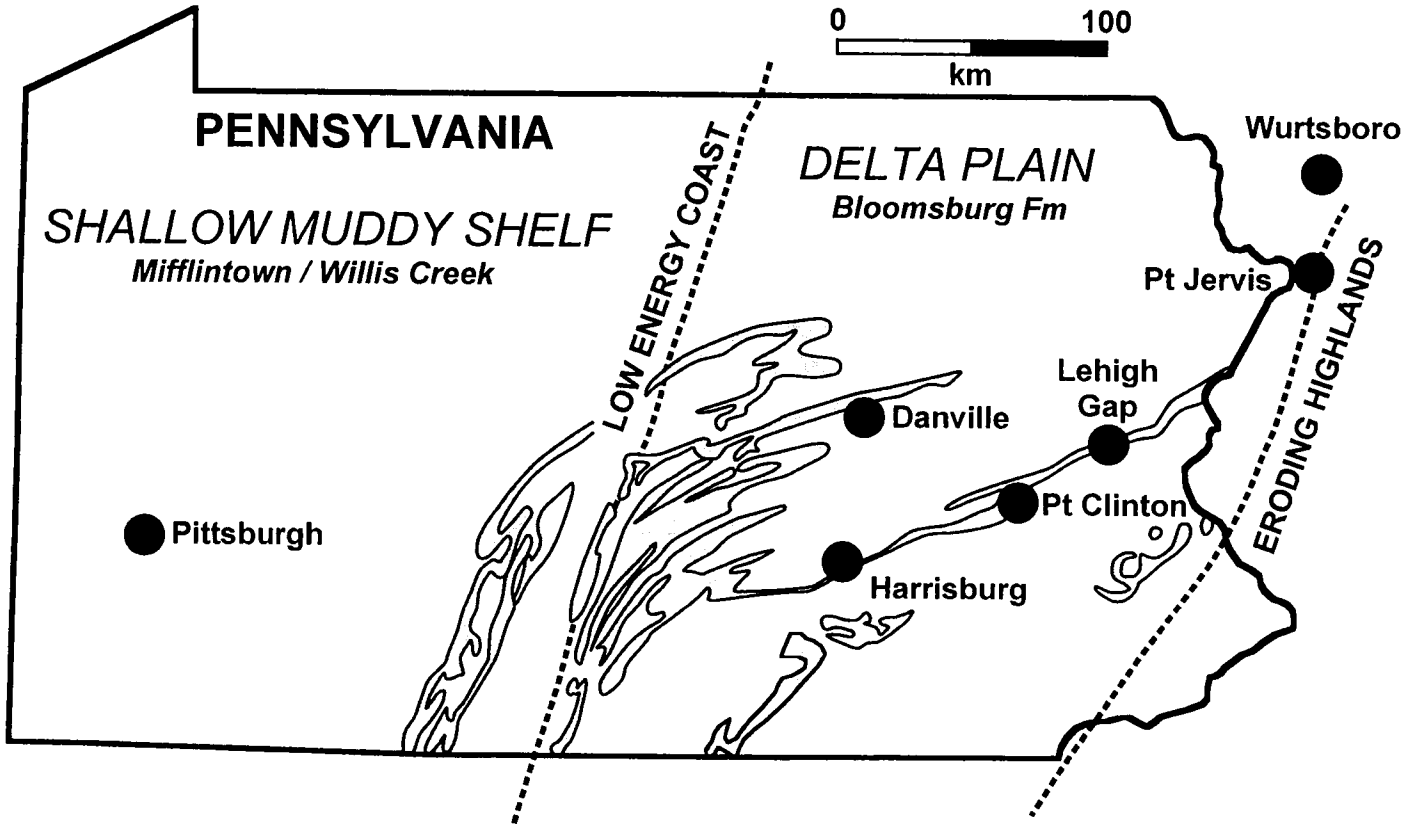

Figure 11. Map of Pennsylvania, illustrating paleosol localities and occurrence of the Bloomsburg outcrop belt. The source of clastic sediments (eroding highlands) was located near eastern Pennsylvania. The low energy coast is the approximate position of the paleoshoreline at maximum westward migration. The transition from the Bloomsburg Formation to the Mifflintown/Wills Creek Formation is to the west of all outcrop localities. To the east, the Bloomsburg Formation grades into the Shawangunk Formation.

approximately in the same position as the modern Appalachian Mountains. This resulted in a westward distal trend of increasing carbonate-rich, open-marine conditions and a progressive westward migration of the paleoshoreline during the deposition of the Bloomsburg. Paleogeographic studies have determined that the location of Pennsylvania during the Late Silurian was between 20 and 25° south (Scotese, 1984; Van der Voo, 1988). The climate was typically warm and moist in winter and hot and dry in summers (Ziegler et al., 1979; Driese et al., 1992).

CATSKILL FORMATION

The Upper Devonian (upper Famennian) Catskill Formation (Fig. 12) was deposited in the foreland basin as a generally westward-thinning, coarsening-upward, transgressive sequence of sandstone, mudstone, and conglomerates of alluvial origin (Gordon and Bridge, 1987). The subaerial portion of the delta was restricted to New York, Pennsylvania, Maryland, West Virginia, and northwestern Virginia (Faill, 1985). The terrigenous source terrain also served as an orographic boundary influencing the weather patterns during the Devonian. During this time, the climate was typically tropical to sub-tropical, highly seasonal, and of a monsoonal nature (Cotter et al., 1993). Paleogeographic studies have determined the location of Pennsylvania to be between the equator and 10-15°S during the Upper Devonian (Zeigler et al., 1979; Scotese et al., 1979; Kent and Miller; 1988; Van der Voo, 1988).

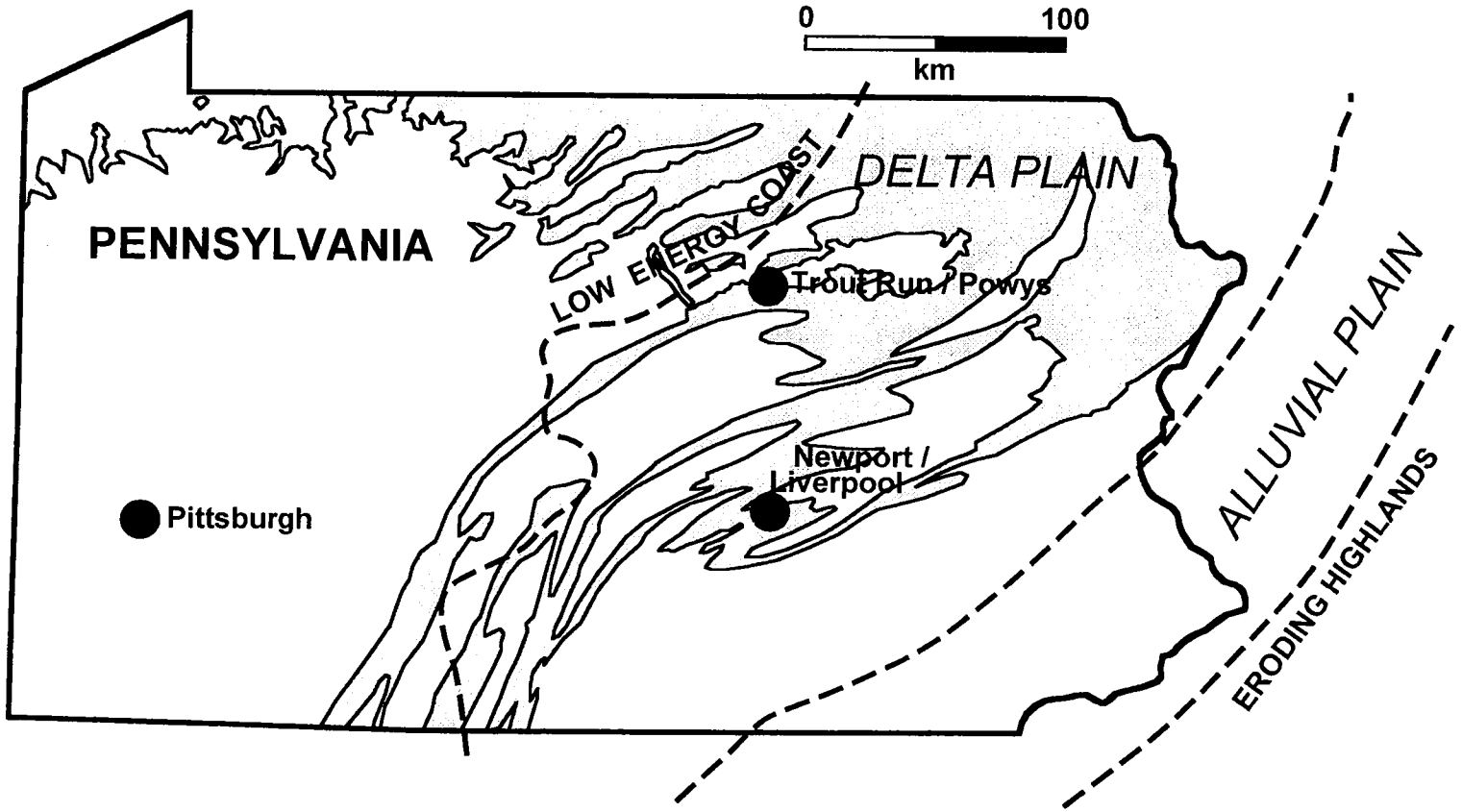

Figure 12. Map of Pennsylvania, illustrating paleosol localities and occurrence of the Catskill outcrop belt. The source of clastic sediments (eroding highlands) was located near eastern Pennsylvania. The low energy coast is the approximate position of the Late Devonian paleoshoreline.

IV. Methods

Sampling and measurement of the paleosols at Lehigh Gap, Wurtsboro, Port Jervis, Port Clinton, Danville, and Harrisburg, occurred during the summer of 1995 by Mora and Driese; the Lehigh Gap, Port Clinton, Danville, Liverpool, and Powys localities were subsequently sampled and measured in 1996 by Mora and King. The paleopedology and isotope geochemistry of some Silurian-Devonian paleosol localities (Trout Run, PA, Newport, PA, and Danville, PA) were previously described in detail (Driese et al., 1992; Driese et al., 1993a, 1993b) and were helpful in this study for baseline values. New isotopic data are reported herein for the Danville and Trout Run localities. A summary of samples that were collected, slabbed and thin-sectioned, and analyzed for isotope compositions is presented in Table 1.

Field analysis consisted of collecting and describing the paleosols in their stratigraphic/sedimentological context in order to evaluate development of pedogenic

Table 1. Summary of sample acquisition for both Bloomsburg and Catskill paleosols

Paleosol locality and number of paleosol sequences measured	# outcrop samples	# carbonate bearing paleosols analyzed	# carbonate bearing samples analyzed	# carbonate isotope analyses
Wurtsboro (6)	14	2	3	4
Port Jervis (3)	7	1	2	4
Harrisburg (3)	4	1	1	12
Lehigh Gap (1)	2	1	1	3
Port Clinton (5)	14	3	4	17
Danville (1)	2	1	2	4
Powys (5)	12	5	6	23
Trout Run (1)	2	1	2	9
Liverpool (1)	4	1	1	1

fabrics (hackly fabric, slickensides), depth of rooting, pedogenic carbonate deposition, soil features that satisfy a rhizome-like appearance as described by Klappa (1980), and to find evidence for physical and biological turbation. For each paleosol, one to six intervals were sampled based on the presence of carbonate morphologies that appeared to be pedogenic. The location of each paleosol sequence is described in Appendix A.

Macro- and mesoscopic paleosol features were described in the field using terminology proposed by Retallack (1988; 1990). At the outcrop scale, the vertical and lateral distribution of pedogenic carbonate was determined, noting the number of carbonate phases present. Mora et al. (1993) provided a summary of the differences between pedogenic vs. groundwater carbonates to ensure proper sampling of materials. Individual rock samples were duct-taped on the exposed surface, carefully chiseled out, and completely wrapped in tape for transport back to the lab.

Once in the lab, one or more coats of boat resin were used to preserve the sample during preparation of thin sections. For especially fragile samples, vacuum impregnation with epoxy was necessary. All hand samples were slabbed and at least one thin section was made for each of the samples. During the sawing and slabbing of the rock samples, the billets had to be recoated in order to maintain the integrity of the paleosol. Multiple thin sections of the carbonate bearing billets were made on 2 x 3" plates for analysis of mineralogy, micro-fabrics, and post-pedogenic features. A preliminary survey of carbonate phases was performed using Alizarin Red S and a mixture of Alizarin Red S stain and potassium ferricyanide to distinguish calcite and dolomite (Dickson, 1965;

1966). Thin sections were then examined by transmitted light (TL) and cathodoluminescence (CL) petrography using a Citl Cold Cathode Luminescence 8200 mk3 (CL) microscope. TL/CL were used to evaluate the carbonate paragenesis and degree of recrystallization and to guide sampling for isotopic analysis (Solomon and Walkden, 1985; Machel and Burton, 1991). A wide range of carbonate phases and morphologies (calcite/dolomite, rhizoliths/nodules, spar/microspar/micrite) were identified and all were sampled for isotopic analysis. Only the least recrystallized micritic rhizoliths were used for determination of pCO_2 concentrations (Driese and Mora, 1993).

A small dental drill mounted on a binocular microscope was used to drill microsamples of carbonate powders to be isotopically analyzed. The samples were roasted at 375° C for one hour to remove volatile organic matter. The carbonate was then reacted under a vacuum with 100% orthophosporic acid (H_3PO_4) at 25°C, using techniques based on McCrea (1950). Average sample sizes ranged from 4 to 8 mg. Calcite was reacted for 24 hours, whereas dolomite was reacted for 48, after Al-Aasm et al. (1990). Some micro-samples (0.5 to 2 mg) were measured using a Finnigan-Mat Carbo-Flo helium sparged common acid bath. Both calcite and dolomite samples were reacted in the Carbo-Flo for ~15 minutes with 100% H_3PO_4 at 120°C and then inlet into the mass spectrometer. Isotopic ratios were measured on the Finnigan-Mat Delta Plus mass spectrometer at the University of Tennessee, Knoxville. The reported values for samples obtained by the Carbo-Flo procedure were corrected to 25°C. Results are

reported in standard δ-permil notation relative to PDB. Precision for all carbon and oxygen samples was +/- 0.2 per mil. All isotopic results are listed in Appendix B.

V. Results

Isotopic analyses of pedogenic carbonate for Siluro-Devonian paleosols provides an opportunity to evaluate the preservation potential of primary isotope compositions in these ancient paleosols. Ideally, $\delta^{13}C$ values of coeval pedogenic carbonates should be similar. However, given similar physical constraints, the results presented here indicate that there is a wide range of isotope compositions in the different Silurian and (to a lesser extent) Devonian paleosols (Figs. 13 and 14). Any individual paleosol sequence will have less $\delta^{13}C$ variation. Tables 2 and 3 contain a summary of carbonate and matrix micromorphologies. Results for each locality are discussed below.

Of the six Bloomsburg outcrops sampled in this study, the principle carbonate mineralogy for three of the paleosols (Port Jervis, Harrisburg, and Wurtsboro) was dolomite. These outcrops had consistently more negative $\delta^{13}C$ and more positive $\delta^{18}O$ values than the paleosols (Lehigh Gap, Port Clinton, and Danville) that had calcite as the principle carbonate mineral. The four Catskill paleosols [Powys (Sherman Creek Member), Trout Run (Duncannon Member), Newport (Duncannon Member), and Liverpool (Duncannon Member)] exhibit far less variation in carbonate morphology and isotope composition than the Bloomsburg paleosols possibly due to similarities in pedogenic processes or because they share similar temperature and fluid histories.

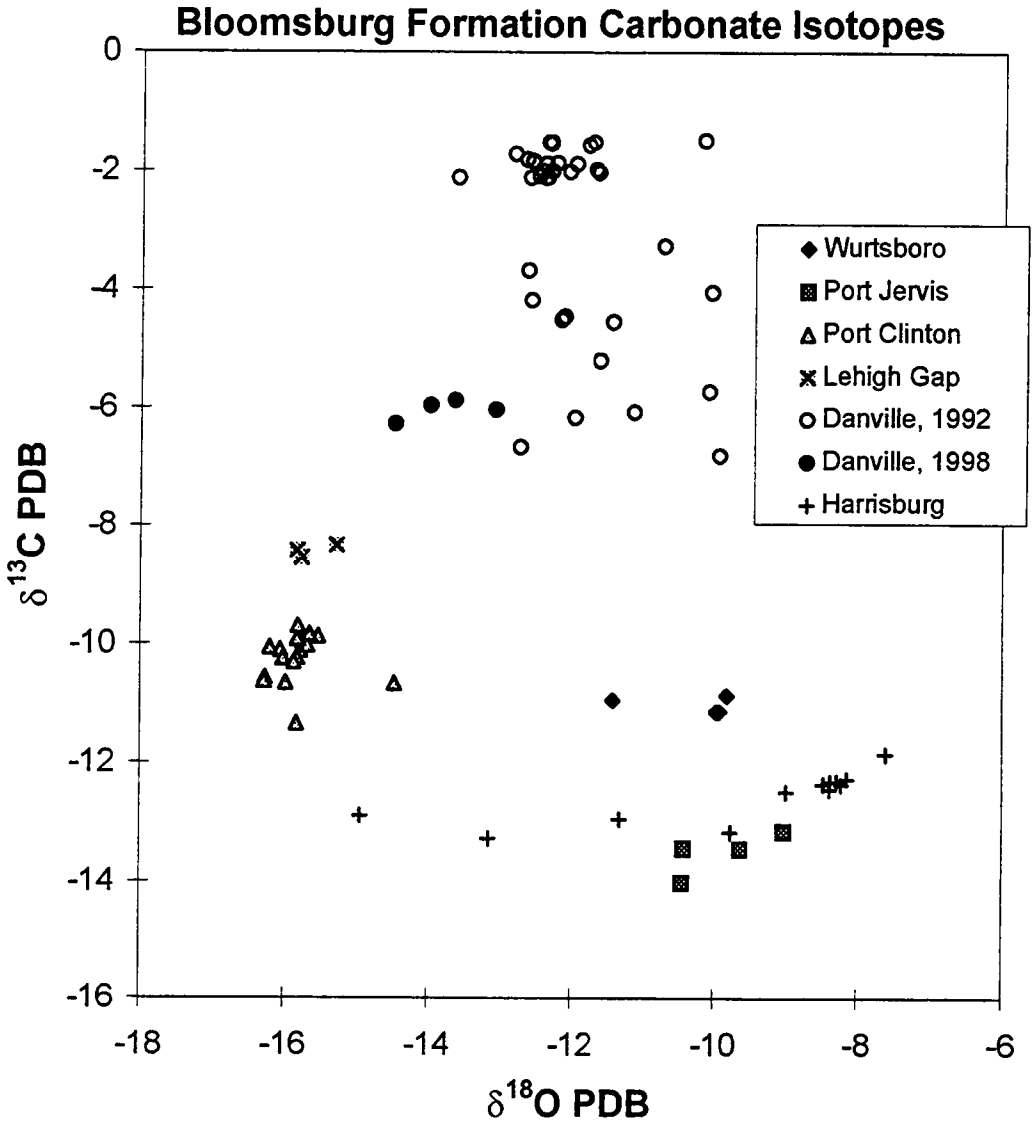

Figure 13. Bloomsburg (Upper Silurian) Formation stable isotope compositions from various localities in Pennsylvania and New York. The isotope values fall into three groups; (1) low $\delta^{13}C$, high $\delta^{18}O$ of dolomite bearing paleosols (Wurtsboro, Port Jervis, and Harrisburg), (2) low $\delta^{13}C$, low $\delta^{18}O$ of paleosols located along the Blue Mountain Structural Front (Port Clinton and Lehigh Gap), and (3) high and variable $\delta^{13}C$, variable $\delta^{18}O$ of the Danville paleosol.

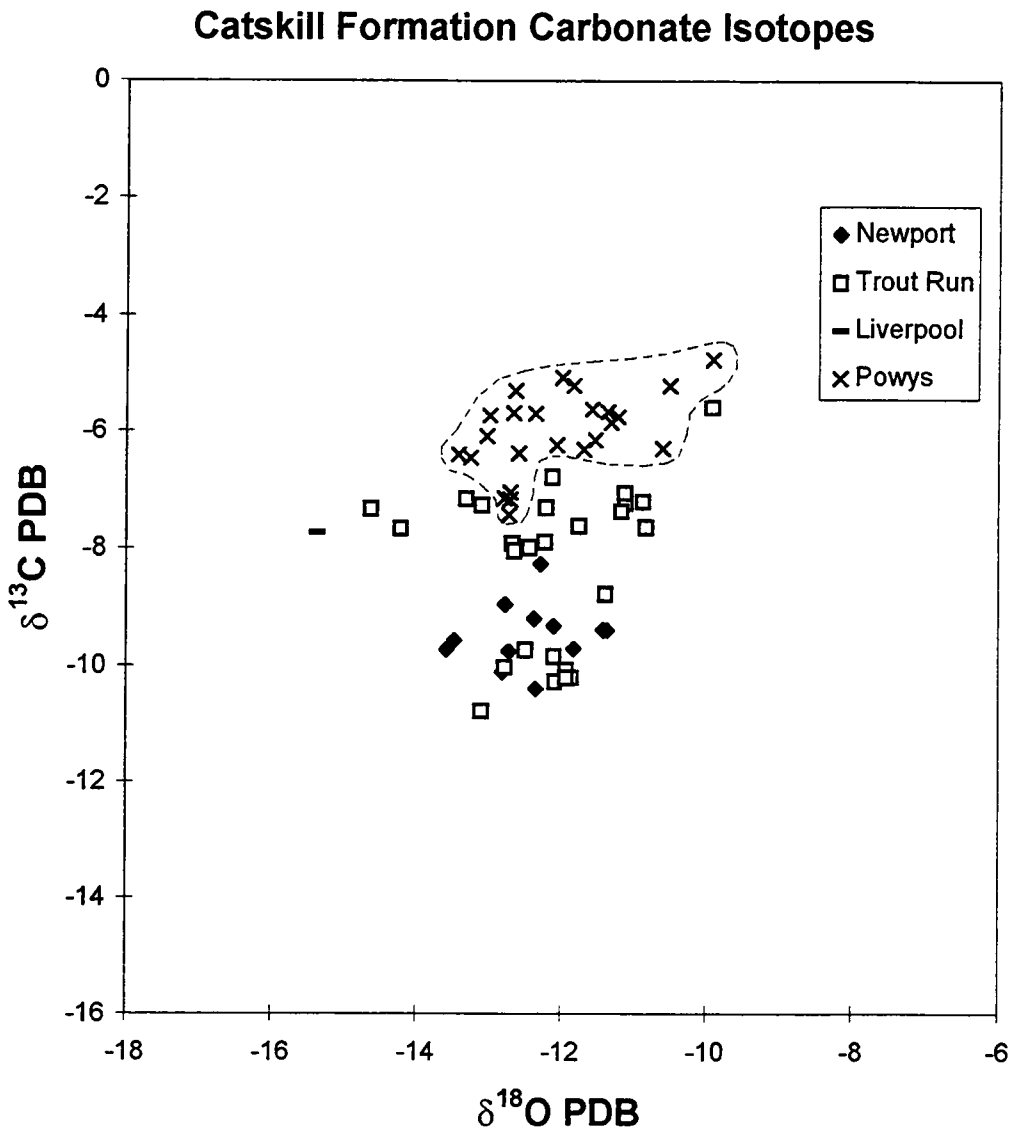

Figure 14. Catskill (Upper Devonian) Formation stable isotope compositions from various localities in Pennsylvania. The Powys paleosol represents the Sherman Creek Member and have the least negative $\delta^{13}C$ values (inside the dotted boundary). The Newport, Trout Run, and Liverpool paleosols represent the overlying, Duncannon Member and have more negative $\delta^{13}C$ values.

Table 2. Summary of carbonate and matrix morphologies for Bloomsburg paleosols.

Location and principal carbonate	Paleosol Matrix	Rhizoliths	Nodules	Other	CL
Wurtsboro (Dolomite)	Muddy siltstone to silty sandstone	None	Sparse, ferroan dolomite microspar nodules with some planar-e baroque spar	Contained quartz sand up to 1 mm diameter; carbonate very similar to Harrisburg	Bright red-orange
Port Jervis (Dolomite)	Muddy to sandy siltstone	None	Sparse, nodules consisting entirely of ferroan, non-baroque dolomite microspar	Most homogeneous carbonate morphology of dolomite-bearing paleosols	Bright red-orange
Harrisburg (Dolomite)	Muddy siltstone	Abundant, filamentous microspar and spar rhizome-like features	Sparse, ferroan dolomite micrite and microspar as ~1 cm nodules with some planar-e baroque spar in nodules	Contained dolomite filled veins that crosscut the paleosol; and abundant micro-fractures oriented 30° to the horizon; carbonate very similar to Wurtsboro	Very dull orange
Lehigh Gap (Dolomite and calcite spar)	Muddy siltstone	Sparse, filamentous, and orthogonal to bedding; ferroan, non-baroque dolomite microspar with calcite spar at center of rhizolith	Abundant, composed of a mixture of ferroan, non-baroque dolomite microspar and calcite spar, horizontally elongated in most cases (1 X 2 cm)	Contains many silty interlayers reminiscent of foliation and banding; one case of a ferroan Calcite vein, formed parallel to interlayers	Red-orange
Port Clinton (Calcite)	Mudstone to silty mudstone	Abundant, filamentous microspar and spar	Abundant, amorphous dense micrite, micrite, and microspar nucleating in proximity to or around rhizome-like feature (1 X 2 cm)	Carbonate morphologies most similar to Danville	Yellow to reddish-orange
Danville (Calcite)	Mudstone to silty mudstone	Abundant, filamentous microspar and spar	Sparse, amorphous microspar and spar nucleating in proximity to or around rhizome-like feature (1 X 2 cm)	Carbonate morphologies most similar to Port Clinton	Non lumin-escent

Table 3. Summary of carbonate and matrix morphologies for Catskill paleosols.

Location and principal carbonate	Paleosol Matrix	Rhizoliths	Nodules	Other	Lumin-escence under CL
Powys (Calcite)	Mudstone to silty mudstone	Mostly small diameter (<2 cm) rhizoliths consisting of three distinct concentric carbonate zones	Homogeneous carbonate; Larger nodules consist of microspar whereas micronodules (<2 mm) consist of micrite	Amorphous brecciated micrite present in silty interlayers	Orange to reddish-orange
Trout Run (Calcite)	Mudstone to silty mudstone	Mostly large diameter (2 to 5 cm) rhizoliths present consisting of three distinct concentric carbonate zones	Homogeneous microspar carbonate; very abundant and dense near root and stump casts described in Driese et al. (1997)	"Rosette" microspar morphology (see Figure 38)	Bright yellowish -orange
Liverpool (Calcite)	Mudstone	None	Argillaceous micrite with septarian Fe-calcite sparry infills. Micrite exhibits radial, fibrous fabric	Clay layers (~0.1 mm), aligned parallel to bedding exhibit varying degrees of iron-oxide staining	Dull, orange lumin-escence

BLOOMSBURG FORMATION

Wurtsboro and Port Jervis

In southeastern New York, near the Pennsylvania and New Jersey border, the Bloomsburg Formation consists of the upper Basher Kill Tongue and lower Wurtsboro Tongue, separated by the Ellenville Tongue of the Shawangunk Formation (Epstein, 1993). Outcrops at Port Jervis and Wurtsboro are both part of the Wurtsboro Tongue. The Wurtsboro Tongue is about 70 m thick at Port Jervis and about 35 m thick at the type section near Wurtsboro (Epstein, 1993). The proximity of the Wurtsboro and Port Jervis localities suggests that they had similar depositional environments and diagenetic histories. Compared to the other Bloomsburg paleosols examined, the Wurtsboro and Port Jervis paleosols are more proximal to the terrigenous source area and are much coarser grained. Prave et al. (1989) identified 45 fining-upward sequences at Port Jervis and 41 at Wurtsboro. The two sections are very similar with respect to paleosol thickness and the ratio of fine to coarse lithologies. The type section at Wurtsboro consists of interbedded red, green, and gray, cross-bedded polymictic conglomerate, sandstone, siltstone, and shale with fining-upward sequences as thick as 3.7 m. Polymictic conglomerates are more prevalent at the Wurtsboro locality than at the Port Jervis outcrop. Siltstone-shale interbeds were found to be more prevalent lower in the outcrops and contained mudcracks, burrows and ripples, and the nodules were reported to be composed of siderite (Epstein, 1993). The depositional environment for the New York paleosols are inferred to be one of a high-energy alluvial plain.

The entire exposed Wurtsboro type section was recorded by Driese and Mora in 1995 (Fig. 15), with special consideration to 6 paleosol sequences. Only sequences 1 and 6 were carbonate bearing (Fig. 16 and 17) with the carbonate consisting of dolomite. Paleosol 1 contains carbonate nodules associated with slickensides in the top 20 cm of the paleosol sequence. Paleosol 6 contained dolomite at the 10 and 20 cm intervals below the top of the paleosol sequence. Relict stratification and burrows were common below the slickenside zones.

The carbonate micromorphology of the Wurtsboro paleosol consists primarily of ferroan dolomite microspar (Fig. 18). Although nodules are distinct at outcrop scale, most carbonate occurs as an amorphous matrix cement with some elongate planar-e baroque spar infills. The matrix is the most coarse grained of the three paleosols that have dolomite as the principle carbonate. Overall micromorphology is most similar to the Harrisburg paleosol. Wurtsboro carbonates exhibit relatively constrained carbon ($\delta^{13}C$ = -11‰ PDB) and variable oxygen ($\delta^{18}O$ = -10 to -12‰ PDB) values.

Three stratigraphic intervals were measured at Port Jervis by Driese and Mora in 1995. The stratigraphically highest paleosol 3 was the only sequence to yield carbonate (Fig. 19). Burrows and dolomite concretions were abundant throughout the entire 70 cm interval in addition to gley reduction along the burrows. Dolomite concretions were especially dense between 40 and 50 cm depth where one of the two samples was taken. A second sample was taken between the 20 and 30 cm depth.

The carbonate micromorphology of the Port Jervis paleosol consists entirely of ferroan dolomite microspar (Fig. 18). Although nodules are distinct at outcrop scale,

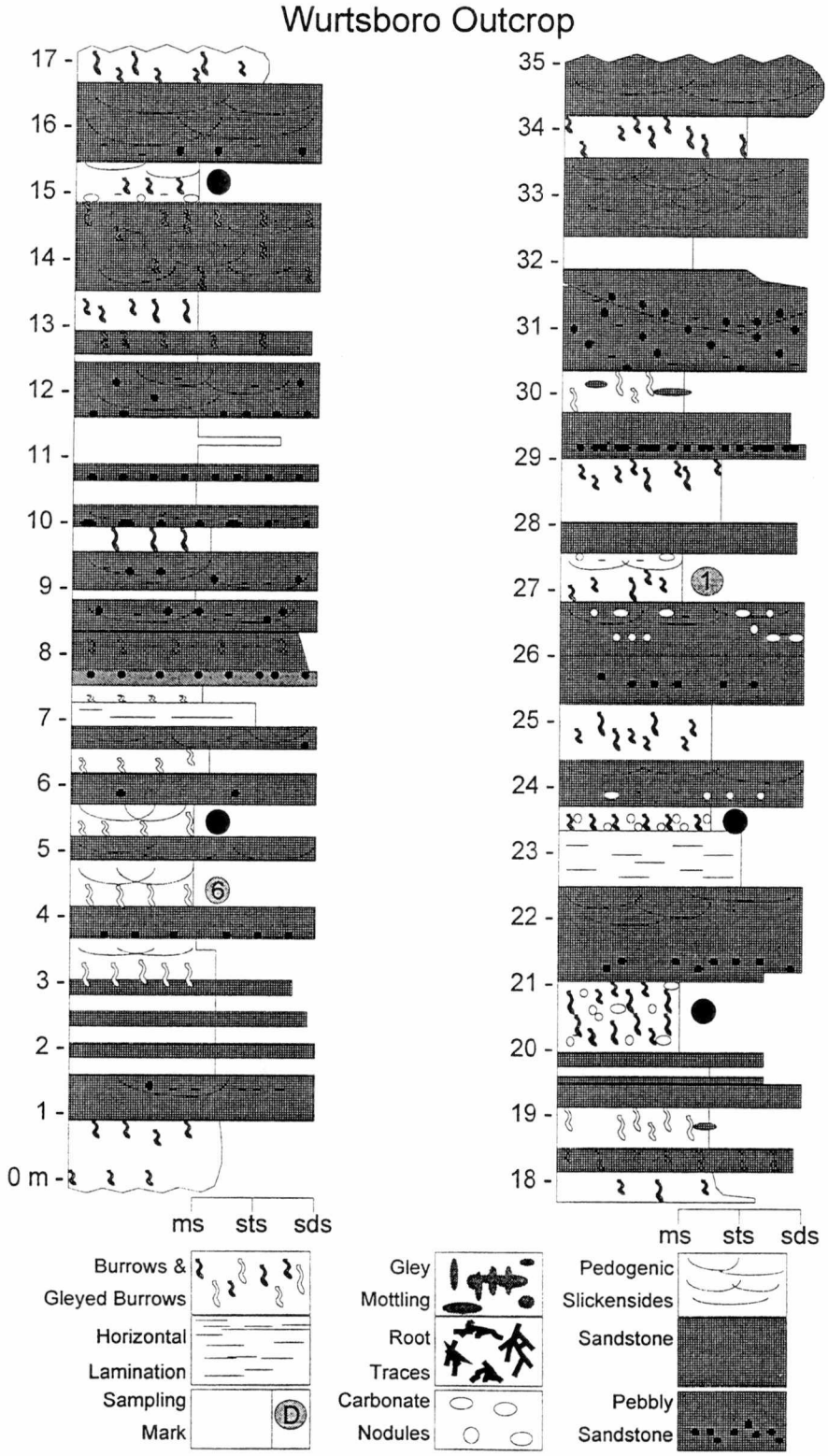

Figure 15. Schematic profile of the Wurtsboro, NY outcrop including the location of two carbonate-bearing paleosols. These palesosols (numbered circles) were sampled and described in more detail (see Figure 16 and 17). Four other sampled sequences were not carbonate-bearing (black dots).

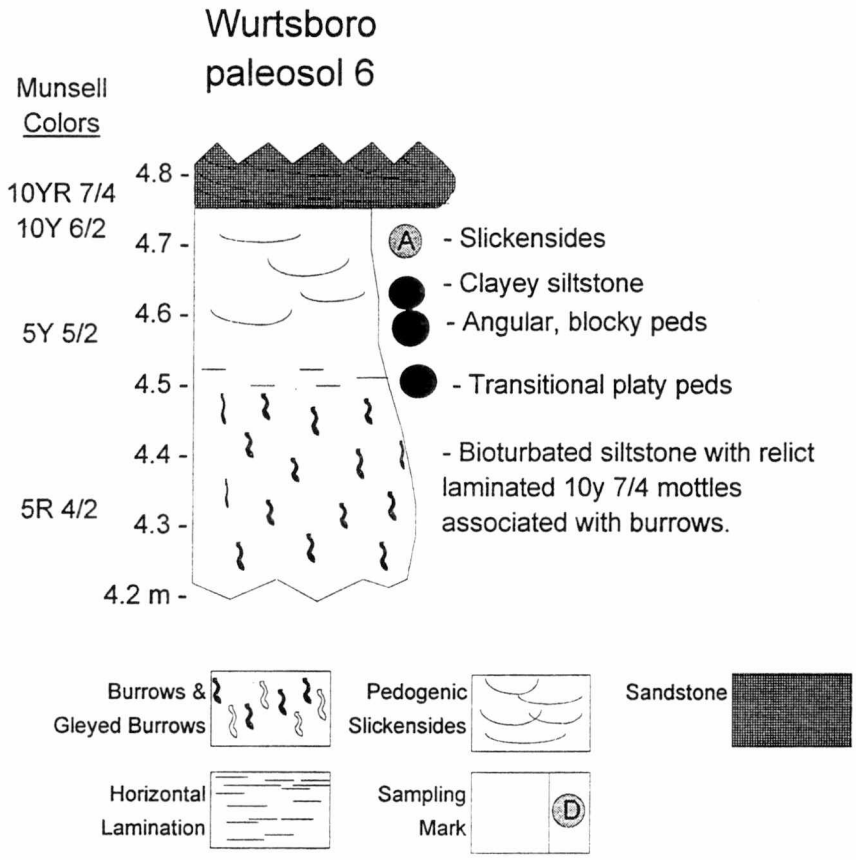

Figure 16. Schematic profile of the carbonate-bearing Wurtsboro, NY paleosol 6 including sample locations. One sample (95-BL-5-6A) contained carbonate. Three other samples were not carbonate-bearing (black dots). The depth intervals correspond to the outcrop measurements (see Figure 15).

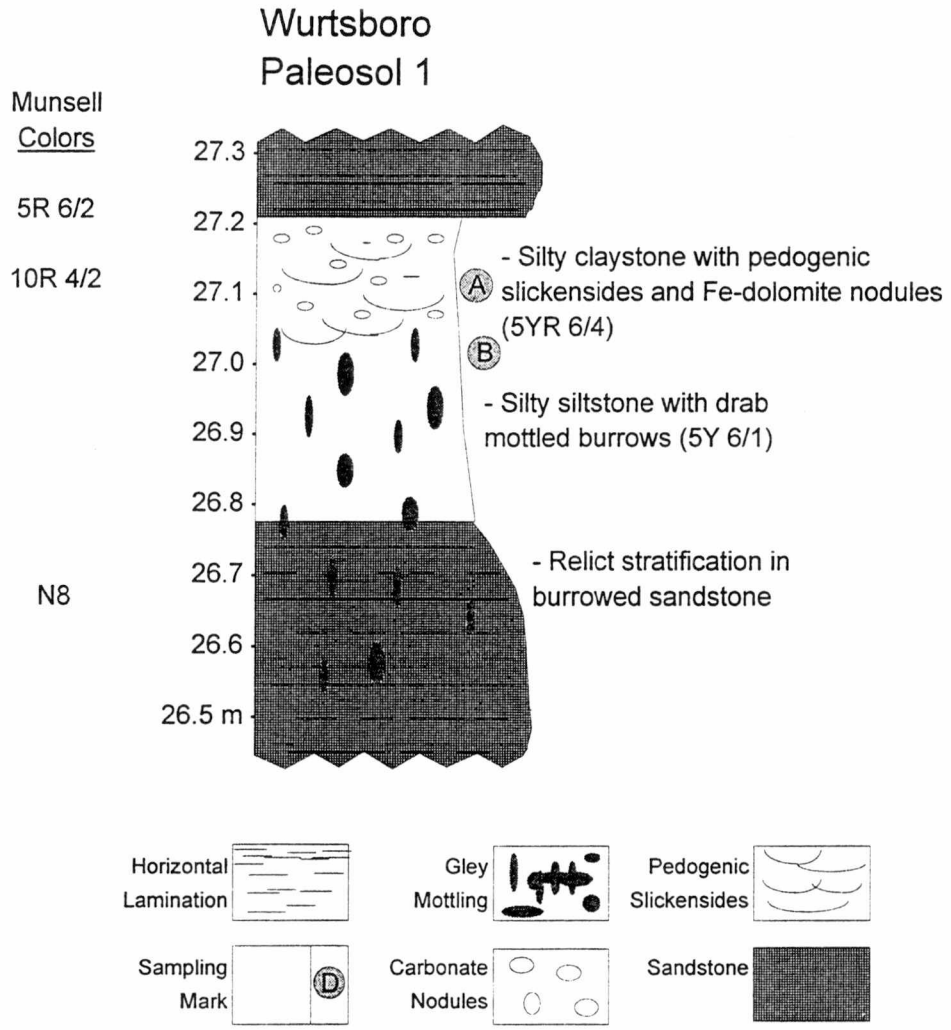

Figure 17. Schematic profile of the carbonate-bearing Wurtsboro, NY paleosol 1 including sample locations. (see Figure 15) Both samples contained carbonate (95-BL-5-1A and 95-BL-5-1B). The depth intervals correspond to the outcrop measurements.

Figure 18. Photomicrographs of Wurtsboro, NY, Port Jervis, NY, and Harrisburg, PA paleosols carbonate morphologies. (a) Wurtsboro (95-BL-5-1B) ferroan, non-baroque dolo-microspar (TL) intergrown with the matrix material (carbonate sample 62-A). (b) Same field of view as (a) under CL has a uniform, very bright red-orange luminescence (luminescence also representative of Port Jervis). (c) Port Jervis (95-BL-4-4B) ferroan, non-baroque dolo-microspar under TL (carbonate sample 72-A). The right portion of the slide has been treated with a mixed Alizarin Red S and potassium ferricyanide stain. The left-hand portion is untreated. (d) Harrisburg (95-BL-1-1) carbonate composed of a typical ferroan, non-baroque dolo-microspar (ms) nodule (carbonate sample H1-C) on the left (TL) with several light patches of spar (carbonate sample H1-D). A cross cutting vein (v) is filled with baroque, planar-e dolo-spar (carbonate sample H1-B). The microspar nodule (ms) on the right (carbonate sample H1-A) has undergone post-pedogenic alteration in conjunction with the vein precipitation.

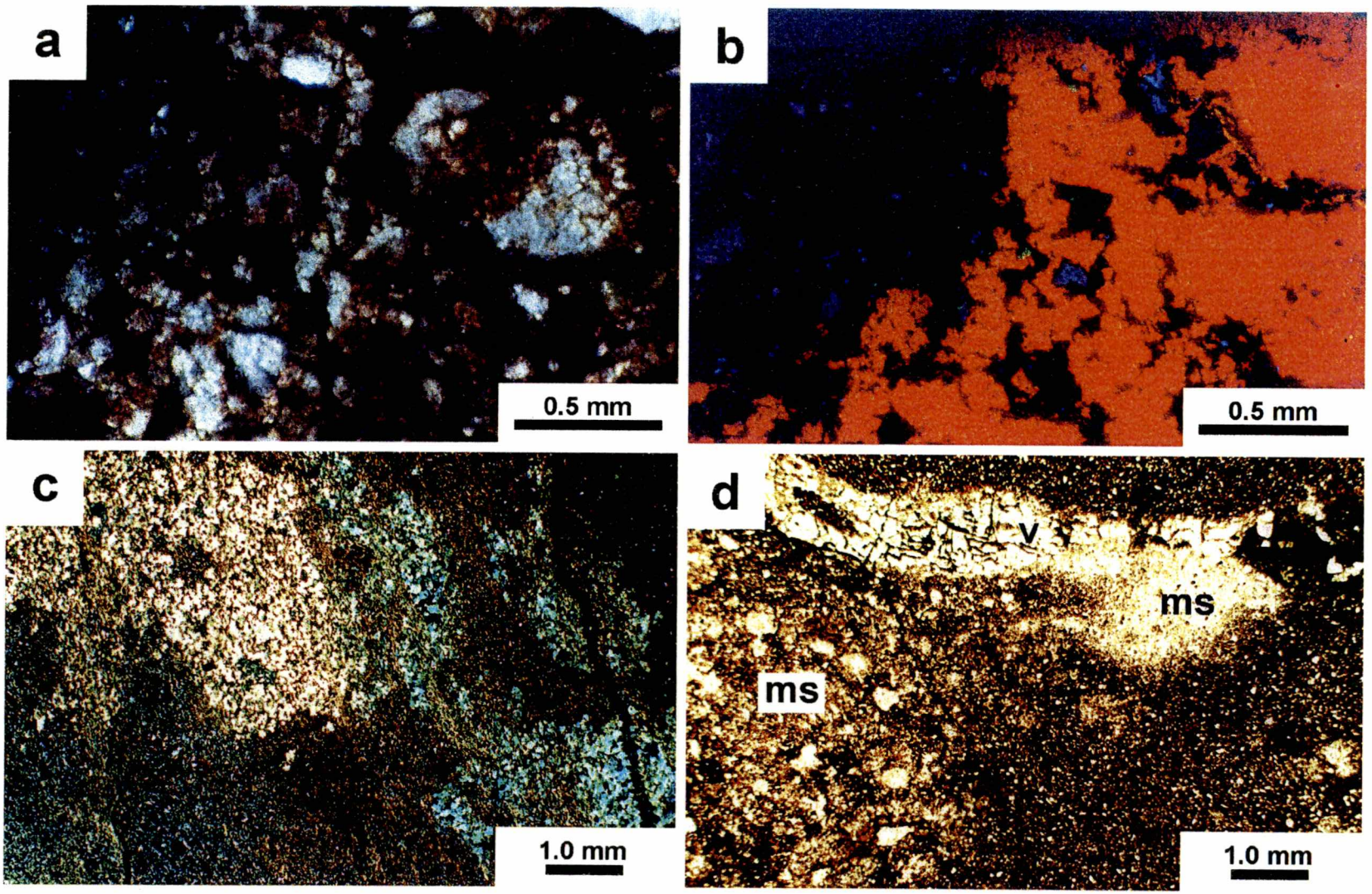
a
0.5 mm
b
0.5 mm
c
1.0 mm
d
v
ms
ms
1.0 mm

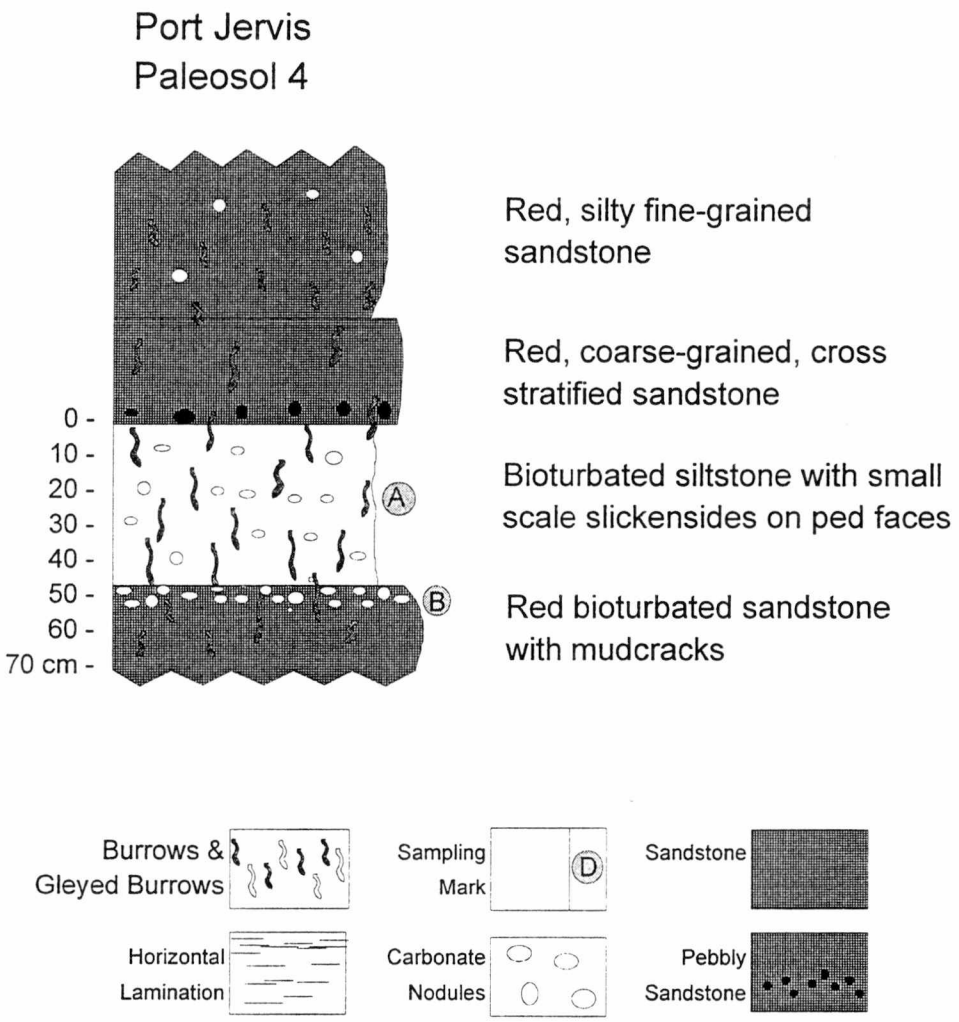

Figure 19. Schematic profile of the carbonate-bearing Port Jervis, NY paleosol including sample locations. Gley reduction mottles of burrows were present throughout the entire sequence. Both samples were conatined carbonate (95-BL-5-4A and 95-BL-5-4B).

most carbonate occurs as an amorphous matrix cement. The carbonate morphology is the most homogeneous of all the paleosols studied. The $\delta^{13}C$ values are slightly more negative (-13 to -14‰ PDB) and $\delta^{18}O$ values more positive (-9 to -11‰ PDB) compared to Wurtsboro.

Harrisburg

The Harrisburg paleosol, locate just north of Harrisburg PA, is exposed at Blue Mountain. At this location, the Bloomsburg Formation is a claystone, siltstone, to fine-grained sandstone sequence with a thickness of approximately 330 meters (Hoskins, 1961). The sandstones are sometimes cross-bedded and the claystones weather into small chips. Each paleosol is typically 0.8 to 3.1 meters thick and is composed primarily of siltstone containing red-orange filamentous carbonate. Marine body fossils (ostracods and lingulids) are present intermittently within the outcrop section. The depositional environment is interpreted to have been marginal marine.

The stratigraphically lowest paleosol was analyzed in the field by Driese and Mora in 1995 (Fig. 20). The upper 40 cm consists of gleyed gray-green siltstone. A mottled contact occurs at 40 cm and sparse filamentous carbonate is found between 50 to 90 cm. Beneath the carbonate is ~1 meter of bioturbated red siltstone with hackly weathering, grading downward into a fine to very-fine grained sandstone containing gley bands.

The carbonate micromorphology of the Harrisburg paleosol consists primarily of ferroan, dolo- micrite and microspar (Fig. 18). Most carbonate occurs as (~1 cm) nodules with some elongate planar-e baroque sparry infills, or as dense, filamentous

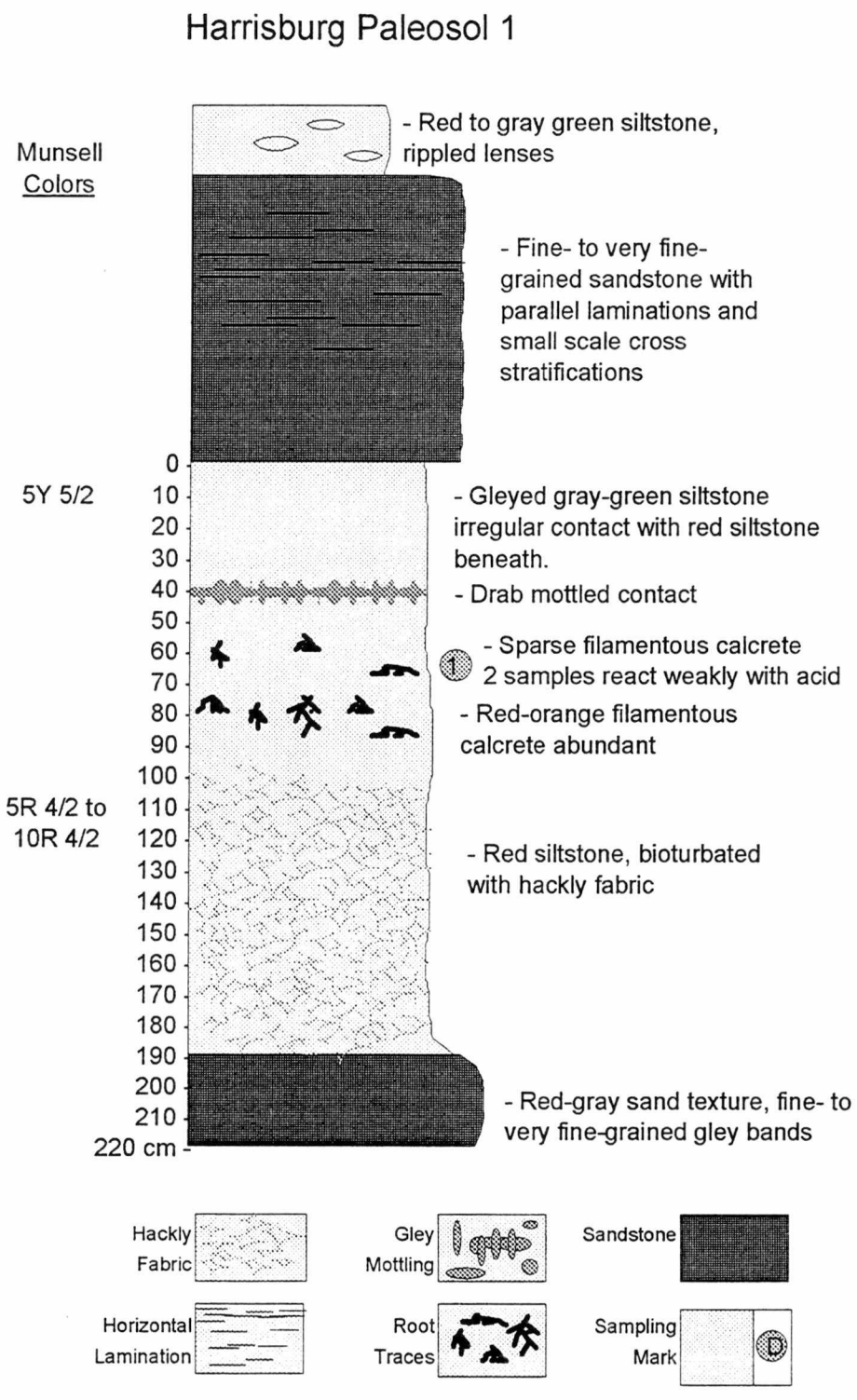

Figure 20. Schematic profile of the carbonate-bearing Harrisburg, PA paleosol including sample location. (Sample 95-BL-1-1)

rhizome-like features. Several veins within the paleosol are occluded with baroque, planar-e dolomite cement. These veins, in addition to abundant microfractures, tend to cross-cut the nodule and rhizolith morphologies at ~30° relative to bedding. The matrix is the most fine-grained of the three paleosols that have dolomite as the principle carbonate. Overall carbonate micromorphology is most similar to the Wurtsboro paleosol. The isotopic values for Harrisburg fall between those of Port Jervis and Wurtsboro ($\delta^{13}C$ = -12 to -13‰ PDB; $\delta^{18}O$ = -8 to -15‰ PDB).

Lehigh Gap

The Lehigh Gap outcrop of the Bloomsburg Formation is located just south of Palmerton, PA exposed at Blue Mountain. Dolomitic concretions and fining-upward sedimentary cycles at Lehigh Gap were first noted by Epstein et al. (1974). Retallack (1985) was the first to describe paleosols at Lehigh Gap where the total thickness of the Bloomsburg Formation is thought to be approximately 460 meters (Epstein et al., 1974). More than 50 fining-upward sequences are found at Lehigh Gap, averaging one to four meters in thickness, in addition to small-scale channels, shale intraclasts, cross-bedding, mudcracks, ripples, bioturbation, and sandstone channel-fills deposited by meandering streams (Gillmeister and Springer, 1990, Epstein et al., 1974).

Paleosol 4 was measured by Mora and King in 1996 and is located approximately 3 meters stratigraphically above paleosol 2 of Retallack (1985). It consists primarily of siltstone and contains many large burrows and bioturbated features in the upper 70 cm (Fig. 21). Calcrete nodules are abundant between 80 and 120 cm depth, in a silty matrix that has retained some relict bedding features.

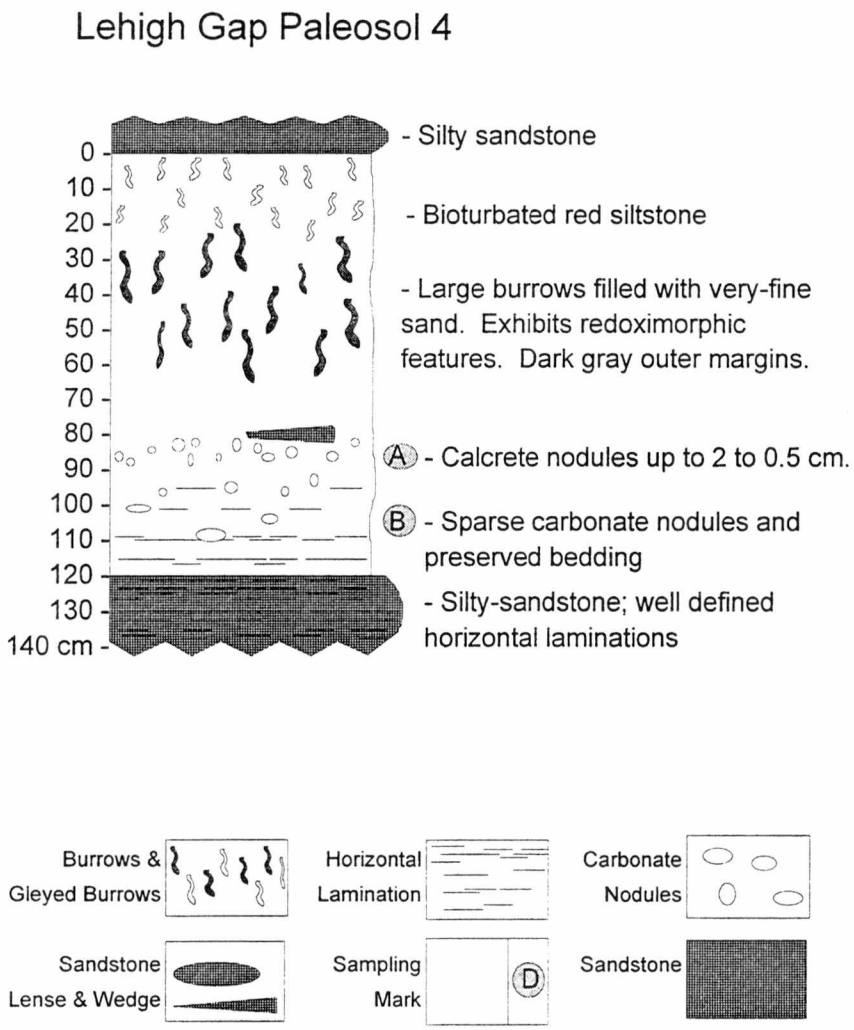

Figure 21. Schematic profile of the carbonate-bearing Lehigh Gap, PA paleosol including sample locations. Paleosol located stratigraphically 3 meters above Retallack's (1985) Paleosol 2. Both samples conatined carbonate, but sample (96-BL-LG-4-) B was not isotopically analyzed. Sample (96-BL-LG-4-) A was isotopically analyzed.

The carbonate micro-morphology at Lehigh Gap consists of a mixture of ferroan, non-baroque dolomite microspar and calcite spar (Fig. 22). Rhizolith morphologies are consist of sparse, filamentous strands, oriented perpendicular to bedding. Typically, the rhizolith are occluded with calcite spar, with ferroan, non-baroque dolomite microspar, lining the outside margins. Nodules also consist of a mixture of ferroan, non-baroque dolomite microspar and calcite spar, but are elongated and aligned horizontal to bedding (1 X 2 cm). In one sample, a ferroan calcite vein is present and aligned parallel to bedding. Silty interlayers (present throughout the paleosol matrix) oriented parallel to bedding were unique to this paleosol and reminiscent of metamorphic foliation and banding. The stable isotope compositions of all morphologies are fairly constant for both carbon ($\delta^{13}C$ = -8 to -9‰ PDB) and oxygen ($\delta^{18}O$ = -15 to -16‰ PDB).

Port Clinton

The Port Clinton paleosols of the Bloomsburg Formation is exposed at the Schuylkill Water Gap at the northern town line of Port Clinton, PA (Fig. 23) at Blue Mountain, west of Lehigh Gap. The thickness of the Bloomsburg Formation here is approximately 260 meters according to Smith (1968). At least 10 fining-upward sequences were described by Smith (1968) as consisting of a basal erosional surface, overlain by a coarse basal deposit, then a sequence of thinly interlaminated greenish-olive shales and sandstones, and finally a red, burrow-mottled argillaceous siltstone. Minor amounts of marine fossils were also described in Strother (1988) and Giffin (1979). Clay content, carbonate, and soil features become more prevalent up section, whereas burrows

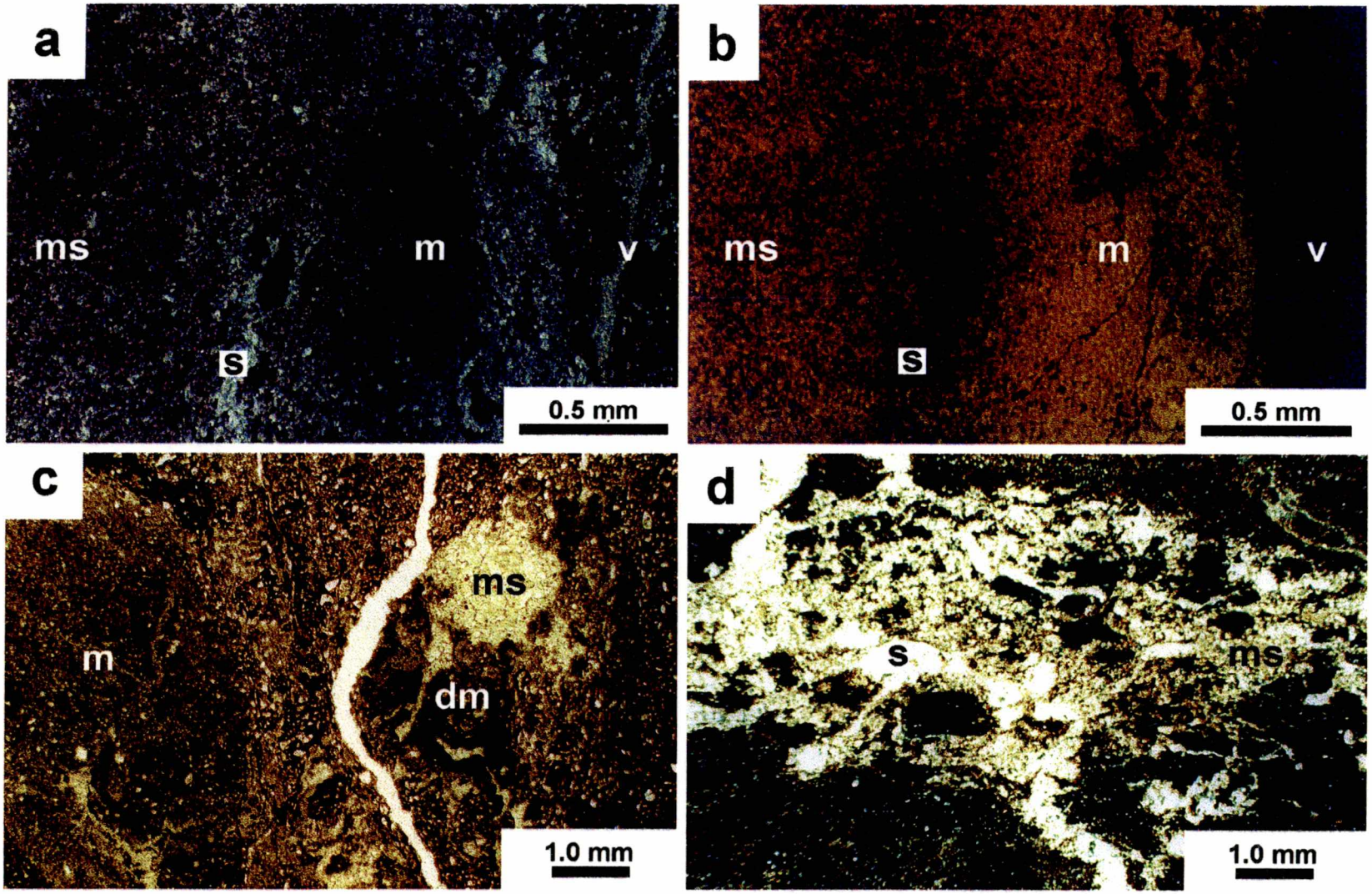
a
ms
m
v
s
0.5 mm
b
ms
m
v
s
0.5 mm
c
ms
m
dm
1.0 mm
d
s
ms
1.0 mm

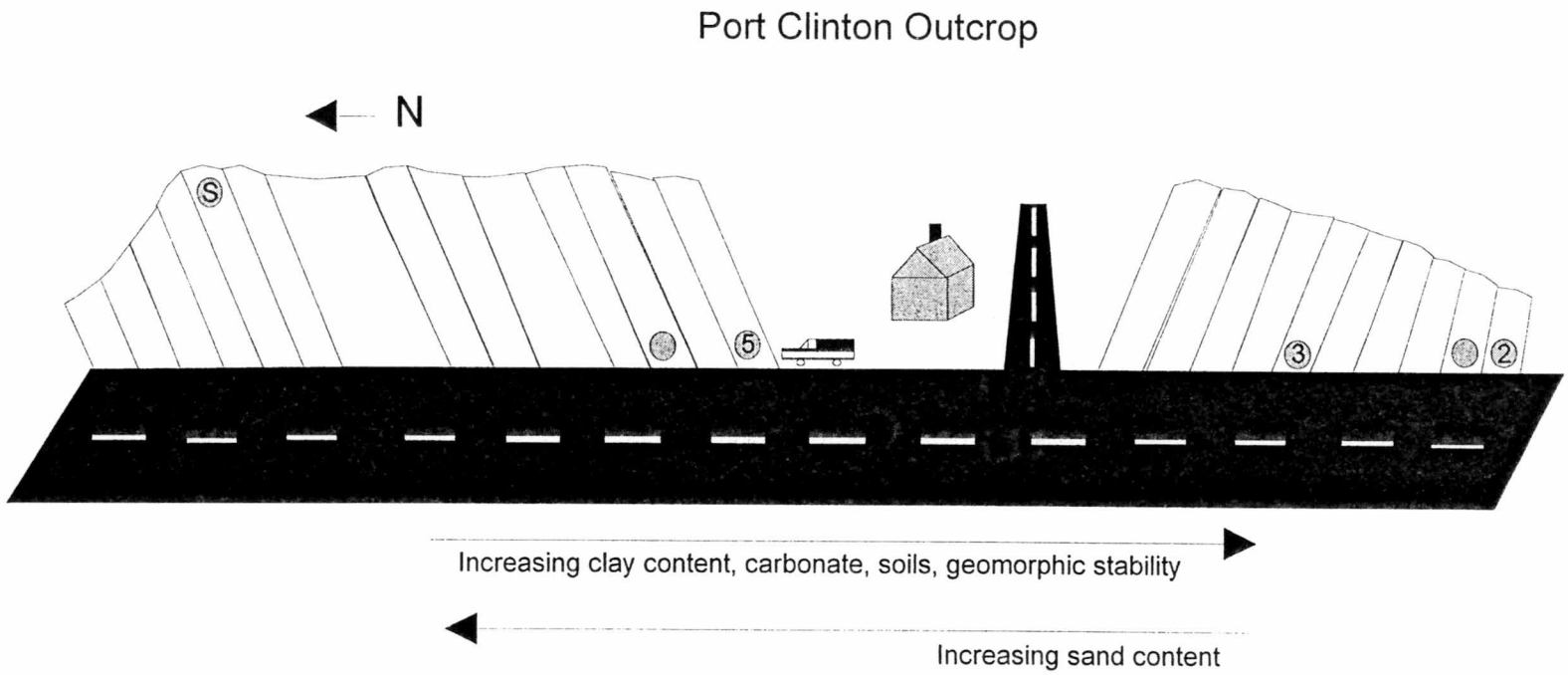

Figure 23. Schematic sketch of the Port Clinton, PA outcrop exposed along approximately one mile of highway (Route 61). Outcrop sketch includes the location of five paleosols which were sampled and described in more detail (see Figures 24 and 25) and the organic carbon rich interval (S) of Strother (1988).

and sandstone thickness decrease. The depositional environment is described as marginal marine, alternating between a tidal flat and lagoon (Smith, 1968).

All five Port Clinton paleosols contained abundant nodules, but no pedogenic slickensides or apparent carbonate rhizoliths at outcrop scale. Paleosols 1 through 4 were measured by Driese and Mora in 1995 and Paleosol 3 was reexamined by Mora and King in 1996. Paleosols 1, 2 and 4 were only outcrops measured (Figs. 24 and 25) and analyzed for carbonate isotope composition. Gley mottling is abundant throughout the paleosols. Nodules were typically located less than 50 cm below a sandstone bed or a layer that included evidence of gley mottling.

The carbonate micromorphology at Port Clinton primarily consists of dense micrite, micrite, ferroan microspar and non-ferroan spar calcite (Fig. 26). The rhizome-like morphologies are typically downward-tapering, filamentous and tubular fenestrae formed in concentrated zones very similar to the Danville locality. Larger rhizoliths are occluded with clear, equant calcite spar cement. Smaller-diameter tubules branch off from the larger fenestral pores and are typically filled with microspar and spar. Port Clinton also contains abundant nodules of approximately the same dimensions as the concentrated filamentous rhizolith zones (1 x 2 cm), which could serve as an initial nucleation surface. Other amorphous nodules of similar size are composed entirely of dense micrite and micrite. Isotopic compositions are relatively homogeneous ($\delta^{13}C$ = -9.5 to –11.5‰ PDB; $\delta^{18}O \cong$ -16‰ PDB). The Port Clinton carbonate has the most negative $\delta^{18}O$ values (similar to Lehigh Gap) of all Bloomsburg paleosol carbonates.

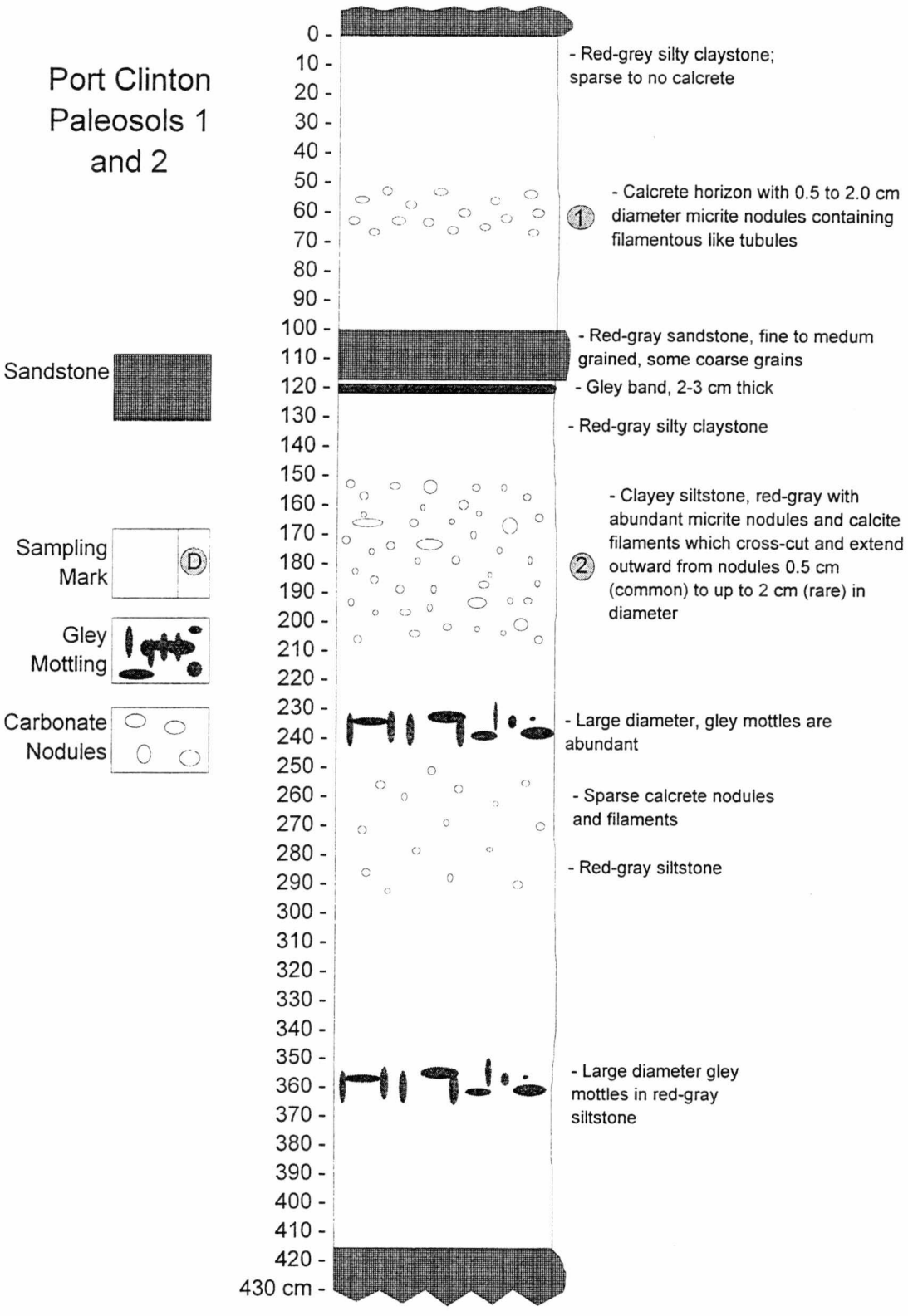

Figure 24. Schematic profile of the carbonate-bearing Port Clinton, PA paleosols 1 and 2 including sample locations. (Samples 95-BL-2-1 and 95-BL-2-2)

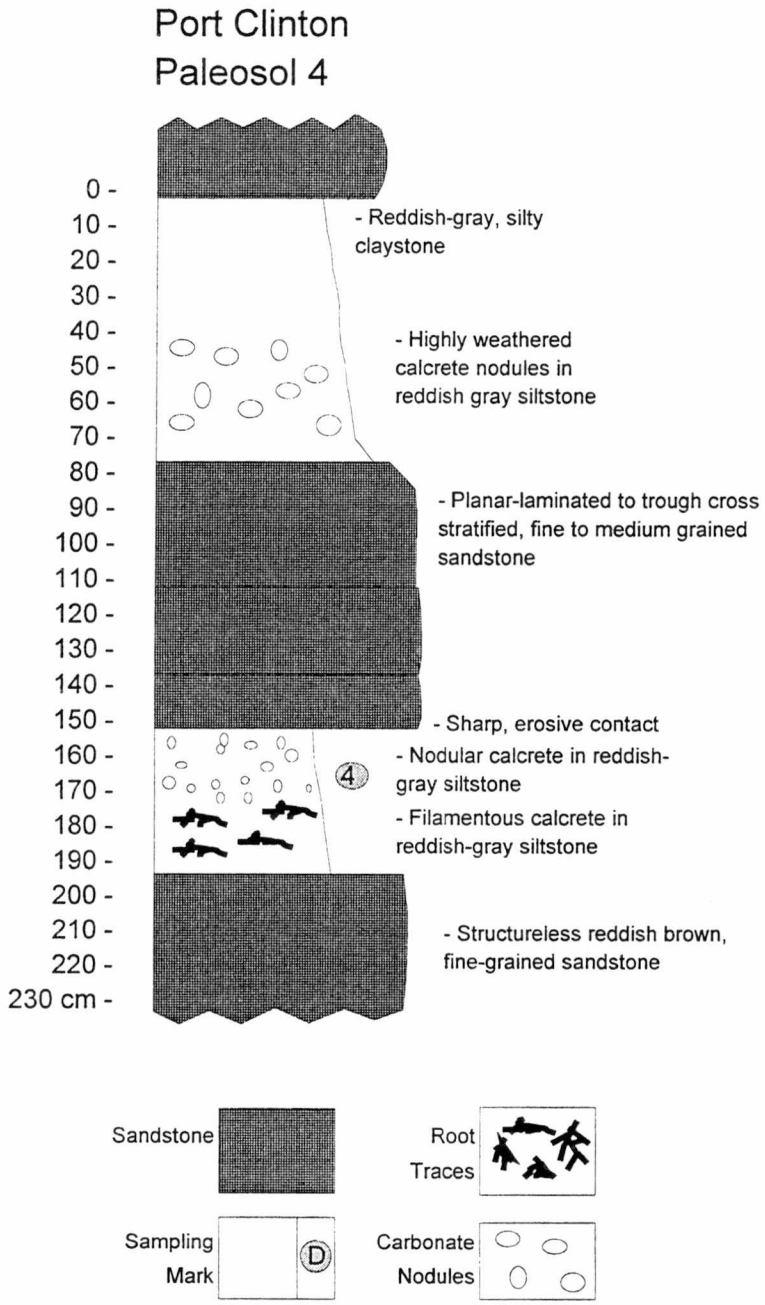

Figure 25. Schematic profile of the carbonate-bearing Port Clinton, PA paleosol 4 including sample location. (Sample 95-BL-2-4)

Figure 26. Photomicrographs of Port Clinton, PA and Danville, PA paleosols carbonate morphologies. (a) Port Clinton (95-BL-2-4) paleosol exhibiting an irregular nodule with physical morphology representing all three primary carbonate morphologies under TL: microspar (ms), micrite (m), and spar (s). A small tectonic vein (v) filled with sparry cement cross-cuts the paleosol. (b) Same field of view as (a) under CL. Each carbonate phase present has a uniform and distinct luminescence: micrite (m) is yellow-orange, microspar (ms) is reddish orange, and spar (s) is non-luminescent. (c) Port Clinton (95-BL-2-4) paleosol exhibiting three carbonate morphologies: micrite (m), dense micrite (dm), and spar (ms). (d) Danville (96-BL-DAN-A), ferroan calcite microspar (ms) with sparry occlusions (s) present in a dense filamentous, downward-tapering, tubular fenestrae under TL. Danville carbonate is non-luminescent.

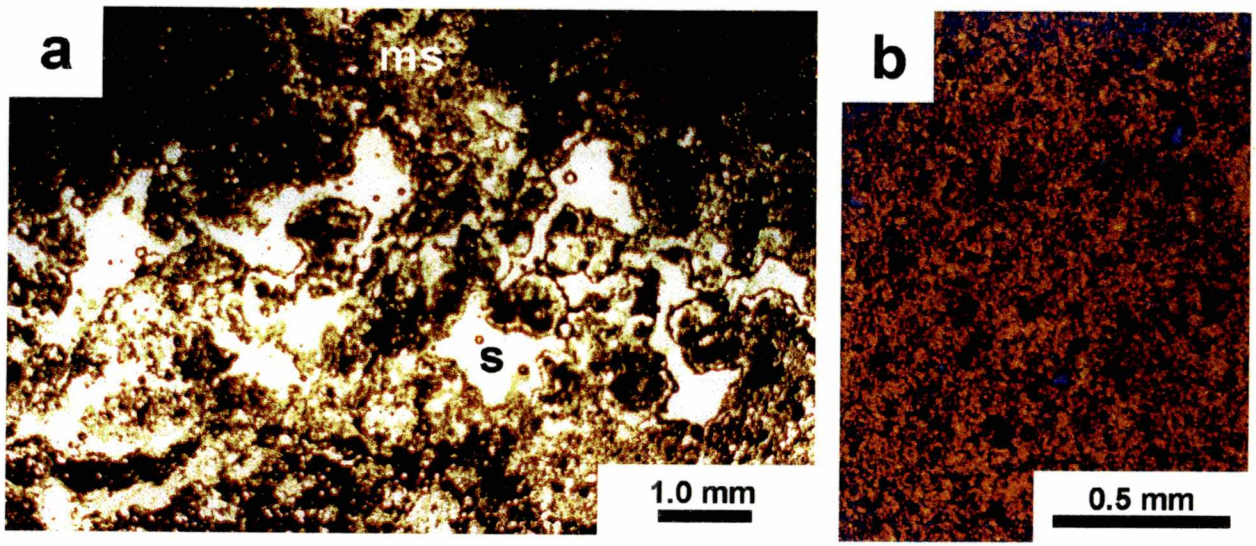

Figure 22. Photomicrographs of Lehigh Gap, PA paleosol carbonate morphologies. (a) ferroan, non-baroque dolo-microspar (96-BL-LG-4-B) exhibiting fairly distinct zonation with occluding spar cement (s) under TL. (b) Microspar (96-BL-LG-4-A, carbonate sample 89-C) has fairly uniform luminescence under CL and was the most prevalent morphology at Lehigh Gap.

Danville

This highway outcrop, located just west of Danville, PA, provides one of the best exposures of the Bloomsburg Formation. The probable thickness of the Bloomsburg at the Danville locality is approximately 150 meters (Hoskins, 1961) and is similar to the delta-plain sequence described in Sevon (1985). Twenty fining-upward cycles were defined at this nearly-complete Bloomsburg sequence (Driese et al., 1992, 1993a). The lower 100 meters consists of grayish-red silty claystone with a few olive green beds near the base; the upper contact is covered and a fault of unknown displacement cuts through the redbeds. The upper 27 m consists of interbedded, very fine-grained sandstone, siltstone, and silty claystone, stacked in fining-upward sequences. Terrestrial plant macro-fossils occur in the upper 10 meters. Pedogenic carbonate and slickenside features are abundant in the lower portion of each paleosol, whereas desiccation cracks are prevalent near the top. Evidence of marine hydromorphism, in the form of gray-green reduction, is present near the tops of several paleosols and marine layers containing open- to restricted-marine fauna. The environmental interpretation of a low-energy, delta plain system, is based upon previous work on the stratigraphically lower portion of the Danville sequence (Driese et al., 1992, 1993a).

For this study, the stratigraphically highest complete fining-upward sequence was sampled (Fig. 27). Hackly weathering and gley mottling are present in the upper 30 cm and carbonate nodules are abundant from the 30 to 40 cm depth, in association with pedogenic slickensides. Below 40 cm depth, fine rhizoliths and nodules are present, in addition to relict bedding features.

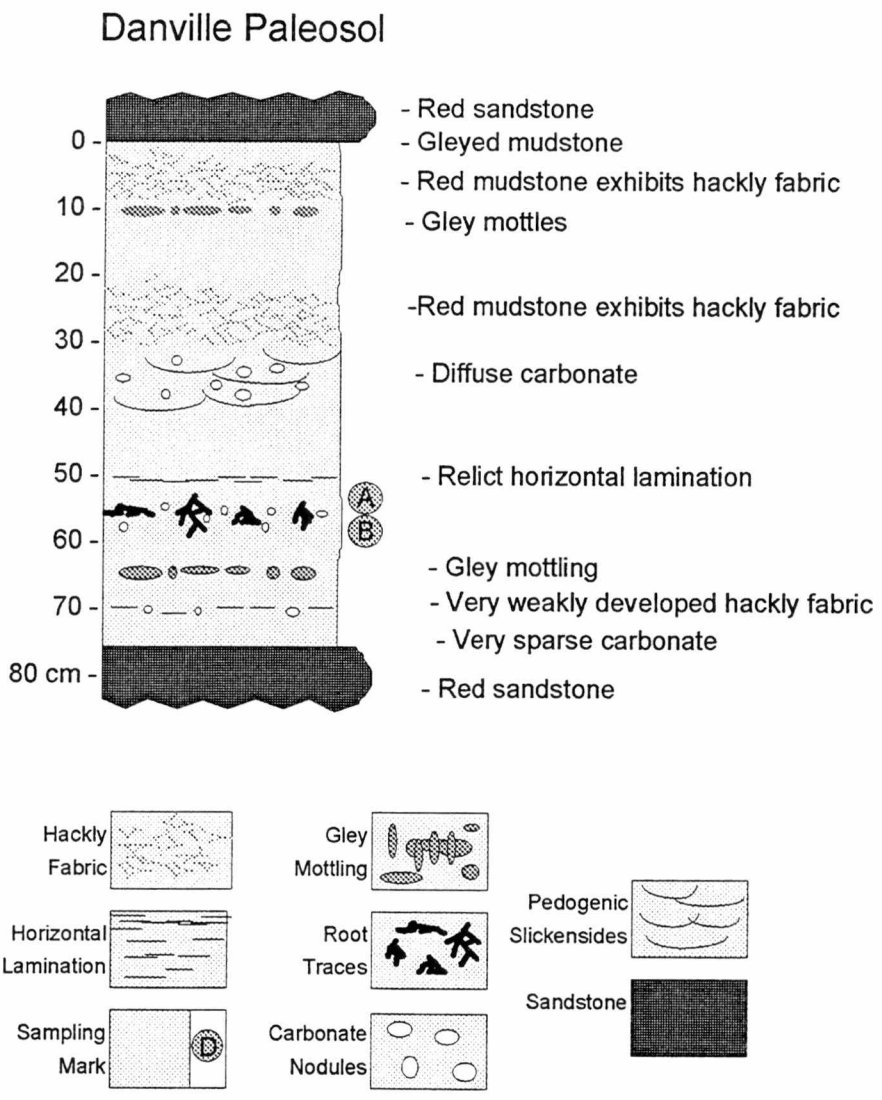

Figure 27. Schematic profile of the carbonate-bearing Danville, PA paleosol including sample locations. Both samples contained carbonate (96-BL-DAN-A and 96-BL-DAN-B).

The carbonate micromorphology at Danville primarily consists of ferroan microspar, and non-ferroan spar calcite (Fig. 26). The rhizome-like morphologies are typically downward-tapering, filamentous and tubular fenestrae formed in concentrated zones. Larger rhizoliths are occluded with clear, equant calcite spar cement. Smaller-diameter tubules branch off from the larger fenestral pores and are typically filled with microspar and spar. The $\delta^{13}C$ values for this paleosol were similar to pedogenic carbonate values reported in Driese et al. (1992; $\delta^{13}C$ = -6.0‰), with greater variation in $\delta^{18}O$ values (-13 to -14.5‰ PDB). However, most of the stratigraphically lower samples analyzed by Driese et al. (1992) demonstrate a variety of $\delta^{13}C$ values associated with marine water alteration that occur in several paleosols sequences throughout the lower 100 meters of the Bloomsburg Formation (Fig. 28).

CATSKILL FORMATION

Powys (Sherman Creek Member)

This new Catskill Formation highway exposure is located a few miles south of the Trout Run paleosols South of Powys (PA) and was measured by Mora and King in 1996 (Fig. 29). The Powys paleosols were the only representatives from the Sherman Creek Member analyzed in this study. Cotter and Driese (1998) report paleosols in stratigraphically more distal Sherman Creek exposures near Selilnsgrove, PA. The entire thickness of the Sherman Creek member in Central Pennsylvania ranges from 360 to 540 meters (Williams, 1985), much of which is exposed at the Powys locality. Sevon (1985) described the Sherman Creek Member as lower coastal alluvial plain deposits consisting

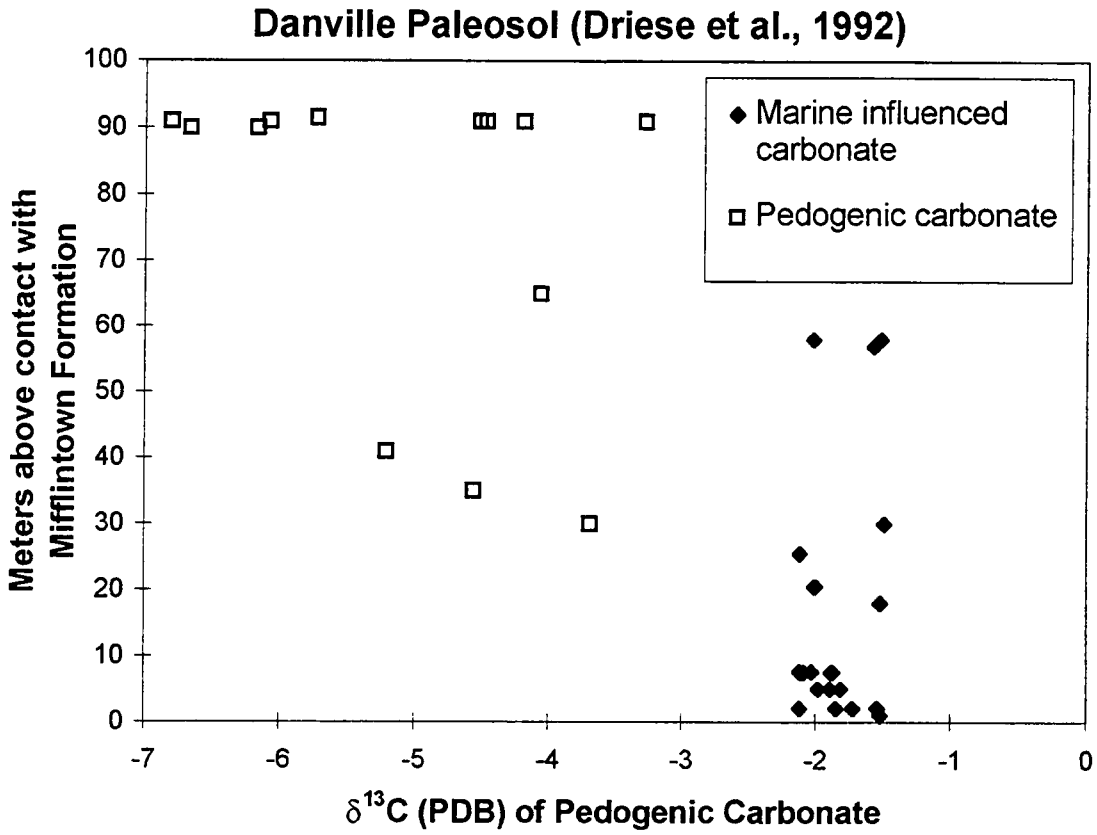

Figure 28. Danville paleosol $\delta^{13}C$ signatures with respect to stratigraphic position relative to the Mifflintown Formation contact (from Driese et al., 1992). Paleosols sampled within the first 50 meters of the contact retain a marine carbon signature with few exceptions. Ninety meters above the contact, the $\delta^{13}C$ signatures vary significanly, reflecting a more pedogenic influence.

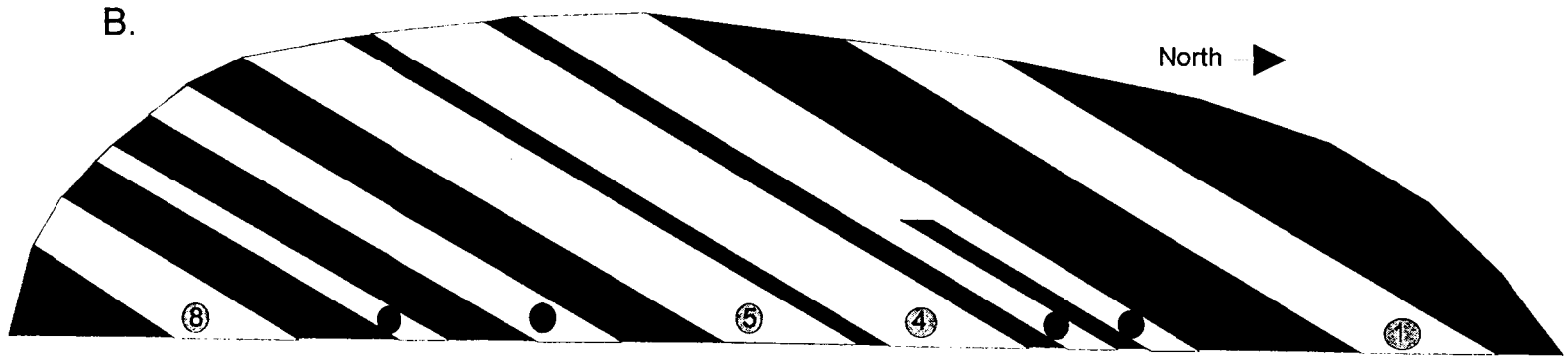

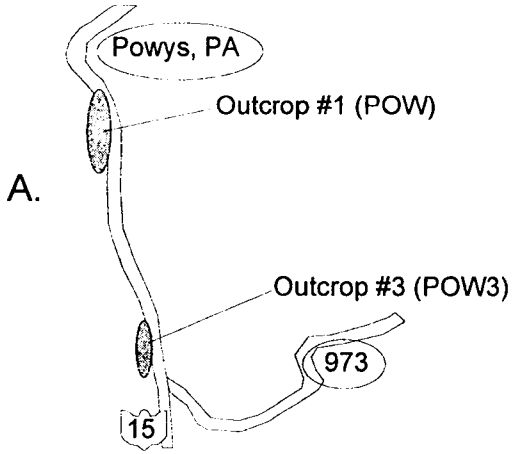

Figure 29. Schematic sketch of the Powys, PA outcrops including the location of five carbonate-bearing paleosols. (A) Powys road-cuts along Route 15. The first outcrop is approximately 1 mile south of Powys, PA. (B) Schematic sketch of the first road-cut (approximately 1 mile along Route 15) including 4 sampled paleosol sequences (numbered circles; see figures 30 to 32). Other fining-upward sequences contained very little carbonate or pedogenic features (black dots).

of mudrock-dominated fining-upward cycles a few meters thick (approximately half as thick as comparable cycles in the Duncannon Member), although the ratios of coarse- to fine-grained sequences is approximately the same (Diemer, 1992). At least 12 fining-upward paleosol sequences were present in three outcrop sections. The fining-upward sequences grade from sandstones characterized by planar cross-lamination and some horizontal stratification to red silt- and mudstones. The mudstones typically contain calcareous nodules, roots, desiccation cracks, and burrows. Most sandstone deposits are interpreted as having been deposited on point bars of shallow, sinuous rivers (Diemer, 1992). Cotter and Driese (1998) suggest that deposition of many sandstones occurred in estuarine or tidal environments based on evidence of marine incursion, trace and body fossils, and wave-rippled sandstone.

The first of three outcrops encountered traveling south on Route 15 (Fig. 29) contain numerous paleosols characterized by abundant carbonate nodules, and carbonate rhizoconcretions (similar to the morphology described in Sherman Creek Member paleosols near Selinsgrove, PA; Cotter et al., 1993; Capelle and Driese, 1995; Driese et al., in preparation). Other paleosol features observed include pedogenic slickensides, gley mottling, ripple marks, relict bedding and gley reduction mottles, and thin gley bands. Several layers of large carbonate nodules present along mudstone horizons are were interpreted as groundwater deposits. Five fining-upward sequences were sampled (Figs. 30 through 32).

Carbonate micromorphology is diverse for the Powys paleosols (Figs. 33 through 35). Usually viewed in cross section, these morphologies consist of circular carbonates

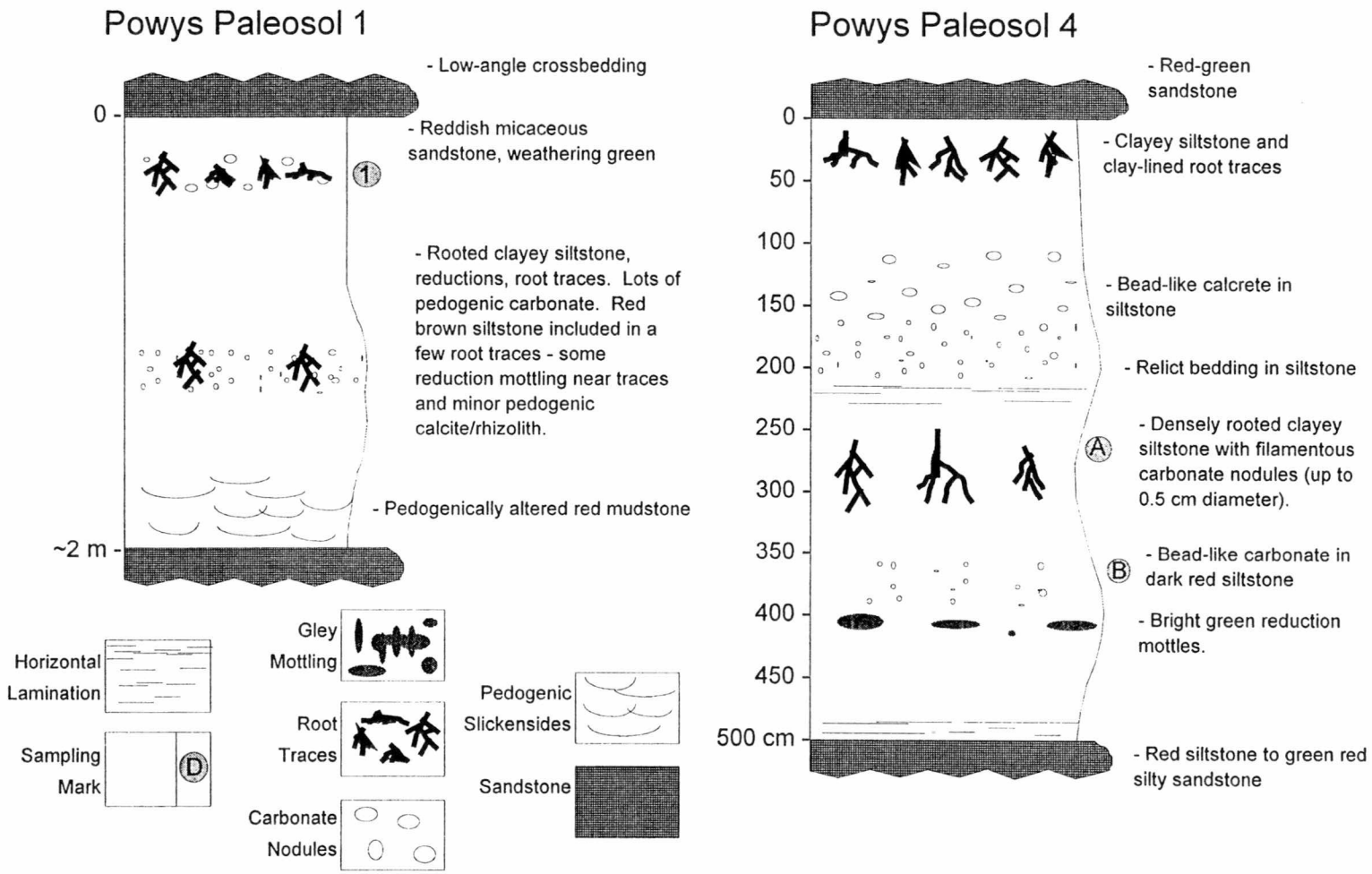

Figure 30. Schematic profile of the carbonate-bearing Powys, PA paleosols 1 and 4 including sample locations. All samples conatined carbonate (96-SC-POW-1, 96-SC-POW-4A, and 96-SC-POW-4B).

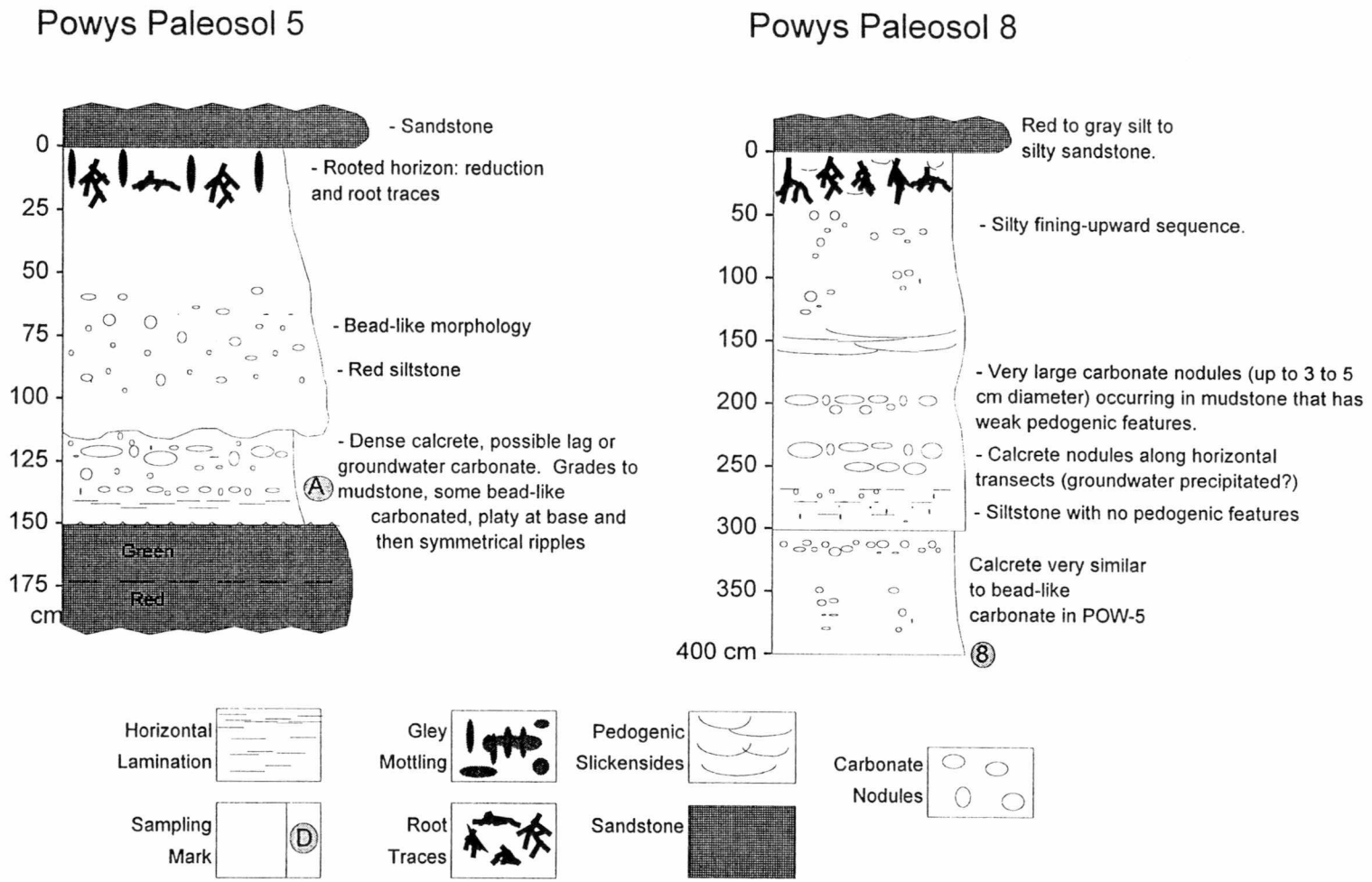

Figure 31. Schematic profile of the carboante-bearing Powys, PA paleosols 5 and 8 including sample locations. (Samples 96-SC-POW-5A and 96-SC-POW-8).

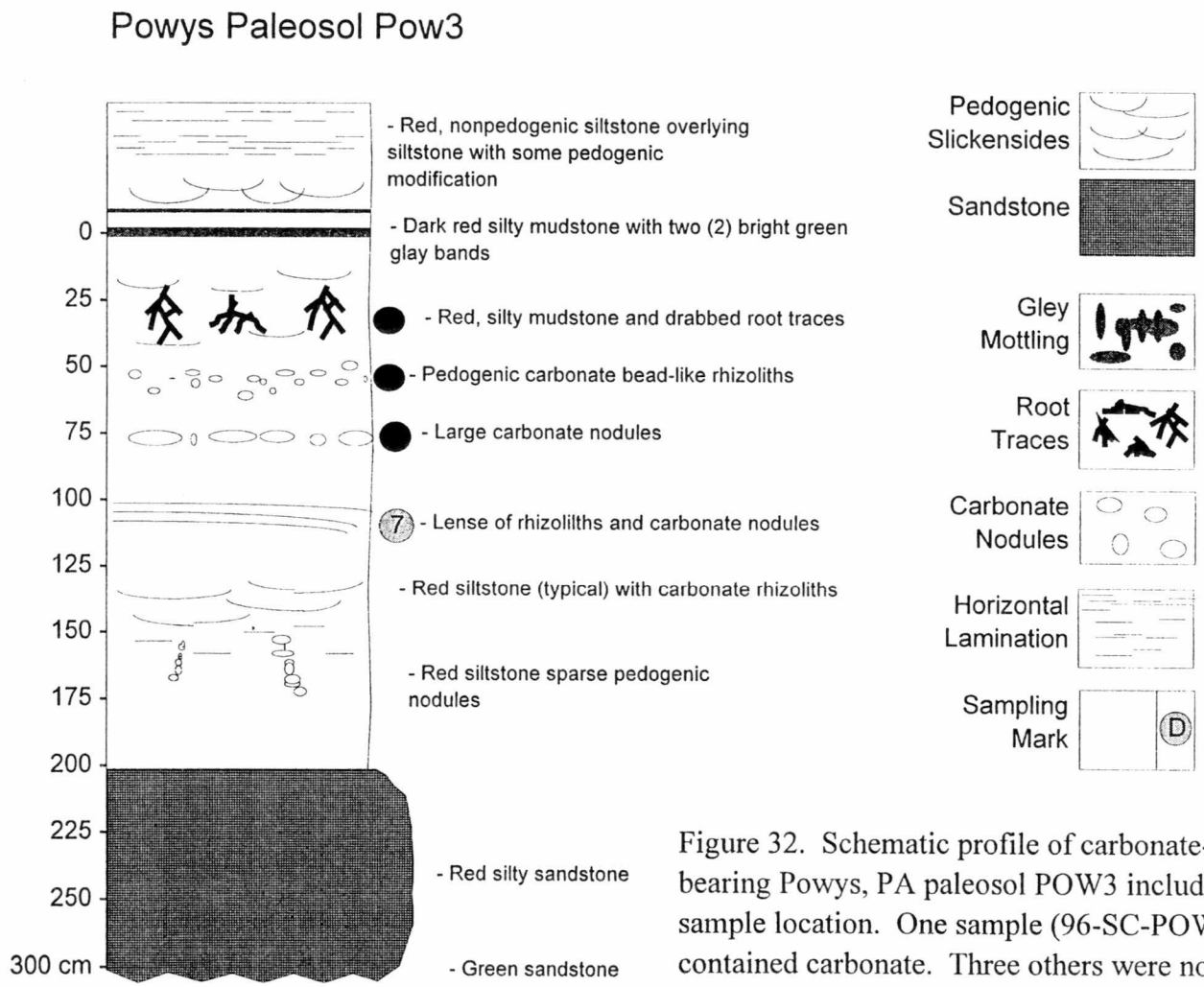

Figure 32. Schematic profile of carbonate-bearing Powys, PA paleosol POW3 including sample location. One sample (96-SC-POW3-7) contained carbonate. Three others were not carbonate-bearing (black dots).

Figure 33. Photomicrographs of Powys, PA paleosols (1st suite) carbonate morphologies. (a) Powys (96-SC-POW-8) microspar within a large (~2 cm diameter) nodule (carbonate sample 100-P). (b) Same field of view as (a) under CL has a uniform, orange luminescence. (c) Powys (96-SC-POW-4B) nodule composed of microspar (ms) nucleating around a bead-like feature (cross section) exhibiting micrite (m) occluded with equant spar cement (s, carbonate sample 97-R). (d) Same field of view as (c) under CL. Brighter zones of carbonate luminescence within the nodule and the surrounding matrix suggest several stages of carbonate precipitation post-dating precipitation of the bead-like feature, which exhibits a dull, red-orange luminescence.

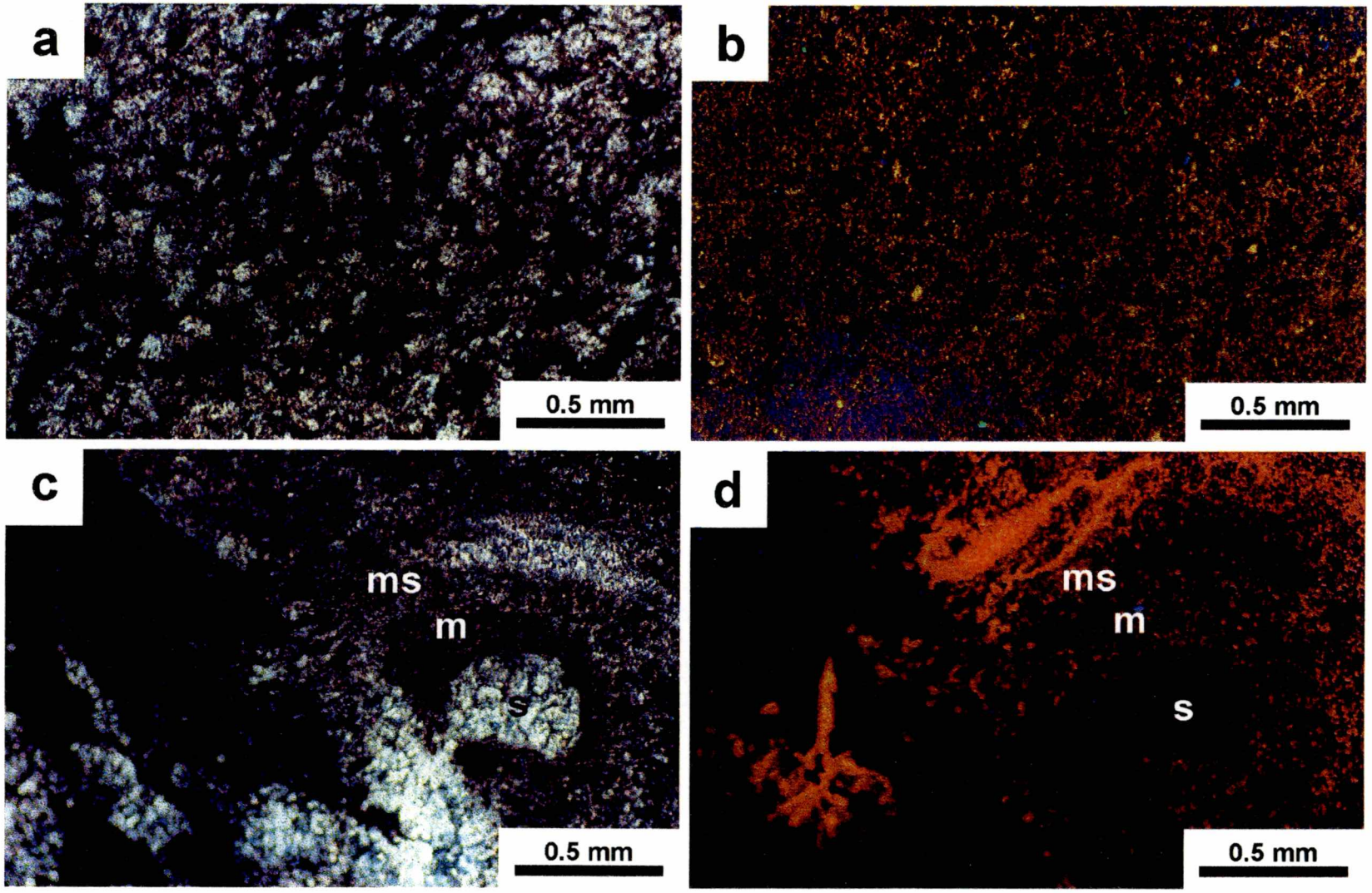
a
0.5 mm
b
0.5 mm
c
ms
m
s
0.5 mm
d
ms
m
s
0.5 mm

Figure 34. Photomicrographs of Powys, PA paleosols (2nd suite) carbonate morphologies. (a) Powys (96-SC-POW-4B) ferroan micrite and microspar, viewed under crossed-nicols. Spar cement is represented by the clear, white patches and exhibits a radial, prismatic morphology. (b) Powys (96-SC-POW-4B) bead-like feature; these features typically consist of micrite (m) occluded by spar cement and surrounded by a cortex of microspar or spar cement (s). In this case, the cortex is relatively thick and elongated parallel to bedding. (c) Powys (96-SC-POW-8) bead-like feature viewed in cross section along the long axis. Carbonate consists of several concentric layers of relatively dark micrite that has varying degrees of iron-oxide staining. Bead-like feature is occluded by a microspar cement and has a relatively thick microspar cortex. (d) Powys (96-SC-POW-8) microspar within a large nodule, approximately 2 cm diameter (carbonate sample 1-J).

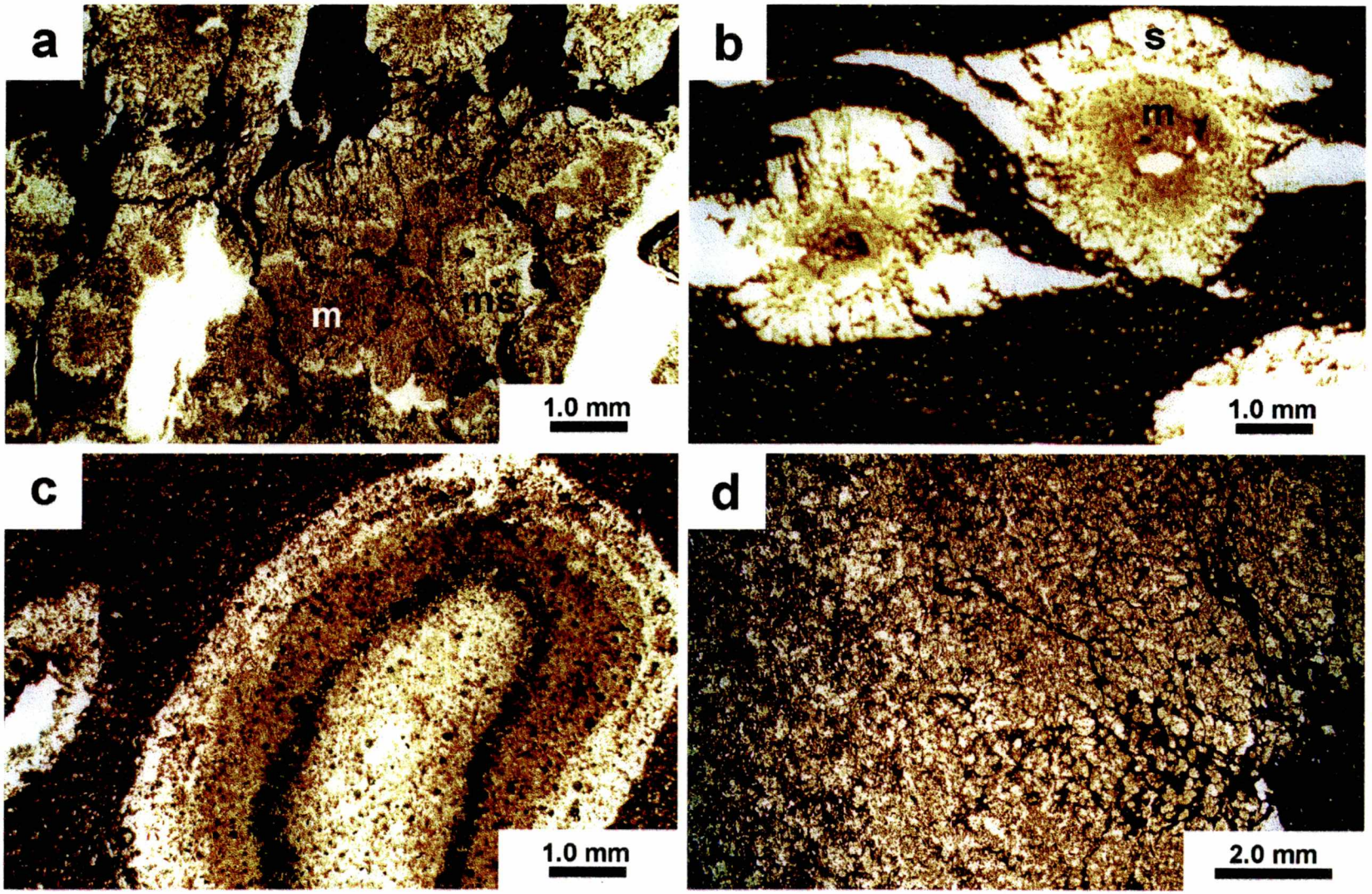
a
m
ms
1.0 mm
b
s
m
1.0 mm
c
1.0 mm
d
2.0 mm

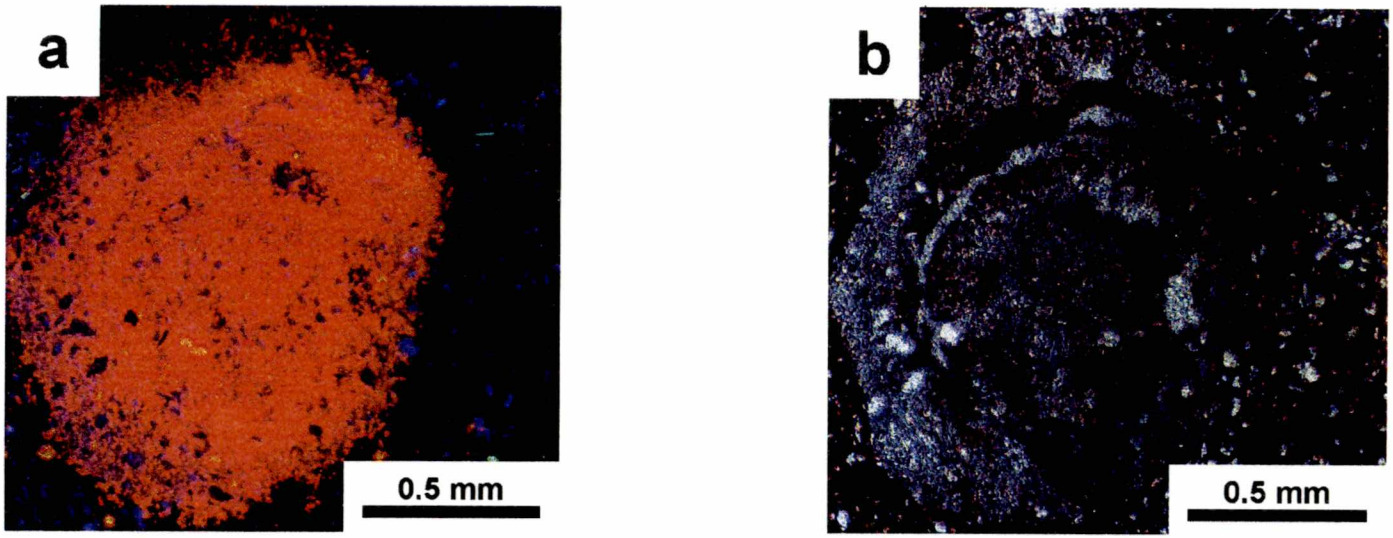

Figure 35. Photomicrographs of Powys, PA paleosols (3rd suite) carbonate morphologies. (a) Powys (96-SC-POW-1) micrite micronodule exhibiting a microspar-filled circumgranular crack. (b) Same field of view as (a) under CL. The darkest micrite in TL exhibits the brightest orange luminescence, whereas microspar tends to exhibit a more dull, red-orange luminescence.

of varying diameters. Carbonate is represented by (a) small rhizoliths (< 5 mm) that have a "bead-like" morphology at outcrop scale and large rhizoliths (0.5 to 1 cm), (b) micronodules (< 2 mm) and nodules (0.2 to 1 cm), and (c) amorphous brecciated micrite (~0.5 to 1 cm). While all three morphologies are present to some degree in all the paleosols, the rhizoliths tend to be the most abundant (and have the most distinct boundaries with the clay matrix) in clay-rich beds that exhibiting no bedding characteristics. Nodules have a more homogeneous calcite morphology consisting of micrite, although microspar and "rosette" morphology (similar to Trout Run) is more prevalent in large nodules. The nodules and amorphous brecciated micrite are most abundant where there is bedding and millimeter-scale siltstone layers. The amorphous micrite is located within these layers and appears to have been broken up by pedogenesis or soft sediment deformation that occurred after the bulk of carbonate precipitation. Where there is evidence of post-pedogenic deformation, calcite spar is most abundant.

The small rhizoliths are the most abundant morphology present and are typically viewed in cross section where the calcite has a coarse-grained core and two outer concentric layers. The center of the larger rhizoliths usually consists of equant spar or sparry microspar, whereas smaller rhizoliths contain very little to no spar. The middle layer is usually thickest and consist of multiple zones of micrite. Each layer varies in color, from light gray to brown, according to the degree of iron-oxide stain. The outer layer is usually relatively thin (0.1 to 0.3 millimeters), and is composed of microspar or thicker, radial prismatic-arrays of spar. For all rhizoliths analyzed, spar is always present to some degree as a void-filling cement in circumgranular and septarian cracks. In CL,

the intensity and color of luminescence are similar to carbonates in the Trout Run paleosols. Pedogenic carbonate in the Powys paleosols exhibits a range of isotope values ($\delta^{13}C$ = -5.0 to –7.5‰ PDB; $\delta^{18}O$ = 10 to -14‰ PDB) according to carbonate morphology (Fig. 36).

Trout Run (Duncannon Member)

Located just north of the Valley and Ridge province near Williamsport, PA, the Trout Run localities are the most paleogeographically distal Catskill Formation (Duncannon Member) paleosols studied. The Duncannon Member paleosols consist of 5-10 meter thick fining-upward sequences consisting of an erosive based, non-red, cross-stratified channel sandstone that grades into a red-brown, ripple cross-laminated to parallel-laminated fine-grained sandstone, then into a red-gray silty mudstone containing paleosol features (Driese and Mora, 1993). The thickness of the Duncannon Member at this locality is ~360 meters (Williams, 1985), most of which is exposed along the east side of highway 15N, 2.5 km north of the town of Trout Run. The lithology is consistent with high-sinuosity fluvial systems where the sandstones represent fluvial and point bar deposits and the silty mudstones are overbank and floodplain deposits. Nodular fragments are included in overlying, erosively-based, channel sandstone. In a study by Driese et al. (1997), large root and tree stump casts were described. Detailed petrographic analysis is also discussed in Driese et al. (1997) and a small number of analyses were originally presented in Mora et al. (1993).

For this study the fifth Trout Run outcrop north of the Route14/15 split was analyzed (Fig. 37). Samples were taken from the lower portion of the upper paleosol at

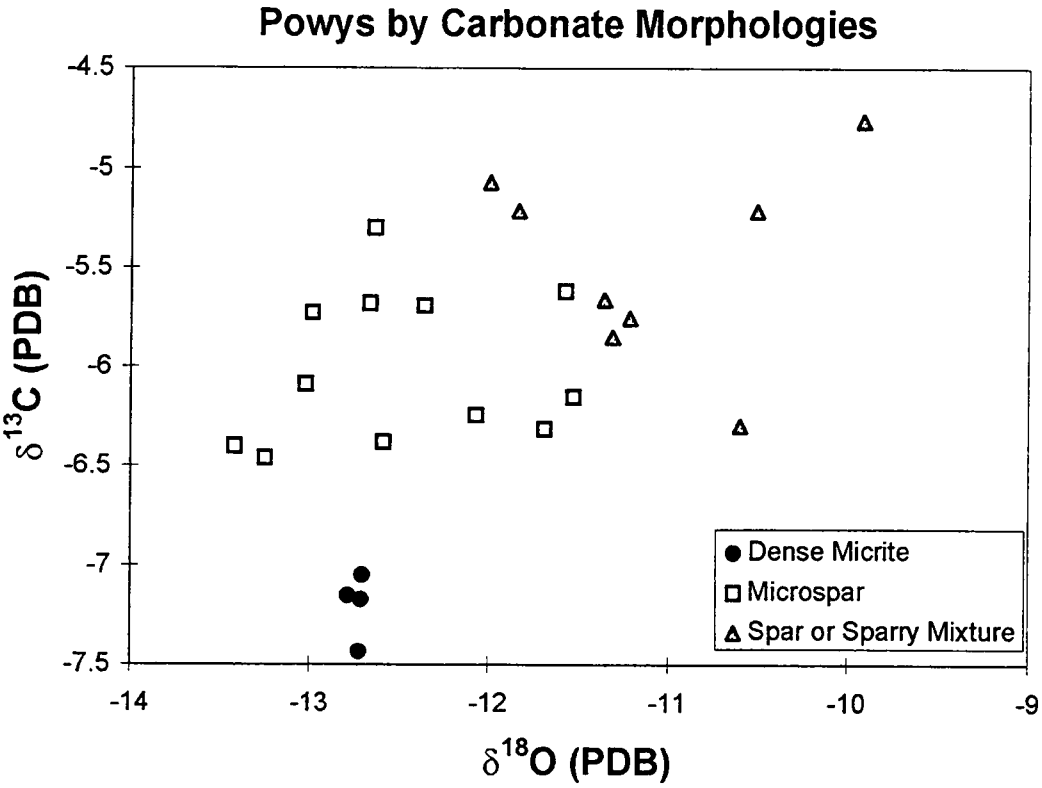

Figure 36. Powys paleosol carbonate isotope compositions. Micrite represents the least altered pedogenic signature and is used in paleobarometric estimates. Microspar and spar are more variable with respect to both $\delta^{13}C$ and $\delta^{18}O$ due to reequilibration during post-pedogenic burial diagenesis.

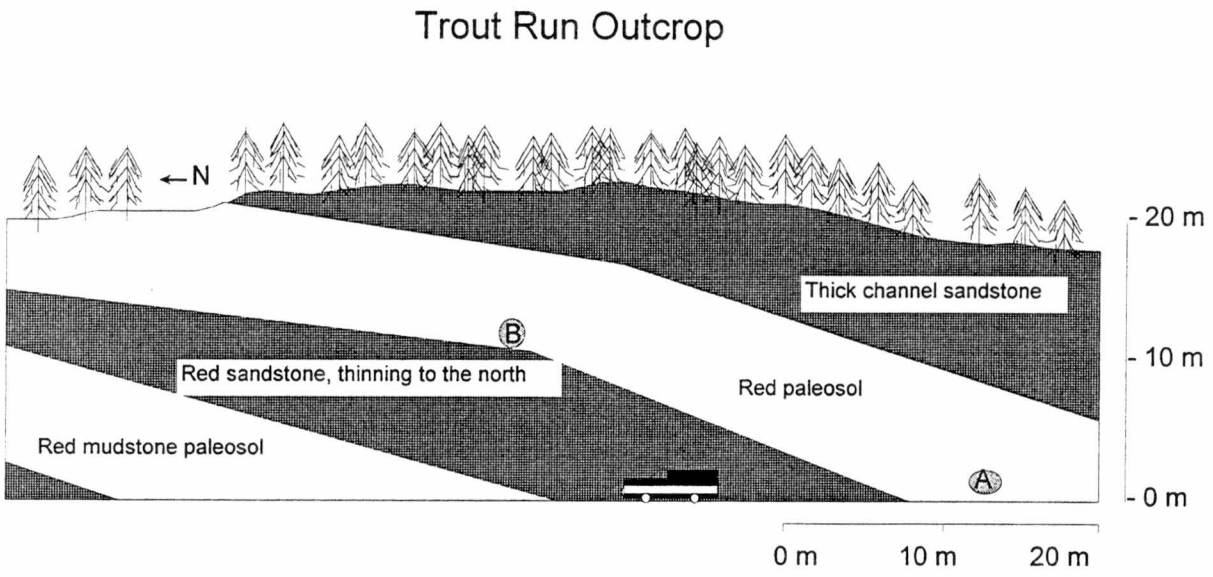

Figure 37. Schematic profile of the carbonate-bearing Trout Run, PA outcrop including sample locations. Sample (96-CAT-TR5-) A was collected *in situ*. Sample (96-CAT-TR5-) B was a float block apparently from lower in the same paleosol, above road level. Rhizoliths were abundant in sample B, but not for A.

this locality. The entire paleosol exhibited pedogenic slickensides and local variability of carbonate abundance. At road level (A), carbonate was sparse, whereas 20 meters north (B), the paleosol was extremely carbonate rich.

The Trout Run paleosols exhibit a variety of carbonate micromorphology (Figs. 38 and 39) and is similar to Powys. However, Trout Run carbonate tends to be slightly larger in diameter, amorphous, and more localized and abundant. Most carbonate is represented by (a) small rhizoliths (< 1 cm) that have a "bead-like" morphology at outcrop scale and large rhizoliths (1 to 1.5 cm), (b) micronodules (< 2 mm) and nodules (0.2 to 2 cm), and (c) amorphous micrite (~1 to 2 cm). All morphologies have distinct boundaries with the

clay matrix and exhibit no bedding characteristics. Nodules at Trout Run have a more homogeneous calcite morphology than Powys, consisting of micrite, although microspar is more prevalent in the larger nodules. The amorphous micrite is located in close proximity to localized zones of abundant carbonate, possibly originating as a cemented aggregate of two or more nodules. The rhizoliths viewed in cross section are similar to the small rhizome-like morphology present in the Powys paleosols which have three distinct concentric layers of carbonate discussed earlier. However, many of the Trout Run paleosols have only one or two of these layers, especially in the smaller rhizoliths. For all rhizoliths analyzed, spar is always present to some degree as a void filling cement in circumgranular and septarian cracks.

Of special interest for the Trout Run carbonate morphology is the presence of "rosette" microspar which is best defined at Trout Run, but which is also present at the

Figure 38. Photomicrographs of Trout Run, PA paleosol (1st suite) carbonate morphologies. (a) Trout Run (96-CAT-TR5-B) amorphous nodule exhibiting dense micrite (dm) and micrite (m) morphologies. (b) Trout Run (96-CAT-TR5-B) micronodules (mn) exhibiting zonation in the form of an iron-oxide stained micrite center and a microspar cortex. A large amorphous nodule seen on the left contains several carbonate morphologies, but is primarily composed of spar (s). (c) Trout Run (96-CAT-TR5-A) microspar within a cluster of well defined "rosette" morphology. This morphology occurs within the most dense and darkest iron-oxide stained matrix. (d) Enlargement of field of view in (c). The microspar rosettes exhibit iron-oxide staining very similar to the micronodules in (b). Rosette micromorphology is also present in the Powys paleosols, but less distinct.

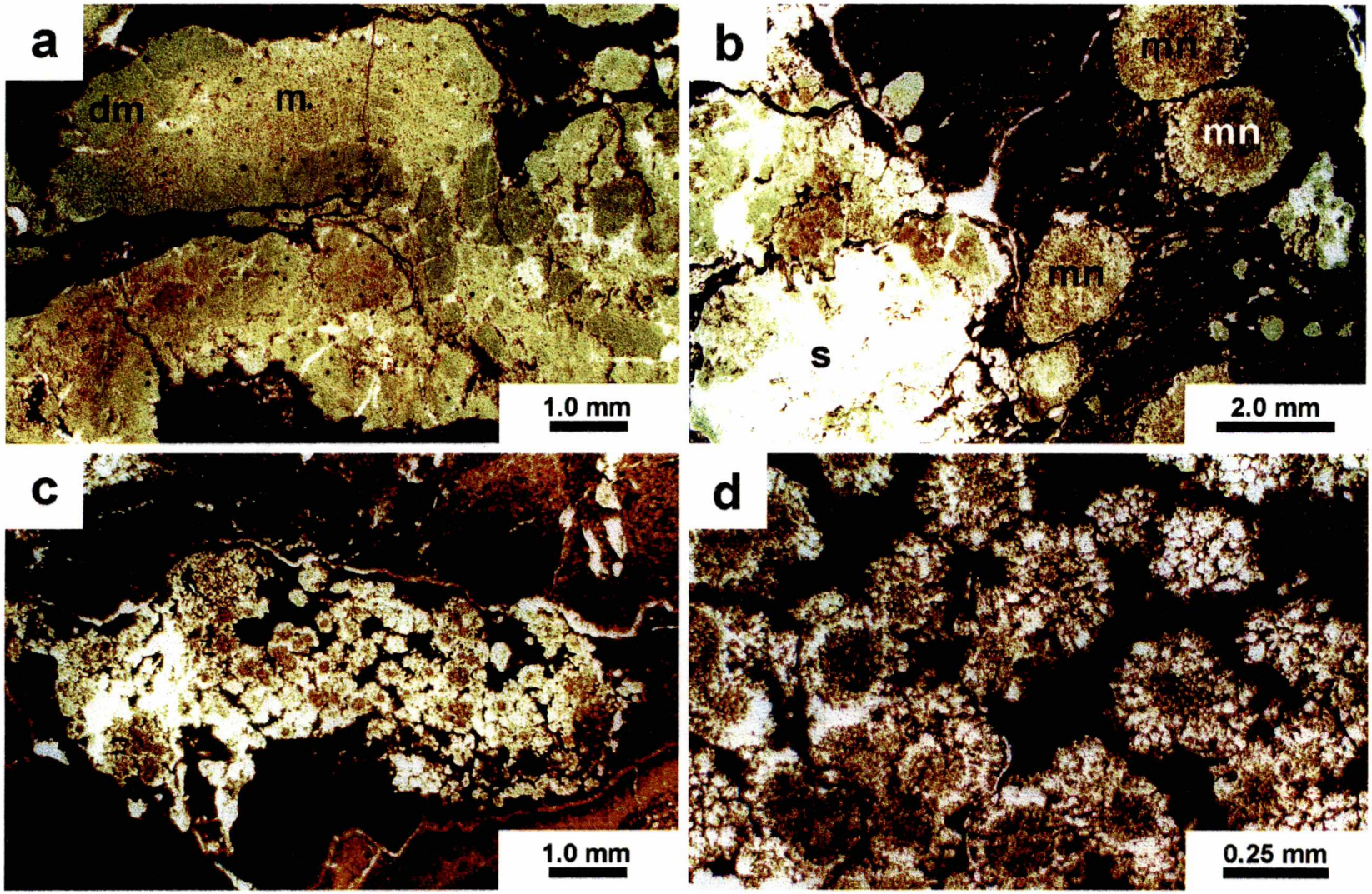
a
dm
m
1.0 mm
b
mn
mn
mn
s
2.0 mm
c
1.0 mm
d
0.25 mm

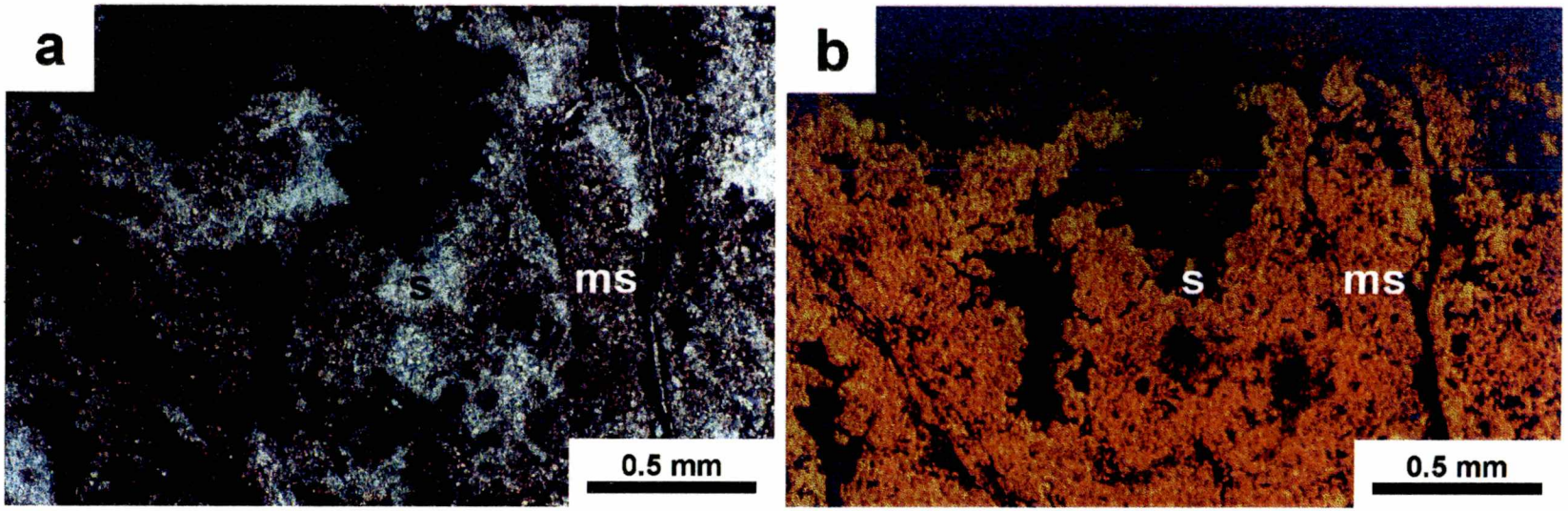

Figure 39. Photomicrographs of Trout Run, PA paleosol (2nd suite) carbonate morphologies. Trout Run (96-CAT-TR5-A) amorphous nodule exhibiting spar (s) and microspar (ms) morphologies. (b) Same field of view as (a) under CL. Microspar has a uniform, bright orange luminescence, whereas the spar has very dull luminescence.

rhizoliths within a clay-rich, ferroan matrix and occur either as a cluster (see Fig. 38c) or singular feature. Each rosette has a morphology similar to small rhizoliths with a iron-oxide-rich core and a more-coarse grained cortex, but has a uniform size and is much smaller in diameter (0.25 mm). In CL, the Trout Run samples are highly luminescent and have distinct boundaries within the matrix, unlike CL patterns in the Bloomsburg. Isotopically, this paleosol exhibits a range of carbon and oxygen values ($\delta^{13}C$ = -7.0 to −10.0‰ PDB; $\delta^{18}O$ = -11 to -13‰ PDB) that are divisible into two distinct $\delta^{13}C$ ranges (Fig. 40). The isotopic range for nodules within the channel sandstone tend to have more negative $\delta^{13}C$ values (-2‰), but are also isotopically similar to nodules sampled from the paleosol. Most paleosol carbonate values, however, fall into a range of -6.8 to -8.1‰ PDB, which are considered pedogenic in origin.

Newport and Liverpool (Duncannon Member)

Both Liverpool and Newport, PA represent the exposures of the Catskill Formation (Duncannon Member) that are most proximal to the Blue Mountain Structural Front. The geographic proximity indicates they experienced similar depositional environments and diagenetic histories. The sedimentology of these paleosols is described by Diemer (1992) and the paleopedology is described in Driese and Mora (1993). The general stratigraphy at Newport consists of numerous fining-upward sequences, five to ten meters thick. The typical sandstone-mudstone sequence consists of: (1) an erosive-based bedset, (2) non-red, cross-stratified, medium to coarse-grained channel sandstone, (3) red-brown, ripple cross-laminated to parallel-laminated, very fine to fine grained sandstone and (4) red-gray silty mudstone with common paleosol features

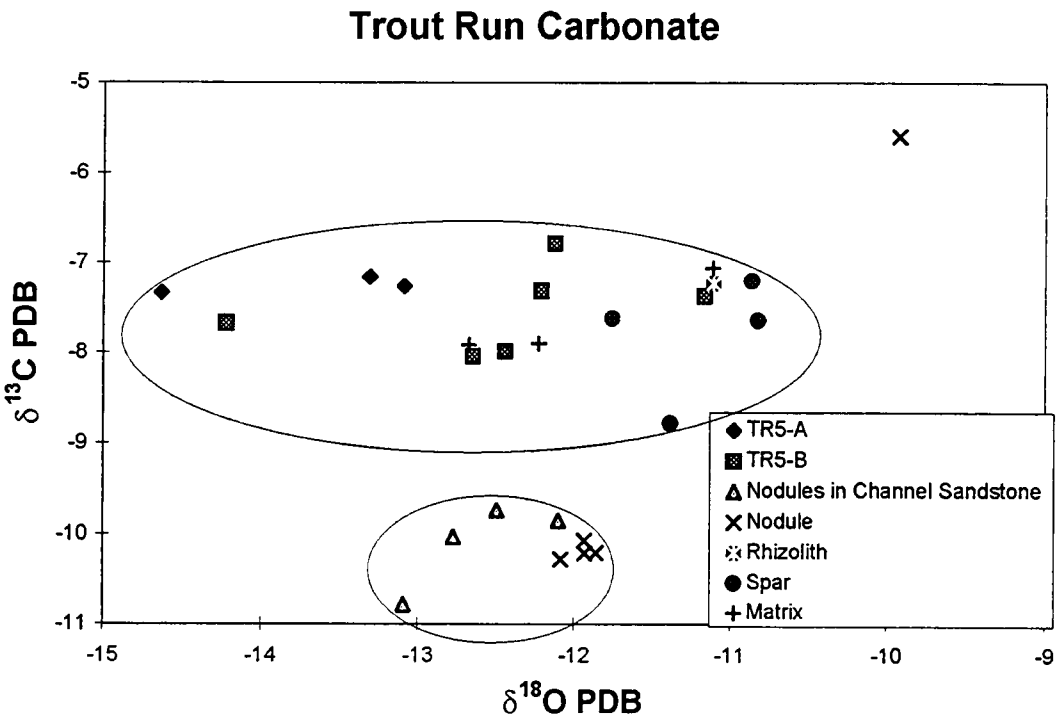

Figure 40. Trout Run paleosol carbonate isotope compositions with respect to carbonate morphology. The nodules and nodules in the channel sandstone carbonates both have been altered by a ^{13}C-depleted source. However, most of the carbonate located in the paleosol sequence has a fairly uniform $\delta^{13}C$ signature (+/- 0.8)

(Driese and Mora, 1993; Driese et al., 1993b). These sequences are deposits of high-sinuosity fluvial systems, where silty mudstones represent overbank and floodbasin deposits (Walker and Cant, 1984; Bridge and Gordon, 1985; Gordon and Bridge, 1987; Bridge, 1988; Diemer, 1992). The coarser sandstone units were deposited in lower point bar and fluvial channel environments. Thicker mudstone units exhibit pseudoanticlines, formed by shrink swell cycles during pedogenesis orthogonal to bedding (Diemer, 1992). The mudstones exhibit hackly texture and are shiny on pedogenic slickenside surfaces. Mudstones locally contain downward branching, clay lined tubules, one or more millimeter in diameter, and several centimeters long. Driese and Mora (1993) and Driese et al. (1997) also report larger root casts up to 5 cm in diameter and 15 to 30 cm long. In addition, they are often bioturbated and contain calcareous concretions, plant remains, peds, and burrows.

The Newport paleosol is typical of a Duncannon Member mudstone paleosol described as a cumulative paleosol complex with abundant pedogenic carbonate (Driese and Mora, 1993; Fig. 41). Hackly soil fabric is present in the upper portions of the paleosol. Carbonate nodules are restricted to the active shrink-swell zone, with pedogenic rhizoliths forming below this zone from 3.5 to 4 meters; most carbonate occurs between 3.5 and 4.8 meters depth. Pedogenic slickensides are present throughout the cumulative paleosol. Two gley-mottled layers are present at 1 and 4 meters depth. Pedogenic micrite has a very dull luminescence, whereas sparry pore-filling calcite and tectonic calcite veins that cross-cut the paleosol are both brightly luminescent (Driese

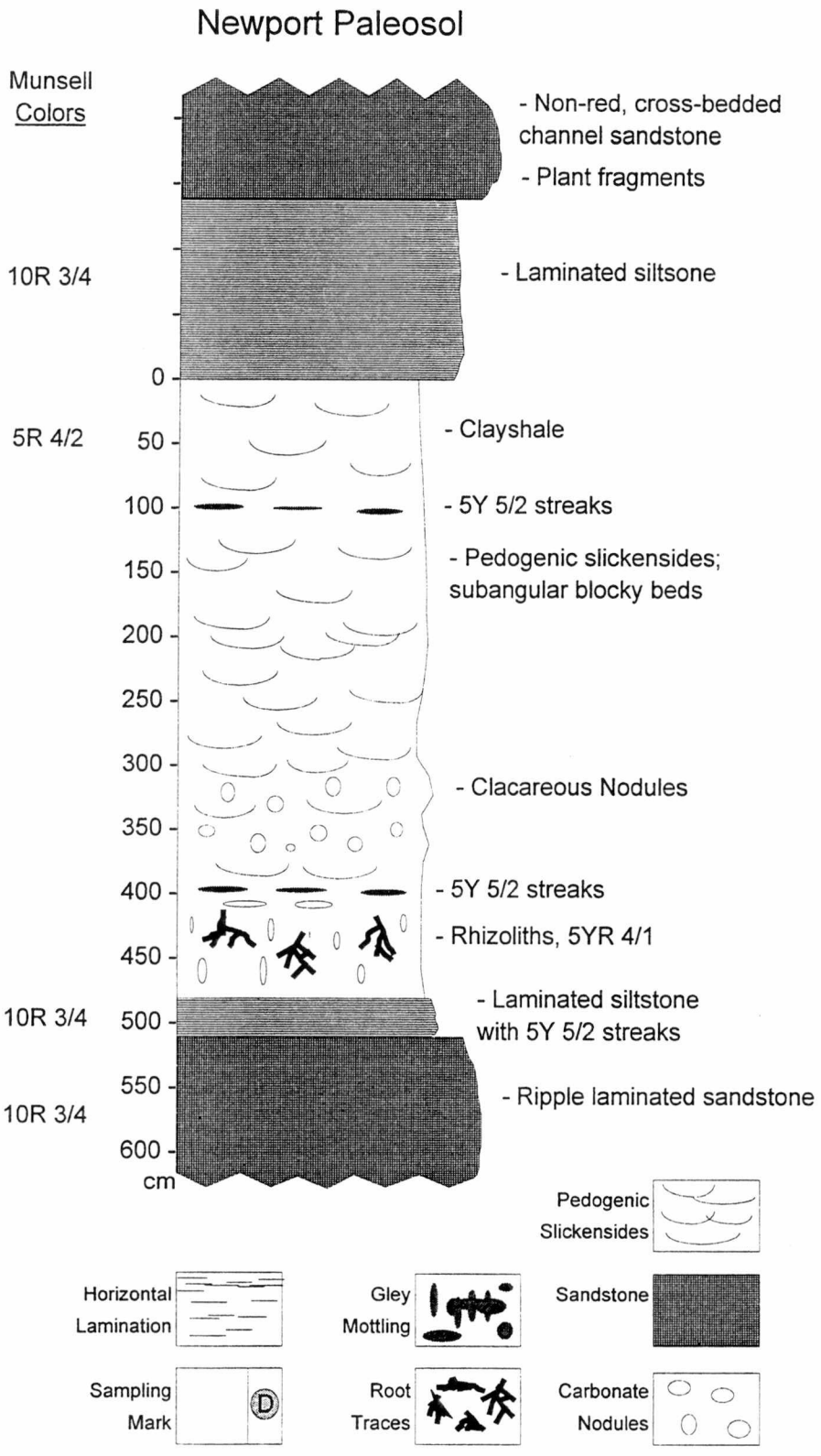

Figure 41. Schematic profile of the Newport, PA paleosol (from Driese and Mora, 1993).

and Mora, 1993). Isotopically, nodules and rhizoliths exhibit a range of values ($\delta^{13}C$ = -7.0 to –10.5‰ PDB; $\delta^{18}O$ = -11 to -14‰ PDB).

The Duncannon Member paleosol exposed near Liverpool, PA has very few carbonate nodules (Fig. 42). The Liverpool carbonate micromorphology is unique in comparison to the other paleosols of this study present as a well defined (~4 cm) thick layer in one of the four hand samples collected. The carbonate consisted of argillaceous micrite exhibiting a radial, fibrous fabric with septarian ferroan-calcite sparry infills. The matrix was the most clay-rich of any paleosols studied and exhibited clay layers (~ 0.1 mm) of variable iron-oxide stain, parallel to bedding. The one carbonate sample analyzed has a relatively low $\delta^{18}O$ value of -15.4‰ PDB compared to the other Duncannon Member paleosols, suggesting a different late diagenetic history. The carbonate composition of this sample, however, may not be representative of the entire unit because of the small sample size.

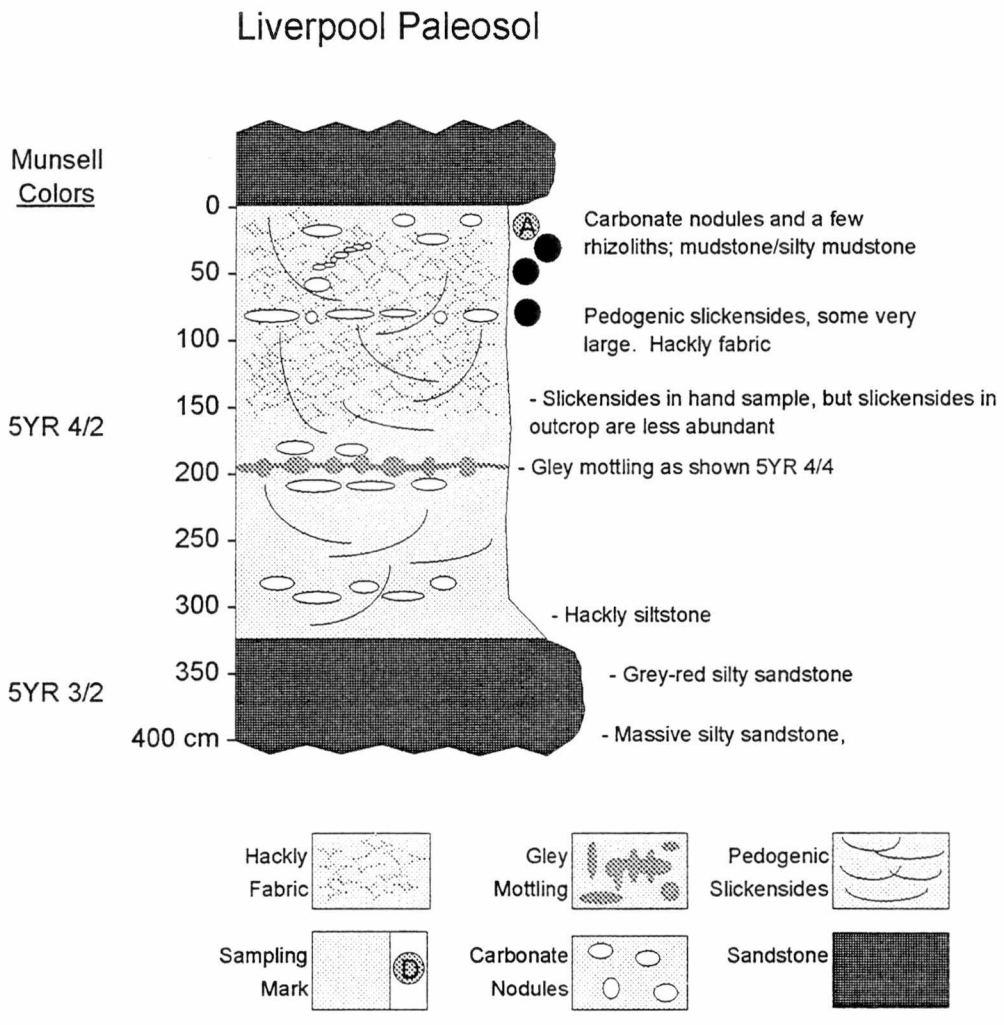

Figure 42. Schematic profile of the carbonate-bearing Liverpool, PA paleosol including sample locations. One sample (96-CAT-LIV-A) contained carbonate. Three other samples were not carbonate-bearing (black dots).

VI. Discussion

Carbonate precipitation and chemical re-equilibration can occur at any point throughout the history of a paleosol. It is important to evaluate the origin of the carbonate before considering its isotopic composition in paleoclimatic or pCO_2 studies. When studying paleosols formed during the Paleozoic, consideration should be taken for alteration of the original isotopic compositions of soil-carbonate by isotopic exchange occurring within: (1) the pedogenic environment, (2) the early burial diagenetic environment, and (3) for Appalachian paleosols, a later burial environment dominated by hot, tectonically driven fluid (Mora et al., 1998). Variations in isotopic compositions reflect the different environments in which carbonate reached final equilibrium. Carbonate precipitation in each of these environments is briefly described below.

PEDOGENIC CARBONATE

Pedogenic calcite forms as a result of dissolution-reprecipitation processes in the soil largely driven by alternating wet-dry cycles (Bellanca and Neri, 1993; Salomons and Mook, 1976; Amundson et al., 1989). Following a wetting cycle, and under normal soil conditions, smectite clays remain fully hydrated and Vertisols are reported to have a relatively high moisture retention at all water potentials (Coulombe et al., 1996). Therefore, carbonate precipitation in Vertisols is favored during the dry season. In humid to sub-humid climates, carbonate precipitation is primarily attributed to CO_2 degassing and occurs more prevalently with depth in clay-rich soil profiles (Dever et al., 1987).

The stable isotopic compositions of pedogenic carbonate reflect the composition of soil-respired CO_2 ($\delta^{13}C$; see discussion in earlier section) and soil water (Savin and Hsieh, 1998). The two primary pedogenic carbonate morphologies present in most carbonate-bearing paleosols (rhizoliths and nodules) may be isotopically distinct, reflecting formation of nodules in the zone of active shrink-swell and therefore in the presence of increased atmospheric input and variable amount of heavy atmospheric CO_2 (Driese and Mora, 1993).

EARLY DIAGENETIC CARBONATE

Early diagenetic changes in the physical conditions of the soil, including (a) marine flooding and (b) anaerobic decay of organic matter, may lead to recrystallization and exchange of oxygen and carbon isotope compositions of pedogenic carbonate. This is most common in marginal marine environments in which the uppermost preserved horizon in a fining-upward sequence commonly shows evidence of physical and chemical alteration referred to as marine hydromorphism (Driese and Foreman, 1992; Driese et al., 1993a). Flooding of this nature often results in erosional truncation of the uppermost soil horizon(s). Physical evidence that can be preserved in the rock record of marine hydromorphism is most easily recognized by the reduction of oxidized iron, presence of framboidal pyrite (or pseudomorphs), abundance of marine trace or body fossils, and physical sedimentary features. Depending on the nature and length of time the paleosol is submerged, the effect on carbonate can be extensive.

Dolomitization of pedogenic calcite is reported in a Late Mississippian Pennington Formation paleosol (Caudill et al., 1996). A dolomicrite crust is present in gilgai microlows. Dolomicrite carbonate nodules occurring deeper in the profile retain many petrographic features consistent with a pedogenic origin. These include (1) pedogenic fabrics and cathodoluminescence similar to pedogenic calcite nodules from other vertic Paleozoic paleosols (Driese and Mora, 1993); (2) dolomite is restricted to a nodular morphology and the clay matrix does not contain any carbonate, and (3) isotopically, carbon and oxygen values occurred in a range between values typical to a pedogenic origin and typical values for shallow, evaporative environments. For these reasons, Caudill et al. (1996) favored dolomitization of the dolomite nodules in an early post-pedogenic environment.

Clays are resistant to isotopic alteration under surface and near-surface conditions, except during mineralogical alteration (Savin and Hsieh, 1998). Rapid burial rates that exceed the rate of diagenesis tend to preserve carbonate isotope compositions through the insulating effect of clay minerals (Alpay, 1996). However, during slow burial, dolomitization and gley reduction may occur (Alpay, 1996). More coarse-grained paleosols may allow penetration of early diagenetic fluids or modified marine seawater through the entire sequence and as a consequence of dolomitization, pedogenic carbonate will reflect carbon and oxygen isotope compositions of the environment of dolomitization.

LATE DIAGENETIC CARBONATE

Late diagenetic fluids may be pore fluids evolved locally as a result of diagenetic mineral reactions such as the smectite-to-illite transformation or hot, saline tectonic fluids expelled from more deeply buried and deformed parts of the Appalachian Basin (Oliver, 1986). Hot, tectonic fluids often induce short-term thermal and chemical anomalies on a regional scale (Oliver, 1986; Elliott and Aronson, 1987; Ge and Garven, 1989; Cathles, 1990; Schedl et al., 1992; Qing and Mountjoy, 1992). There is widespread evidence for basin-wide fluid migration in response to Alleghanian tectonism, including textural, isotopic and geochemical evidence (Schedl et al., 1992), and K-Ar (from illites) and Ar/Ar ages (from authigenic K-feldspar) of the Valley and Ridge and Appalachian Plateau (Elliott and Aronson, 1987; Hearn et al., 1987; Schedl et al., 1992).

Uplift of foreland basins can create large-scale basinal fluid flow, but local hydrological factors also may control fluid flow (Qing and Mountjoy, 1992). Shaly basinal facies act as aquitards, impeding flow and there may be very little fluid communication between stratigraphic intervals (Nelson and Read, 1990). However, fluid flow is often concentrated along fracture and or fault zones.

Pedogenic carbonate is almost invariably recrystallized during burial diagenesis, at least to some degree, and oxygen isotopes are often good indicators of maximum burial temperatures (Mora et al., 1998). In Pennsylvania, there is a general westward trend of decreasing burial, with deepest burial occurring along the anthracite belt (Figs. 9 and 10). Levine (1986) calculated average burial depths to the lower Mississippian

rocks, based on vitrinite reflectance data, and suggest a more northwest trend of burial estimates. Of the Bloomsburg paleosols, the Danville locality has experienced the least amount of burial. Of the Catskill paleosols, the Powys/Trout Run localities were the least buried. The relatively ^{18}O-depleted composition of the pedogenic carbonates examined indicate that all samples have experienced isotopic resetting during diagenesis. Slight variation in $\delta^{18}O$ values reflect relatively deeper depths of burial or position along the Blue Mountain Structural Front (in the case of Lehigh Gap and Port Clinton). Less negative oxygen isotope compositions analyzed for the dolomite bearing paleosols (Wurtsboro, Port Jervis, Harrisburg) can be accounted for by less burial of dolomite-bearing paleosols and differences in the fractionation pathways for dolomite relative to calcite. Despite extensive resetting of oxygen isotope compositions, many diagenetic fluids have a low carbon content and diagenetic recrystallization may not significantly alter the original pedogenic carbon isotope composition (Mora et al., 1998).

VII. INTERPRETATION

BLOOMSBURG FORMATION

The principal carbonate phases occurring in Bloomsburg Formation paleosols included both dolomite and calcite; mean isotope compositions are presented in Table 4.

Wurtsboro, Port Jervis, and Harrisburg

Dolomite is the principal carbonate at three localities (Wurtsboro, Port Jervis, and Harrisburg). The $\delta^{18}O$ values range from -8 to -15‰ PDB. Excluding Harrisburg samples drilled in proximity to tectonic carbonate veins (Fig. 18d), the range is smaller ($\delta^{18}O$ = -8 to -10‰ PDB). Oxygen isotopic compositions for dolomites at Wurtsboro, Port Jervis, and Harrisburg are enriched by 3-5‰ compared to the carbonate in the calcite bearing paleosols from Danville. Taking into account the equilibrium isotopic fractionation between dolomite and calcite (2-3‰; Land, 1980), the oxygen isotope composition are consistent with dolomite equilibration during peak burial diagenesis of these paleosols, which experienced less burial then the other localities examined (Figure 9).

Table 4. Mean $\delta^{13}C$ and $\delta^{18}O$ values for carbonate in Bloomsburg Formation paleosols

Location	Mean $\delta^{13}C$ (PDB)	Mean $\delta^{18}O$ (PDB)	Principal carbonate	Sample Quantity ($\delta^{13}C$ only)	Standard Deviation (1σ)
Port Jervis	-13.5	-9.9	Dolomite	4	0.36
Harrisburg	-12.4	-8.4	Dolomite	7	0.08
Wurtsboro	-11.0	-10.3	Dolomite	4	0.14
Port Clinton	-10.3	-15.8	Calcite	17	0.41
Lehigh Gap	-8.4	-15.6	Calcite/Dolomite	3	0.10
Danville	-6.0	-13.8	Calcite	4	0.17

Carbon isotope compositions are consistent with dolomite precipitation during early diagenetic sulfate reduction ($\delta^{13}C < -12‰$ PDB; Alpay, 1996) at shallow depths. Equilibration with diagenetic fluids having low carbon concentrations could reset the oxygen isotope compositions while having no effect on the carbon compositions such that carbon $\delta^{13}C$ values could reflect early diagenesis, whereas the $\delta^{18}O$ values reflected a deeper burial environment. But, burial fluids can also be carbon-bearing. The oxygen isotope compositions and the similar $\delta^{13}C$ values of dolomicrite and later, coarser dolomite phases, however, are most consistent with dolomite formation and isotopic equilibration during deeper burial.

Unlike early post-pedogenic dolomicrite nodule in the Pennington Formation (Caudill et al., 1996) which have distinct boundaries, dolomite in the Bloomsburg paleosols is a mixture of carbonate and matrix material. Dolomitic Bloomsburg paleosols have a more coarse grained matrix relative to the other Bloomsburg paleosols. Harrisburg is not as coarse grained as Port Jervis and Wurtsboro, but has a carbonate micromorphology that is very similar to the Wurtsboro paleosol. A coarse-grained matrix can allow externally derived diagenetic fluids to penetrate the paleosol sequence and reset the pedogenic chemistry more readily than a clay-rich paleosol.

The bulk of the Harrisburg isotope data fall into a narrow range of both carbon and oxygen isotope compositions and are interpreted as having equilibrated in the same manner as Wurtsboro and Port Jervis. However, carbonate samples drilled from (or in proximity to) the dolomite veins that crosscut the paleosol have more negative $\delta^{13}C$ and

$\delta^{18}O$ values (Fig. 13). The slightly more negative values of $\delta^{13}C$ could be a result from differences in temperature of equilibration. Oxygen values are as much as 6.5‰ more negative for vein dolomite than the bulk paleosol dolomite, most likely reflecting higher temperatures during vein precipitation. The vein dolomite is interpreted to have precipitated from a late pulse of hot, carbon-poor diagenetic fluid passing through the paleosol after wholesale diagenetic isotopic equilibration of the paleosol. Dolomite spars that have recrystallized in conjunction with a tectonic influence, by being in close proximity to vein propagation, yield $\delta^{18}O$ values that lie between values for the carbonate veins and values for the bulk of paleosol dolomite.

Port Clinton and Lehigh Gap

Port Clinton and Lehigh Gap are examples of clay-rich paleosols that physically appear to be pedogenic in origin (show little evidence of recrystallization), but probably retain little of their original pedogenic chemistry based on several lines of evidence. Both the Port Clinton and Lehigh Gap paleosols are located in the portion of the basin that has been most deeply buried and occur in close proximity to the Blue Mountain Stuctural Front (Fig. 9). The natural evolution of pore waters could have easily reset the oxygen isotope compositions during burial. However, carbon isotope compositions in these paleosols are also very negative ($\delta^{13}C$ = -8 to -11‰ PDB).

A possible source of the ^{13}C-depleted carbon is the decomposition and fermentation of previously-buried organic matter (Martens et al., 1991; Ali, 1995). Kisch and van den Kerkhof (1991) have studied fluid inclusions in eastern Pennsylvania and have found methane within Siluro-Devonian Rocks. The Blue Mountain Structural

Front would provide a conduit for migrating, methane-bearing tectonic fluids (Orkan and Voight, 1983) and supports the interpretation that pedogenic carbonate in these paleosols has reequilibrated during diagenesis. Wholesale recrystallization of calcite during burial seems inconsistent with the preservation of micrite calcite, however, molecule by molecule replacement of the original calcite can occur without any evidence of recystallization (Algeo et al., 1992).

An addition line of evidence for a non-pedogenic origin for Port Clinton and Lehigh Gap carbon isotope composition is made through consideration of the Cerling (1991) paleobarometer. Formation of pedogenic calcite in the absence of a significant input of atmospheric CO_2 yields carbonate $\delta^{13}C$ values of approximately -12 ‰ PDB. The carbon isotope compositions at Port Clinton and Lehigh (-8 to -11‰ PDB) would require low atmospheric pCO_2 and/or high soil respiration rates, both of which are counter to modeled pCO_2 (Berner, 1994) and the relatively sparse vegetation inferred for the Late Silurian (Gensel and Andrews, 1987).

Danville

Many carbonate $\delta^{13}C$ values from the Danville paleosol are considered pedogenic based on mineralogy (Driese et al., 1992). Addition lines of evidence for retention of carbon isotope compositions during burial diagenesis can be made based on relative distance from the Blue Mountain Structural Front and a more shallow burial depth relative to the other New York and Pennsylvania localities (Fig. 9). Hot, methane-bearing tectonic fluids that migrated through zones of structural weakness (Kisch and van den Kerkhof, 1991) resulted in more negative carbon isotope compositions. The

Danville $\delta^{13}C$ values, however, are the least negative of any of all the Bloomsburg paleosols.

That the Danville carbonate retains variable carbon isotope compositions argues against wholesale late diagenetic reequilibration of carbon isotopes such as at Port Clinton and Lehigh Gap which yields a narrow range of isotope values throughout. Carbon isotope compositions vary throughout the lower 90 meters of the Bloomsburg Formation (Driese et al. 1992). The heaviest $\delta^{13}C$ values are interpreted as having precipitated in equilibrium with the marine carbon reservoir ($\delta^{13}C \cong$ -2 ‰ PDB; Driese et al., 1992). This interpretation was tempered by evidence of marine hydromorphism in the lower Danville paleosols, where samples had the heaviest carbon isotope compositions (Fig. 28). Stratigraphically higher in the section, the Danville paleosols reflect a more terrestrial origin, based on isotope geochemistry, paleosol morphology, and micromorphology. This is consistent with the theory of a westward migration of the paleoshoreline during Bloomsburg deposition.

The carbonate carbon isotope compositions that are interpreted as pedogenic at Danville by Driese et al. (1992) have $\delta^{13}C$ values that are variable ($\delta^{13}C$ = -3 to -7 ‰ PDB). This variability in both carbon and oxygen isotope compositions ($\delta^{18}O$ = -10 to -14.5 ‰ PDB) may be an expression of heterogeneities in diffusion within the paleosol profile or relatively shallow carbonate precipitation (Fig. 4). An average $\delta^{13}C$ of -6‰ PDB obtained in this study is in agreement with the some of lightest carbon isotope

compositions reported by Driese et al. (1992) and were used for minimum paleoatmospheric pCO_2 estimates (see later section).

LATE DEVONIAN PALEOSOLS

The principal carbonate morphologies occurring in Catskill Formation paleosols include micrite, microspar, and spar which can occur in several distinct physical morphologies (rhizolith, nodule, matrix, cement, or vein). Estimation of representative isotope compositions are presented in Table 5 based on those mineralogies.

Powys

The Powys paleosols are the only paleosols examined in this study from the early Late Devonian Sherman Creek Member of the Catskill Formation. The relatively large distance of the Powys outcrop from the Blue Mountain Structural Front and relatively shallow burial depths imply possible retention of pedogenic isotope composition (Fig. 10). Variability in isotope compositions for both $\delta^{13}C$ (-5 to -7.0‰ PDB) and

Table 5. Mean $\delta^{13}C$ and $\delta^{18}O$ values for carbonate in Catskill Formation paleosols

Location	**Mean $\delta^{13}C$ (PDB)**	**Mean $\delta^{18}O$ (PDB)**	**Principal carbonate**	**Sample Quantity ($\delta^{13}C$ only)**	**Standard Deviation (1σ)**
Liverpool*	-7.7	-15.4	All	1	-
Trout Run	-7.6	-12.2	Not nodules	17	0.48
Trout Run	-10.2	-12.3	Nodules	8	0.32
Newport	-9.5	-12.4	All	13	0.53
Powys	-7.2	-12.7	Micrite	4	0.16
Powys	-6.0	-12.5	Microspar	12	0.38
Powys	-5.5	-11.1	Spar	8	0.50

$\delta^{18}O$ (-10 to -14‰ PDB) is observed (Fig. 36) and average compositions for different carbonate morphologies are also variable (Table 5). Powys micrite that was sampled from, or proximal to, rhizoliths yields the most negative $\delta^{13}C$ values, whereas microspar and sparry mixtures associated with nodular concretions were typically more positive. Variability with respect to carbonate morphology is indicative of pedogenic processes and diffusion heterogeneities as discussed previously. Compared with isotope data presented in Cotter et al. (1993) from the Selinsgrove, PA paleosol ($\delta^{13}C \cong$ -10‰ PDB), the Powys paleosols retained carbonate isotope compositions that were heavier and therefore more pedogenic. The lightest $\delta^{13}C$ values from the dense micrite at Powys were used for a minimum paleoatmospheric pCO_2 estimate (see later section).

Trout Run

Trout Run paleosols (Duncannon Member) are similar in location, paleosol lithology, and carbonate morphology to the Powys paleosols, allowing comparison of isotope compositions during a relatively short interval of geologic time. The relative distance of the Trout Run locality from the Blue Mountain Structural Front and the relatively shallow average burial depths (Fig. 10) suggest possible retention of pedogenic carbon isotope compositions. Like the Powys paleosol, $\delta^{13}C$ values fall into two distinct ranges, however, the nodules at Trout Run represent the ^{13}C-depleted carbonate morphology relative to the other carbonate morphologies analyzed (Fig. 40).

Similar average $\delta^{13}C$ (-10‰ PDB) and $\delta^{18}O$ (-12 to 13‰ PDB) values were derived from both nodules and cement sampled from the overlying channel sandstone

and the nodules sampled from the paleosol, suggesting that all of these phases formed or reequilibrated during the same event. Micritic rhizoliths and microspar rosettes (Fig. 38) in the paleosol retain distinct isotopic compositions and are interpreted, on the basis of morphology and isotopes, to more likely preserve the original pedogenic isotopic composition. Therefore, an average of all carbonate $\delta^{13}C$ values, excluding nodules and cement were used for a paleoatmospheric pCO_2 estimate.

Liverpool and Newport

Both the Liverpool and Newport localities are in relatively close proximity to the Blue Mountain thrust fault (Fig. 10) and may have experienced a degree of isotopic resetting similar to that of the nearby Bloomsburg paleosols discussed above. The $\delta^{13}C$ values of Newport paleosol carbonate is more negative than values in the Trout Run paleosol. In addition, the $\delta^{18}O$ value of Liverpool paleosol carbonate is more negative, reflecting higher temperatures of exchange. These two lines of evidence make the interpretation that pedogenic carbon isotope compositions were preserved in these paleosols suspect and, thus, values derived from these sample were not used for paleoatmospheric pCO_2 estimates.

ESTIMATIONS OF LATE SILURIAN TO LATE DEVONIAN pCO_2

The isotopic data in this study can be used to constrain atmospheric pCO_2 using Cerling's (1991) paleobarometer as described earlier. Three values, representing averages for the Bloomsburg Formation and both the Sherman Creek and Duncannon

Members of the Catskill Formation, were used in this calculation (Figs. 43 through 45) and presented in Table 6.

The $\delta^{13}C$ value of atmospheric CO_2 is -7.0‰ PDB for the Silurian and -5.0‰ PDB for the Devonian, based on the marine carbon isotope data of Popp et al. (1986) and Veizer et al. (1986). The range of S(z) values between 3,000 and 5,000 ppmV for the Silurian and 4,000 and 6,000 ppmV for the Devonian was used based on measurements of modern soils (Cerling, 1991). Using these assumptions, we see a steep drop in atmospheric pCO_2 from the Late Silurian to the Late Devonian. Also, there was an additional drop in pCO_2 of 300 to 500 between the deposition of the Sherman Creek and Duncannon Members of the Catskill Formation. These results are presented in Figure 46.

Table 6. Summary of mean $\delta^{13}C$ values used in paleobarometer and paleoatmospheric pCO_2 estimates

Locality (Age; Formation; Member)	Most representative pedogenic $\delta^{13}C$ value	Paleoatmospheric pCO_2 estimate
Bloomsburg (Late Silurian; Bloomsburg)	-6.0‰ PDB	2,400 - 4,500 ppmV
Powys (Late Devonian; Catskill; Sherman Creek)	-7.2‰ PDB	2,300 - 4,000 ppmV
Trout Run (Late Devonian; Catskill; Duncannon)	-7.6‰ PDB	1,900 - 3,900 ppmV

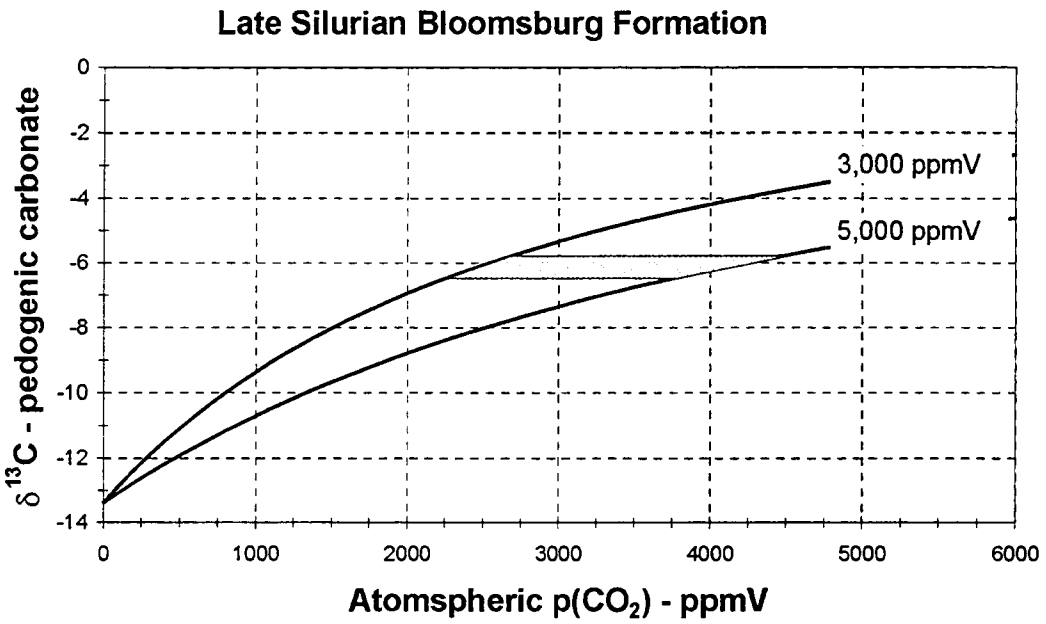

Figure 43. Estimate of Late Silurian atmospheric pCO_2 (Bloomsburg Formation). Estimates are based on Cerling's (1991) paleobarometer and soil CO_2 concentrations between 3,000 and 5,000 ppmV which represent typical modern semi-arid soils (Cerling, 1991). Atmospheric $\delta^{13}C$ = -7.0‰ PDB is based on marine carbonate values (Popp et al., 1996; Veizer et al., 1996). The $\delta^{13}C$ of organic matter = -27.4‰ PDB (Mora et al., 1996). Standard deviation for values used = 0.17.

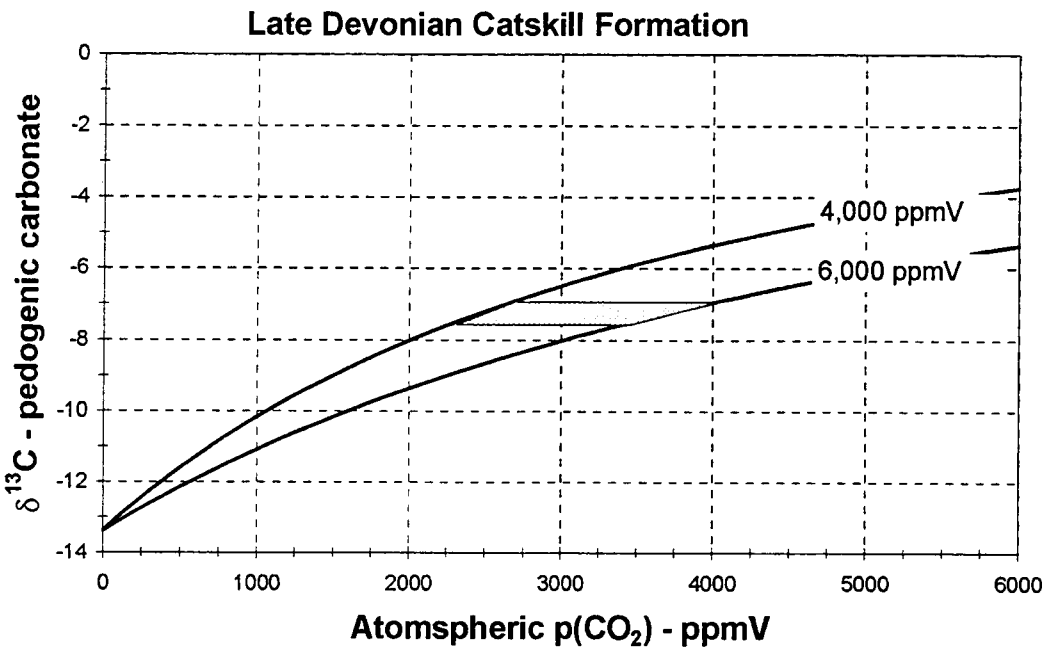

Figure 44. Estimate of early Late Devonian atmospheric pCO_2 (Catskill Formation, Sherman Creek Member). Estimates are based on Cerling's (1991) paleobarometer and soil CO_2 concentrations based on comparison with modern soils (Cerling, 1991). Atmospheric $\delta^{13}C$ = -5.0‰ PDB is based on marine carbonate values (Popp et al., 1996; Veizer et al., 1996). The $\delta^{13}C$ of organic matter = -27.2‰ PDB (Mora et al., 1996). Standard deviation for values used = 0.48.

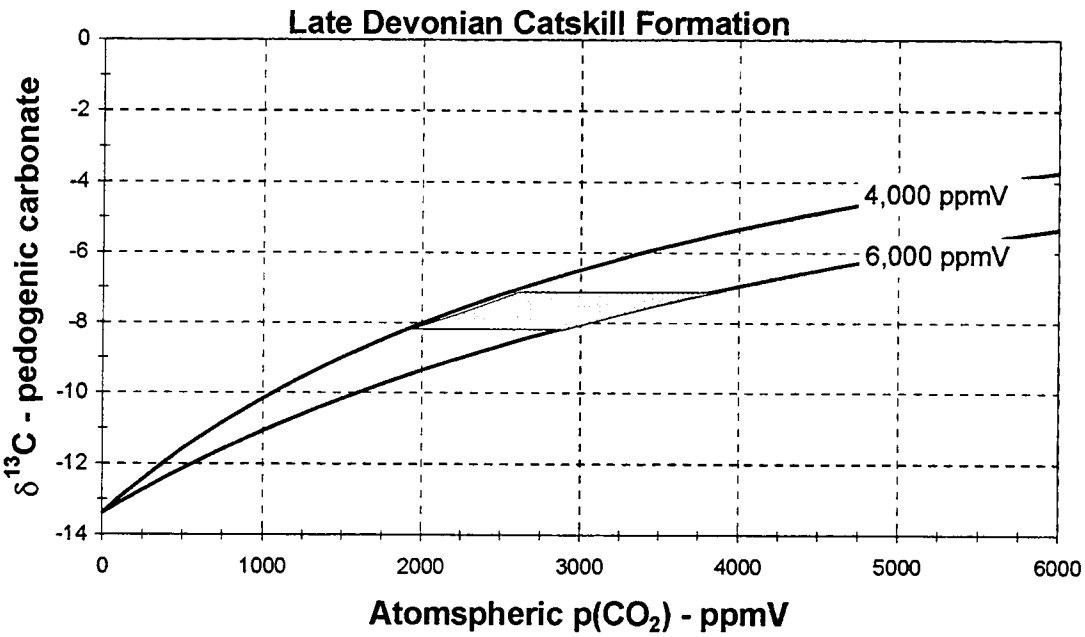

Figure 45. Estimate of (latest) Late Devonian atmospheric pCO_2 (Catskill Formation, Duncannon Member). Estimates are based on Cerling's (1991) paleobarometer and soil CO_2 concentrations based on comparison with modern soils (Cerling, 1991). Atmospheric $\delta^{13}C$ = -5.0‰ PDB is based on marine carbonate values (Popp et al., 1996; Veizer et al., 1996). The $\delta^{13}C$ of organic matter = -27.2‰ PDB (Mora et al., 1996). Standard deviation for values used = 0.16.

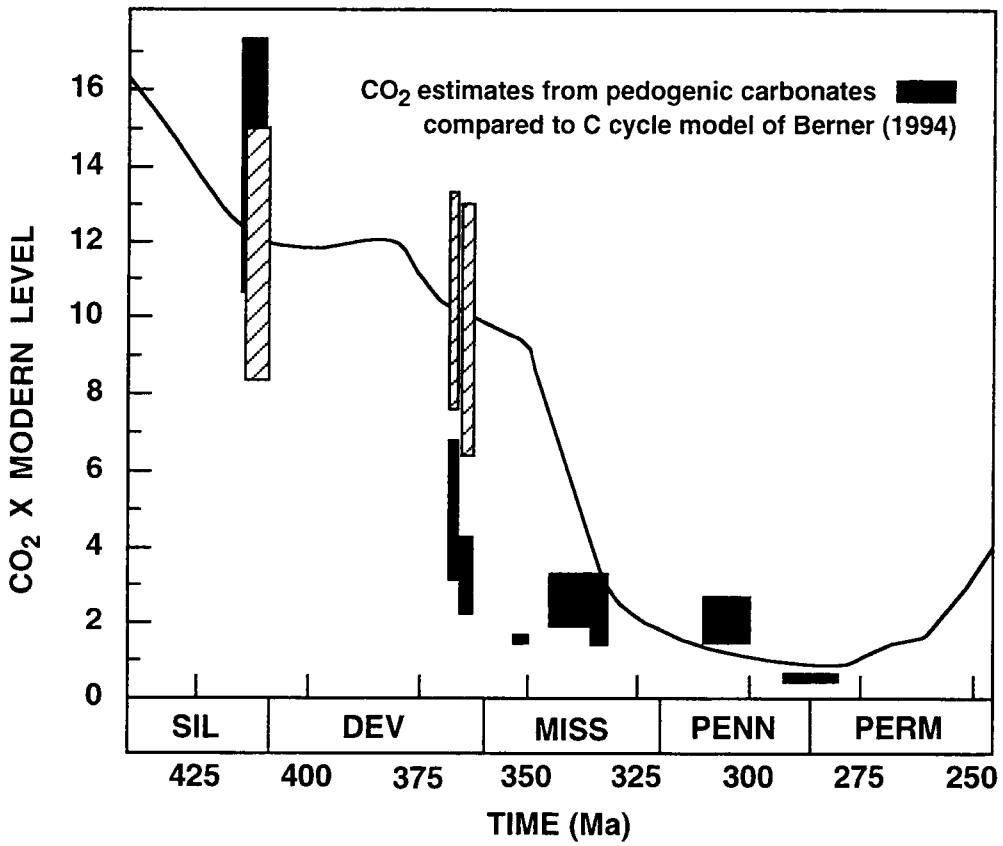

Figure 46. Estimates of Paleozoic atmospheric pCO_2 from pedogenic carbonate in vertic paleosols (from Mora et al., 1996) and Berner's (1994) carbon cycle model compared to estimates from this study. Stippled bars represent data from this work.

VIII. Conclusions

Weighing all the evidence from the multiple localities is important in determining which paleosol has recorded *and preserved* the most original pedogenic carbon isotope composition through diagenesis. Pedogenic carbonate in Late Silurian Bloomsburg Formation paleosols appear, for the most part, to record diagenetic rather than pedogenic isotope geochemistry. Alteration resulted from either the proximity to structural boundaries (i.e. The Blue Mountain Structural Front) or is a result of burial history. For paleosols that can be interpreted as having preserved a pedogenic isotope composition, a clear understanding of sedimentological controls on CO_2 diffusion must be considered before making any kind of interpretation. From the paleosols analyzed in this study, it has been found that:

(1) Sampling of many different carbonate morphologies at multiple stratigraphic levels in a fining-upward paleosol sequence is a good way to ensure recognition of a suite of pedogenic and diagenetic carbonate mineral phases and morphologies present. The presence of a $\delta^{13}C$-depth relationship may argue against wholesale reequilibration by diagenetic fluids or tectonic brines, which might isotopically homogenize the entire unit.

(2) Low permeability (ε) and porosity (ρ) layers within a soil profile affect CO_2 diffusion and therefore may result in isotopic variation. Detailed examination of sedimentology at outcrop and thin section scale is important to document whether there is evidence of such layers.

(3) Estimation of pCO_2 during the Late Silurian range from 2,200 to 6,000 ppmV, whereas estimations of pCO_2 during the Late Devonian range from 1,500 to 4,000 ppmV for the Sherman Creek Member to 1,200 to 3,500 ppmV for the Duncannon Member. These estimates are based on pedogenic carbonate carbon from the Danville ($\delta^{13}C$ = -6.0‰ PDB), Powys ($\delta^{13}C$ = -7.2‰ PDB), and Trout Run ($\delta^{13}C$ = -7.7‰ PDB) localities.

(4) Late diagenetic alteration by hot tectonic fluids appears to be an important mechanism in controlling the isotopic chemistry of many clay-rich Siluro-Devonian (Port Jervis, Lehigh Gap, and Newport) paleosols located at or near zones of structural weakness, such as the Blue Mountain thrust fault of eastern Pennsylvania.

(5) Relatively coarse-grained paleosols appear to have been subject to diagenetic dolomitization and the carbonate isotope compositions reflect equilibration at slightly lower temperatures, consistent with their shallower depths of burial.

(6) Fine grained paleosols such as mud- or claystones are less prone to dolomitization by an externally derived source due to low matrix diffusion.

LITERATURE CITED

LITERATURE CITED

Al-Aasm, I.S., Taylor, B.E., and South, B., 1990. Stable isotope analysis of multiple carbonate samples using selective acid extraction. *Chemical Geology* **80(2)**: 119-125.

Algeo, T.J., Wilkinson, B.H. and Lohmann, K.C., 1992. Meteoric-burial diagenesis of Middle Pennsylvanian limestones in the Orogrande Basin, New Mexico; water/ rock interactions and basin geothermics. *Journal of Sedimentary Petrology* **62(4)**: 652-670.

Algeo, T.J., Berner, R.A., Maynard, J.B. and Scheckler, Stephen.E., 1995. Late Devonian oceanic anoxic events and biotic crises; "rooted" in the evolution of vascular land plants? *GSA Today* **5(3)**:45, 64-66.

Ali, M.Y., 1995. Carbonate cement stratigraphy and timing of diagenesis in a Miocene mixed carbonate-clastic sequence , offshore Sabah, Malaysia; constraints from cathodoluminescence, geochemistry, and isotope studies. *Sedimentary Geology* **99**: 191-214.

Alpay, S., 1996. Diagenetic patterns and processes within a Pleistocene continental slope of mixed carbonate and siliciclastic lithologies; an investigation of results from deep ocean drilling off the Northeast Austrailian margin. Master's Thesis. Carleton University. Ottawa, ON, Canada. Pages 134.

Amundson, R.G., Chadwick, O.A., Sowers, J.M. and Doner, H.E., 1988. Relationship between climate and vegetation and the stable carbon isotope chemistry of soils in the eastern Mojave Desert, Nevada. *Quaternary Research* **29(3)**: 245-254.

Amundson, R.G., Chadwick, O.A., Sowers, J.M., and Doner, H.E., 1989. The stable isotope chemistry of pedogenic carbonates at Kyle Canyon, Nevada. *Soil Science Society of America Journal* **53(1)**: 201-210.

Ayrton, W.G., 1963. Isopach and lithofacies map of the Upper Devonian of Northeastern United States. In: Shepps (ed.), Symposium on Middle and Upper Devonian stratigraphy of Pennsylvania and adjacent states. Pages 3-6.

Beaumont, C., Quinlan, G.M. and Hamilton, J., 1987. The Alleghanian orogeny and its relationship to the evolution of the Eastern Interior, North America. In: C. Beaumont and A.J. Tankard (Eds.), Sedimentary Basins and Basin-forming Mechanisms. *Can. Soc. Petrol. Geol, Mem.* **12**: 425-445.

Beerbower, J.R., 1985. Early Development of Continental Ecosystems. In: Tiffney, B. H. (ed.), Geological Factors and the Evolution of Plants. Pages 47-91.

Bellanca, A. and Neri, R., 1993. Dissolution and precipitation of gypsum and carbonate minerals in soils on evaporite deposits, central Sicily: isotope geochemistry and microfabric analysis. *Geoderma* **59(1-4)**: 263-277.

Berner-Robert-A, 1993. Paleozoic atmospheric CO (sub 2) ; importance of solar radiation and plant evolution. *Science* **261(5117)**: 68-70.

Berner, R.A., 1994, Geocarb II: A revised model of atmospheric CO_2 over Phanerozoic time. *American Journal of Science* **294(1)**: 56-91.

Berner, R.A. and Canfield, D.E., 1989. A new model for atmospheric oxygen over Phanerozoic time. *American Journal of Science* **289(4)**: 333-361.

Blodgett, R.H., 1985. Paleovertisols as indicators of climate. *AAPG Bulletin* **69(2)**: 239.

Boutton, T.W., Nordt, L.C., Archer, S.R., Midwood, A.J. and Casar, I., 1993. Stable carbon isotope ratios of soil organic matter and their potential use as indicators of palaeoclimate. In: Isotope techniques in the study of past and current environmental changes in the hydrosphere and the atmosphere. International Atomic Energy Agency. Vienna, International. Pages 445-459.

Bridge, J.S., 1988. Devonian fluvial deposits of the western Catskill region of New York State: Binghamton, NY, 1988 *Annual Field Trip Guidebook SEPM Eastern Section*, 23 p.

Bridge, J.S., and Gordon, E.A., 1985. Quantitative interpretation of ancient river systems in the Oneonta formation, Catskill Magnafacies. In: Woodrow, D.L., and Sevon, W.D. (eds.), The Catskill delta. *Geological Society of America Special Paper* **201**: 163-182.

Bridge, J.S. and Nickelsen, B.H., 1985. Reanalysis of the Twilight Park Conglomerate, Upper Devonian Catskill magnafacies, New York State. *Northeastern Geology* **7(3-4)**: 181-191.

Capelle, D.G. and Driese, S.G., 1995. Changes in paleosol morphology along a muddy coastal margin-to-alluvial transect: Irish Valley and Sherman Creek Members (Catskill Formation, Upper Devonian), central Pennsylvania. *Geological Society of America, Abstracts with Programs* **27(1)**: 33.

Cathles, L.M., 1990. Scales and effects of fluid flow in the upper crust. *Science* **248**: 323-329.

Caudill, M.R., Driese, S.G. and Mora, C.I., 1996. Preservation of a paleo-Vertisol and an estimate of late Mississippian paleoprecipitation. *Journal of Sedimentary Research* **66(1)**: 58-70.

Cerling, T.E., 1984. The stable isotopic composition of modern soil carbonate and its relationship to climate. *Earth planet. Sci. Lett.* **71**: 229-240.

Cerling, T.E., 1991. Carbon dioxide in the atmosphere: evidence from Cenozoic and Mesozoic paleosols. *American Journal of Science* **291**: 377-400.

Cerling, T.E, 1992. Use of carbon isotopes in paleosols as an indicator of the pCO_2 of the paleoatmosphere. *Global Biogeochem. cycles* **6**: 307-314.

Cerling, T.E. and Hay, R.L., 1986. An isotopic study of Paleosol carbonates from Olduvai Gorge. *Quaternary Research* **25(1)**: 63-78.

Cerling, T.E. and Quade, J., 1993. Stable carbon and oxygen isotopes in soil carbonates. *Geophysical Monograph* **78**: 217-231.

Cerling, T.E., Quade, J., Wang, Y., and Bowman, J., 1989. Carbon isotopes in soils and Palaeosols as ecology and palaeoecology indicators. *Nature* **341(6238)**: 138-139.

Cotter, E., 1993. Overview of Geology of Central Pennsylvania. In: Driese, S.G., Mora, C.I. and Cotter, E. (Leaders), Paleozoic paleosols of central Pennsylvania. *University of Tennessee, Studies in Geology* **22**: 1-29.

Cotter, E., Driese, S.G., Mora, C.I. and Fatovsky, D.E., 1993. Marginal marine and distal alluvial plain paleosols in the Catskill Formation, Sesquehanna river valley, south of Selinsgrove, PA. In: Driese, S.G., Mora, C.I. and Cotter, E. (Leaders), Paleozoic paleosols of central Pennsylvania. *University of Tennessee, Studies in Geology* **22**: 66-76.

Cotter, E. and Driese, S.G., 1998. Incised valley fills and other evidence of sea-level fluctuations affecting deposition of the Catskill Formation (Upper Devonian), Appalachian foreland basin of Pennsylvania. *Journal of Sedimentary Research* **68**: 347-361.

Coulombe, C.E., Dixon, J.B., and Wilding, L.P., 1996. Mineralogy and chemistry of Vertisols. *Developments in Soil Science* **24**: 115-200.

Deines, P., Langmuir, D. and Harmon, R.S., 1974. Stable carbon isotope ratios and the existence of a gas phase in the evolution of carbonate ground waters. *Geochimica et Cosmochimica Acta* **38(7)**: 1147-1164.

Dever, L., Fontes, J.C. and Riche, G., 1987. Isotopic approach to calcite dissolution and precipitation in soils under semi-arid conditions. *Chemical Geology* **66**:307-314.

Dickson, J.A.D., 1966. Carbonate identification and genesis as revealed by staining. *Journal of Sedimentary Petrology* **36(2)**: 491-505.

Dickson, J.A.D., 1965. A modified staining technique for carbonates in thin section. *Nature* **205(4971)**: 587.

Diemer, J.A., 1992. Sedimentology and alluvial stratigraphy of the upper Catskill Formation, south-central Pennsylvania. *Northeastern Geology* **14**: 121-136.

Driese, S.G., and Forman, J.L., 1992, Paleopedology and paleoclimatic implications of Late Ordovician vertic paleosols, southern Appalachians. *J. Sedim. Petrol.* **62**: 71-83.

Driese, S.G., and Mora, C.I., 1993. Physio-chemical environment of pedogenic carbonate formation in Devonian vertic paleosols, central Appalachians, USA. *Sedimentology* **40**: 199-216.

Driese, S.G., Mora, C.I., Cotter, E., and Foreman, J.L., 1992. Paleopedology and stable isotope geochemistry of Late Silurian vertic paleosols, Bloomsburg formation, central Pennsylvania. *Journal of Sedimentary Petrology* **62**: 825-841.

Driese, S.G., Mora, C.I. and Cotter, E., 1993a. Paleosols in Bloomsburg Formation (Upper Silurian) near Danville, PA. In: Driese, S.G., Mora, C.I. and Cotter, E. (Leaders), Paleozoic paleosols of central Pennsylvania. *University of Tennessee, Studies in Geology* **22**: 102-115.

Driese, S.G., Mora, C.I. and Cotter, E., 1993b. Buffalo Mountain paleosol, Duncannon Member of Catskill Formation (Upper Devonian) near Newport, PA. In: Driese, S.G., Mora, C.I. and Cotter, E. (Leaders), Paleozoic paleosols of central Pennsylvania. *University of Tennessee, Studies in Geology* **22**: 50-66.

Driese, S.G., Mora, C.I. and Elick, J.M., 1997. Morphology and taphonomy of root and stump casts of the earliest trees (Middle to Late Devonian), Pennsylvania and New York, U.S.A. *Palaios* **12(6)**: 524-537.

Driese, S.G. and Mora, C.I., in press. Evolution and diversification of Siluro-Devonian root traces: influence on paleosol morphology and estimates of paleoatmospheric CO_2 levels. In: Gensel, P.G., and Edwards, D. (eds.), Early land plants and their environments: International Organization of Palaeobotany Symposium Volume. New York, Columbia University Press.

Dudal, R., and Eswaran, H., 1988. Distribution, properties and classification of Vertisols. In: Wilding, L.P., and Puentes, R. (eds.), Vertisols: Their Distribution, Properties, Classification and Management: College Station, TX, Texas A & M University Printing Center, p. 1-22.

Edwards, D., 1996. New insights into early land ecosystems; a glimpse of a Lilliputian world. *Review of Palaeobotany and Palynology* **90(3-4)**: 159-173.

Ehleringer, J.R., 1988. Carbon isotope ratios and physiological processes in aridland plants. In: Rundel, P.W., Ehleringer, J.R., and Nagy, K.A. (eds.), Applications of stable isotope ratios to ecological research. New York, Springer-Verlag, p. 41-54.

Elick, J.M., Driese, S.G. and Mora, C.I., 1998. Very large plant and root traces from the Early to Middle Devonian; implications for early terrestrial ecosystems and atmospheric p(CO_2). *Geology* **26(2)**: 143-146.

Elliot, W.C. and Aronson, J.L., 1987. Alleghenian episode of K-bentonite illitization in the southern Appalachian basin. *Geology* **15**: 735-739.

Epstein, J.B., Sevon, W.D., and Glaeser, J.D. , 1974. Geology and mineral resources of the Lehighton and Palmerton quadrangles, Carbon and Northampton counties, Pennsylvania. Altas - Pennsylvania. Bureau of Topographic and Geologic Survey. 195cd. Pennsylvania Bureau of Topographic and Geologic Survey. Harrisburg, PA, United States. Pages: 460.

Epstein, J.B., 1993. Stratigraphy of Silurian rocks in Shawangunk Mountain, southeastern New York, including a historical review of nomenclature. *Geological Survey Bulletin*. Pages L1-L40.

Faill, R.T., 1985. The Acadian orogeny and the Catskill Delta. In: Woodrow, D.L., and Sevon, W.D. (eds.), The Catskill Delta. *Geological Society of America Special Paper* **201**: 39-49.

Feakes, C.R. and Retallack, G.J., 1988. Recognition and chemical characterization of fossil soils developed on alluvium; A late Ordovician example: *Geological Society of America Special Paper* **216**: 35-48.

Friedman, I. and O'Neil, J.R., 1977. Compilation of stable isotope fractionation factors of geochemical interest. United States Geological Survey Professional Paper 440-KK, 96 p.

Ge, S. and Garven, G., 1989. Tectonically induced transient groundwater flow in foreland basin. Geophysical Monograph 48; IUGG **3**:145-158.

Gensel, P.G. and Andrews, H.N., 1987. The evolution of early land plants. *American Scientist* **75(5)**: 478-488.

Ghosh, P., Bhattacharya, S.K. and Jani, R.A., 1995. Palaeoclimate and palaeovegetation in Central India during the Upper Cretaceous based on stable isotope composition of the Palaeosol carbonates. *Palaeogeography, Palaeoclimatology, Palaeoecology* **114(2-4)**: 285-296.

Giffin, E.B., 1979. Silurian vertebrates from Pennslyvania. *Journal of Paleontology* **53**: 145-174.

Gillmeister, N.M. and Springer, D.A., 1990. Lehigh Water Gap, Palmerton, Pennsylvania. *Northeastern Geology* **12(1-2)**: 46-50.

Goldstein, R.H., 1991. Stable isotope signatures associated with paleosols, Pennsylvanian Holder Formation, New Mexico. *Sedimentology* **38**: 67-77.

Gordon, E.A. and Bridge, J.S., 1987. Evolution of Catskill (Upper Devonian) river systems: *Journal of Sedimentary Petrology* **57**:234-249.

Hearn, P.P., Sutter, J.F. and Belkin, H.E., 1987. Evidence for late-Paleozoic brine migration in Cambrian carbonate rocks of the Central and Southern Appalachians; implications for mississippi valley-type sulfide mineralization. *Geochimica et Cosmochimica Acta* **51(5)**: 1323-1334.

Hoefs, J., 1987. Stable Isotope Geochemistry, 3rd Edition. Springer Verlag, New York, 241 p.

Holland, H.D., 1984. The chemical evolution of the atmosphere and oceans. Princeton University Press, Princeton, 582 p.

Hoskins, D.M., 1961. Stratigraphy and paleontology of the Bloomsburg Formation of Pennsylvania and adjacent states: Pennsylvania Geological Survey, 4th series, General Geological Report 36, 125 p.

Joeckel, R.M., 1991. Paleosol stratigraphy of the Eskridge Formation; Early Permian pedogenesis and climate in southeastern Nebraska. *Journal of Sedimentary Petrology* **61(2)**: 234-255.

Keller, C.K. and Wood, B.D., 1993. Possibility of chemical weathering before the advent of vascular land plants. *Nature* **364(6434)**: 223-225.

Kenrick, P. and Crane, P.R., 1997. The origin and early evolution of plants on land. *Nature* **389(6646)**: 33-39.

Kent, D.V. and Miller, J.D., 1988. New perspectives from paleomagnetism: Paleozoic drift and Appalachian tectonics: Lamont-Doherty Geological Observatory of Columbia University, Yearbook, p. 12-17.

Kisch, H.J. and van den Kerkhof, A.M., 1991. CH_4-rich inclusions from quartz veins in the Valley-and-Ridge Province and the anthracite fields of the Pennsylvania Appalachians. *American Mineralogist* **76(1-2)**: 230-240.

Klappa, C.F., 1980. Rhizoliths in terrestrial carbonates: classification, recognition, genesis and significance. *Sedimentology* **27**: 613-629.

Kump, L.R., 1989. Chemical stability of the atmosphere and ocean. *Global Planetary Change* **1**: 123-136.

Kump, L.R. and Garrels, R.M., 1986. Modeling atmospheric O_2 in the global sedimentary redox cycle. *American Journal of Science* **286(5)**: 337-360.

Land, L.S., 1980. The isotopic and trace element geochemistry of dolomite: the state of the art. In: Zenger, D.H., Dunhan, J.B., and Ethington, R.L. (eds.), Concepts and Models of Dolomitization. *SEPM Special Publication* **28**: 87-110.

Levine, J.R., 1986. Deep burial of coal-bearing strata, anthracite region, Pennsylvania; sedimentation or tectonics? *Geology* **14(7)**: 577-580.

Machel, H.G. and Burton, E.A., 1991. Factors governing cathodoluminescence in calcite and dolomite and their implications for studies of carbonate diagenesis. In: Luminescence microscopy and spectroscopy; qualitative and quantitative applications. Barker, C.E. and Kopp, O.C. (eds.), *SEPM Short Course Notes* **25**: 37-57.

Martens, C.S., Chanton, J.P. and Paull, C.K., 1991. Biogenic methane from abyssal brine seeps at the base of the Florida Escarpment. *Geology* **19(8)**: 851-854.

McCrea, J.M., 1950. The isotopic chemistry of carbonates and a paleotemperature scale. *Journal of Chemical Physics* **18**: 849-857.

Mora, C.I., Driese, S.G., and Seager, P.G., 1991. Carbon dioxide in the Paleozoic atmosphere; evidence from carbon-isotope compositions of pedogenic carbonate. *Geology* **19(10)**: 1017-1020.

Mora, C.I., Fastovsky, D.E., and Driese, S.G., 1993. Geochemistry and stable isotopes of paleosols. Geological Society of America, Short Course, [University of Tennessee Department of Geological Sciences Studies in Geology, 23] 66 pp.

Mora, C.I., Driese, S.G. and Colarusso, L.A., 1996. Middle to late Paleozoic atmospheric CO_2 levels from soil carbonate and organic matter. *Science* **271(5252)**: 1105-1107.

Mora, C.I., Sheldon, B.T., Elliott, W.C., and Driese, S.G., 1998. An oxygen isotope study of illite and calcite in three Appalachian Paleozoic vertic paleosols. *Journal of Sedimentary Research* **68(3)**: 456-464.

Nelson, W.A. and Read, J.F., 1990. Updip to downdip cementation and dolomitization patterns in a Mississippian aquifer, Appalachians. *Journal of Sedimentary Petrology* **60(3)**: 379-396.

Nickelsen, R.P., 1988. Structural evolution of folded thrusts and duplexes on a first-order anticlinorium in the Valley and Ridge Province of Pennsylvania. *Geological Society of America Special Paper* **222**: 89-106.

Niklas, K.J., Tiffney, B.H., and Knoll, A.H., 1985. Patterns in vascular land plant diversification: and analysis at the species level. In: Phanerozoic Diversity Patterns: Profiles in Macroevolution. Chapter 3.

Oliver, J., 1986. Fluids expelled tectonically from orogenic belts; their role in hydrocarbon migration and other geologic phenomena. *Geology* **14(2)**: 99-102.

Orkan, N.I and Voight, B., 1983. Fracture geometry and vein mineral paleothermometry - Barometry from fluid inclusions, Valley and Ridge province, Pennsylvania. *Geological Society of America, Abstracts with programs* **15(6)**: 656.

Patchen, D.G., Avery, K.L. and Erwin, R.B., 1985. Correlation of stratigraphic units of North America (COSUNA) project, northern Appalachian regiona. Tulsa, OK. AAPG; 1 chart.

Popp, B.N., Anderson, T.F. and Sandberg, P.A., 1986. Brachiopods as indicators of original isotopic compositions in some Paleozoic limestones. *Geological Society of America Bulletin* **97(10)**: 1262-1269.

Prave, A.R., Alcala, M.L. and Epstein, J.B., 1989. Stratigraphy and sedimentology of Middle and Upper Silurian rocks and an enigmatic diamictite, southeastern New York. *Annual Meeting of the New York State Geological Association* **61**: 121-140.

Quade, J., Cerling, T.E., and Bowman, J.R., 1989. Aystematic variations in the stable carbon and oxygen isotopic compositions of pedogenic carbonate along elevation transects in the southern Great Basin, USA. *Geological Society of America Bulletin*, **101**: 464-475.

Quade, J., Cater, J.M.L., Ojha, T.P., Adam, J. and Harrison, T.M., 1995. Late Miocene environmental change in Nepal and the northern Indian subcontinent; stable isotopic evidence from Paleosols. *Geological Society of America Bulletin* **107(12)**: 1381-1397.

Qing, H. and Mountjoy, E.W., 1992. Large-scale fluid flow in the Middle Devonian Presqu'ile barrier, Western Canada sedimentary basin. *Geology* **20**: 903-906.

Retallack, G.J., 1985. Fossil soils as grounds for interpreting the advent of large plants and animals on land. *Biological Sciences* **309**: 105-142.

Retallack, G.J., 1988. Field recognition of Paleosols. In: Reinhardt, J. and Sigleo, W.R. (eds.), Paleosols and weathering through geologic time; principles and applications. *Geological Society of America Special Paper* **216**: 1-20.

Retallack, G.J., 1990. Soils of the Past: Unwin Hyman, Boston, 520 p.
Rose, A.W., Smith, A.T., Gammons, C., 1985. Regional distribution of facies in the Catskill Formation and the controls on red-bed copper-uranium occurrences. In: Central Pennsylvania geology revisited. Guidebook for the Annual Field Conference of Pennsylvania Geologists **50**: 37-43.

Rickard, L.V., 1969. Stratigraphy of the Salina group and origin of its salt beds. Part 1; Pages 49-50.

Robinson, J.M., 1991. Phanerozoic atmospheric reconstructions: a terrestrial perspective. *Palaeogeography, Palaeoclimatology, Palaeoecology* **97**: 51-62.

Salomons, W. and Mook, W.G., 1976. Isotope geochemistry of carbonate dissolution and reprecipitation in soils. *Soil Science* **122(1)**: 15-24.

Savin, S.M. and Hsieh, J.C.C., 1998. The hydrogen and oxygen isotope geochemistry of pedogenic clay minerals: principles and theoretical background. *Geoderma* **82**: 227-253.

Schedl, A., McCabe, C., Montanez, I.P., Fullagar, P.D. and Valley, J.W., 1992. Alleghenian regional diagenesis; a response to the migration of modified metamorphic fluids derived from beneath the Blue Ridge-Piedmont thrust sheet. *Journal of Geology* **100(3)**: 339-352.

Scotese, C.R., 1984. An introduction to this volume: Paleozoic paleomagnetism and the assemblly of Pangea. In: Vand der Voo, R., Scotese, C.R., and Bonhommet, N. (eds.), Plate Reconstruction from Paleozoic Paleomagnetism: *American Geophysical Union, Geodynamics Series* **12**: 1-10.

Scotese, C.R., Bambach, R.K., Barton, C., Van Der Voo, R., and Ziegler, A.M., 1979. Paleozoic base maps. *Journal of Geology* **87**: 217-277.

Sevon, W.D., 1985. Non-marine facies of the Middle and Late Devonian Catskill coastal alluvial plain, in Woodrow, D.L., and Sevon, W.D. (eds.), The Catskill delta: Geological Society of America Special Paper **201**: 79-90.

Smith, N.D., 1968. Cyclic sedimentation in a Silurian intertidal sequence in eastern Pennsylvania. *Journal of Sedimentary Petrology* **38(4)**: 1301-1304.

Soil Survey Staff, 1994. Keys to Soil Taxonomy (6th ed.). U.S. Dept. Agri., Soil Man. Supp. Serv., Blacksburg, VA, 524 pp.

Solomon, S.T., and Walkden, G.M., 1985. The application of cathodoluminescence to interpreting the diagenesis of an ancient calcrete profile. *Sedimentology* **32**: 877-896.

Strother, P.K., 1988. New species of Nematothallus from the Silurian Bloomsburg Formation of Pennsylvania. *Journal of Paleontology* **62(6)**: 967-982.

Thomasson, J.R., Nelson, M.E., and Zakrezewski, R.J., 1988. A fossil grass (Grimineae: Chloridoideae) from the Miocene with Krautz anatomy. *Science* **233**: 876-878.

Van der Voo, R., 1988. Paleozoic paleogeography of North America, Gondwana and intervening displaced terranes: Comparisons of paleo-magnetism with paleoclimatology and biogeographical patterns. *Geological Society of America Bulletin* **100**: 311-324.

Veizer, J., Fritz, P., and Jones, B., 1986. Geochemistry of brachiopods, oxygen and carbon isotopic records of Paleozoic oceans. *Geochimica et Cosmochimica Acta* **50(8)**: 1679-1696.

Walker, R.G. and Cant, D.J., 1984. Sandy fluvial systems. In: Walker, R.G. (ed.), Facies Models, Second Edition. Geoscience Canada Reprint Series Number 1, p. 71-89.

Williams, E.G., 1985. Catskill sedimentation in central Pennsylvania In: Gold, D.P. and others, Central Pennsylvania geology revisited: 50the Field Conference of Pennsylvania Geologists, Guidebook, p. 20-32.

Wright, V.P., (ed.), 1986. Paleosols: their recognition and interpretation: Prinseton, NJ, Princeton University Press, 315 p.

Yapp, C.J. and Poths, Harald, 1994. Productivity of pre-vascular continental biota inferred from the $Fe(CO_3)OH$ contents of goethite. *Nature* **368(6466)**: 49-51.

Ziegler, A.M., Scotese, C.R., McKerrow, W.S., Johnson, M.E., and Bambach, R.K., 1979. Paleozoic paleogeography. *Annual review of Earth and Planetary Science* 7:473-502.

APPENDICES

APPENDIX A:

LOCATION OF PALEOSOL OUTCROPS

WURTSBORO

The Wurtsboro, NY paleosols (95-BL-5-) are located at its type section along N.Y. Route 17, about 1 mile southeast of Wurtsboro. The outcrop can be found in the westcentral portion of the Wurtsboro, NY 7.5' quadrangle (Latitude = 41°33'55"; Longitude = 74°28'15").

PORT JERVIS

The Port Jervis, NY paleosol (95-BL-4-) is located on the southern side of Route 84, 2 miles east of the Delaware River. The best access is by parking at the rest area pull-off and walking downslope. The outcrop can be found in the northeastern portion of the Port Jervis South, NY 7.5' quadrangle (Latitude = 41°21'45"; Longitude = 74°39'30").

HARRISBURG

The Harrisburg, PA paleosol (95-BL-1-) is located on the eastern side of Route 322, 0.9 miles north of intersection with highway 39. The outcrop can be found in the eastcentral portion of the Harrisburg West, PA 7.5' quadrangle (Latitude = 40°20'17"; Longitude = 76°54'15").

PORT CLINTON

The Port Clinton, PA paleosols (95-BL-2-) are located on the eastern side of Route 61, across from the motels and stores in Port Clinton, PA. The outcrop can be found in the eastcentral portion of the Auburn, PA 7.5' quadrangle (Latitude = 40°35'20"; Longitude = 76°01'35"). When approaching this outcrop, even though there is plenty of parking on the western side of the highway, it is suggested that you park on the eastern side of the highway (with permission from the homeowners) to avoid crossing the heavy traffic.

LEHIGH GAP

The Lehigh Gap, PA paleosol (96-BL-LG-) is located on the eastern side of Route 248, 1 miles south of Palmerton, PA. Access is by exiting Route 248 at Palmerton, PA, then turn right onto Mauch Chunk Road. The outcrop can be found in the eastcentral portion of the Palmerton, PA 7.5' quadrangle (Latitude = 40°49'48"; Longitude = 75°31'14").

DANVILLE, PA

The Danville, PA paleosol (96-BL-DAN-) is located on the northern side of Route 11, 3 miles east of Danville, PA. The outcrop can be found in the northeastern portion of the Riverside, PA 7.5' quadrangle (Latitude = 40°58'00"; Longitude = 76°39'00").

APPENDIX A (continued)

POWYS, PA

The Powys, PA paleosols (96-SC-POW-) are exposed at the first and third road cut on the western side of Route 15, south of Powys, PA. Parking is scarce on this busy highway. It is recommended, for the first outcrop, to park at the northern end and walk down section. This road cut is also very steep. Hard hats are a requirement. The outcrop can be found in the northwest and westcentral portion of the Cogan Station, PA 7.5' quadrangle (Latitude = 41°20'45"; Longitude = 77°06'00").

TROUT RUN, PA

The Trout Run paleosol (96-CAT-TR5-) is exposed at the fifth road cut on the eastern side of Route 15, north of the Route 14/15 split. The outcrop can be found in the southcentral portion of the Trout Run, PA 7.5' quadrangle (Latitude = 41°23'45"; Longitude = 77°03'45").

NEWPORT, PA

The Newport, PA paleosol (C1-) is exposed on the eastern side of Route 322, 2 miles north of Newport, PA. The outcrop can be found in the southeastern portion of the Millerstown, PA 7.5' quadrangle (Latitude = 40°30'10"; Longitude = 77°07'40").

LIVERPOOL, PA

The Liverpool, PA paleosol (96-CAT-LIV-) is exposed on the western side of Route 15, 1 mile south of Liverpool, PA. The outcrop can be found in the southeastern portion of the Duncannon, PA 7.5' quadrangle (Latitude = 40°23'00"; Longitude = 77°00'40").

APPENDIX B:

CARBONATE ISOTOPE ANALYSES

KEY FOR CARBONATE MINERALOGY AND MORPHOLOGY:

First Letter;

D = dolomite
C = calcite

Second Letter;

R = rhizolith
N = nodule
M = matrix
C = cement
V = vein
B = bead

* All isotope values recorded using the Carbo-flo method have been temperature corrected to 25°C.

APPENDIX B: CARBONATE ISOTOPE ANALYSIS

Paleosol Locality Wurtsboro Sample Number	Carbonate Sample Number	$\delta^{13}C$	$\delta^{18}O$	Carbonate Mineralogy & Morphology
95-BL-5-6A	56-A	-11.14	-9.93	D;M;dense micrite
95-BL-5-1B	62-A	-11.15	-9.97	D;M;dense micrite
95-BL-5-1A	63-A	-10.87	-9.82	D;M;dense micrite
95-BL-5-1A	63-LL	-10.95	-11.42	D;M;dense micrite with some spar
Port Jervis				
95-BL-4-4A	68-II	-13.46	-9.63	D;M;dense micrite
95-BL-4-4A	68-B	-13.44	-10.42	D;M;dense micrite
95-BL-4-4B	71-A	-14.02	-10.44	D;M;dense micrite
95-BL-4-4B	72-A	-13.16	-9.02	D;M;dense micrite
Harrisburg				
95-BL-1-1	H1-A	-12.95	-11.32	D;M;micrite proximal to vein
95-BL-1-1	H1-B	-13.28	-13.15	D;V;spar
95-BL-1-1	H1-C	-12.37	-8.22	D;N;dense micrite
95-BL-1-1	H1-D	-12.28	-8.14	D;N;spar
95-BL-1-1	H13-A	-12.32	-8.28	D;N;micrite and some microspar
95-BL-1-1	H19-A	-12.37	-8.47	D;N;dense micrite
95-BL-1-1	H19-B	-12.50	-8.99	D;N;micrite
95-BL-1-1	H19-C	-12.33	-8.37	D;N;spar
95-BL-1-1	H22-A	-12.45	-8.38	D;N;micrite
95-BL-1-1	H22-B	-13.18	-9.77	D;N;micrite
95-BL-1-1	H22-C	-11.86	-7.60	D;N;spar
95-BL-1-1	H22-D	-12.90	-14.94	D;V;spar
Lehigh Gap				
96-BL-LG-4-A	89-C	-8.34	-15.28	C;N;microspar
96-BL-LG-4-A	89-D	-8.55	-15.76	C;N;microspar
96-BL-LG-4-A	89-E	-8.43	-15.82	C;N;microspar
Port Clinton				
95-BL-2-1	3 A	-9.70	-15.81	C;N;micrite
95-BL-2-1	3 B	-9.97	-15.75	C;N;micrite
95-BL-2-1	3 C	-9.87	-15.53	C;N;micrite
95-BL-2-1A-a	3 D	-10.03	-15.68	C;N;micrite and some spar
95-BL-2-1A-a	3 F	-9.92	-15.82	C;N;micrite and some spar
95-BL-2-1A-a	3 E	-9.84	-15.65	C;N;spar
95-BL-2-1A-bed	3 G	-10.24	-15.82	C;N;micrite and some spar
95-BL-2-4-bed-a	3 I	-11.35	-15.83	C;N;micrite, spar, and matrix
95-BL-2-4-bed-a	3 J	-10.67	-14.47	C;N;spar

APPENDIX B (continued)

Paleosol Locality Port Clinton Sample Number	Carbonate Sample Number	$\delta^{13}C$	$\delta^{18}O$	Carbonate Mineralogy & Morphology
95-BL-2-4-bed-a	3 L	-10.66	-15.98	C;N;micrite, microspar and spar
95-BL-2-4-bed-b	3 K	-10.31	-15.87	C;N;micrite, microspar and spar
95-BL-2-4-bed-b	3 M	-10.06	-16.20	C;N;microspar, micrite and vein spar
95-BL-2-1A-bed	3 H	-10.25	-16.02	C;N;micrite and some spar
95-BL-2-4	85-H	-10.57	-16.27	C;N;dense micrite and some spar
95-BL-2-4	83-I	-10.63	-16.28	C;N;dense micrite and some spar
95-BL-2-5	79-G	-10.10	-16.05	C;N;dense micrtie and spar
95-BL-2-5	80-BB	-10.12	-15.78	C;R;dense micrite and some spar
Danville (1992)				
BL-1A-91-D	208-13	-1.52	-12.35	C;N;micrite
BL-2A-91-D	207-10	-2.12	-13.61	C;N;micrite
BL-2A-91-D-rr	211-C	-1.84	-12.58	C;N;micrite
BL-2B-91-D	207-1	-1.72	-12.82	C;N;micrite
BL-2B-91-D-rr	212-D	-1.54	-12.32	C;N;micrite
BL-7.5-90-D	178-11	-2.09	-12.49	C;N;micrite
BL-7.5-90-D	180-A	-2.11	-12.37	C;N;micrite
BL-20.5-90-D	191-10	-2.00	-12.45	C;N;micrite
BL-20.5-90-D	179-3	-2.01	-12.31	C;N;micrite
BL-7.6-90-D	178-16	-2.12	-12.39	C;N;micrite
BL-7.6-90-D	177-9	-2.03	-11.65	C;N;micrite
BL-18-91-D	211-11	-1.52	-12.32	C;N;clayey micrite
BL-25.5-90-D	178-15	-2.12	-12.61	C;N;micrite
BL-57-90-A	182-10	-1.57	-11.79	C;N;clayey micrite
BL-58-90-A	181-12	-1.52	-11.72	C;N;clayey micrite
BL-58-90-B	182-C	-2.02	-12.06	C;N;clayey micrite
BL-1-90-NOD	PS	-1.87	-12.24	C;N;
BL-1-90-NOD	PS	-1.88	-12.39	C;N;
BL-90-91-D	211-10	-6.17	-11.97	C;N;
BL-90-91-D	211-15	-6.67	-12.73	C;N;clayey micrite
BL-91-91-D	210-M3	-4.47	-12.12	C;N;clayey micrite
BL-91-91-D	211-9	-4.19	-12.58	C;N;clayey micrite
BL-91-91-D	210-M5	-3.28	-10.73	C;N;clayey micrite
BL-91-91-D	209-2	-4.52	-12.16	C;N;micrite
BL-91.5-91-D	207-14	-5.73	-10.09	C;N;spar filling
BL-91-91-D	210-MWD	-6.08	-11.14	C;N;spar cement
BL-91-91-D	211-MI	-6.81	-9.94	C;N;spar cement

APPENDIX B (continued)

Paleosol Locality Danville (1998) Sample Number	Carbonate Sample Number	$\delta^{13}C$	$\delta^{18}O$	Carbonate Mineralogy & Morphology
96-BL-DAN-B-1	-	-5.97	-13.98	C;N;micrite and some spar
96-BL-DAN-A-3	A	-5.88	-13.64	C;N;micrite
96-BL-DAN-A-3	B	-6.04	-13.07	C;N;micrite
96-BL-DAN-A-3	C	-6.28	-14.47	C;N;spar
Powys				
96-SC-POW-1	99-Q	-6.46	-13.25	C;R;microspar
95-SC-POW-4B	30-AF	-5.21	-10.50	C;R;mix of spar and microspar
96-SC-POW-4B	29-AG	-5.21	-11.84	C;B;micrite and spar
96-SC-POW-4B	29-A	-4.76	-9.91	C;N;spar
96-SC-POW-4B	29-B	-5.66	-11.36	C;N;spar and matrix
96-SC-POW-4B	29-C	-5.62	-11.58	C;N;microspar
96-SC-POW-4B	97-R	-5.07	-12.00	C;B;spar
96-SC-POW-5A	27-AH	-7.44	-12.72	C;B;dense micrite
96-SC-POW-5A	26-AI	-5.75	-11.21	C;N;spar and some microspar
96-SC-POW-5B	24-AJ	-6.30	-10.60	C;N;spar
96-SC-POW-5B	22-N	-7.05	-12.70	C;N;dense micrite
96-SC-POW-5B	22-N	-7.15	-12.78	C;N;dense micrite
96-SC-POW-8	19-AL	-5.30	-12.64	C;N;microspar
96-SC-POW-8	18-L	-5.69	-12.36	C;N;microspar
96-SC-POW-8	100-O	-6.09	-13.02	C;N;microspar
96-SC-POW-8	100-O	-6.40	-13.42	C;N;microspar
96-SC-POW-8	100-P	-5.68	-12.67	C;N;microspar
96-SC-POW-8	100-P	-5.73	-12.99	C;N;microspar
96-SC-POW-8	100-A	-6.38	-12.59	C;N;microspar
96-SC-POW-8	100-B	-7.17	-12.71	C;N;dense micrite
96-SC-POW-8	100-C	-5.85	-11.31	C;N;spar
96-SC-POW3-7	1-J	-6.15	-11.53	C;N;microspar
96-SC-POW3-7	1-K	-6.31	-11.69	C;N;microspar
96-SC-POW3-7	1-K	-6.24	-12.07	C;N;microspar
Trout Run, 1998				
96-CAT-TR5-A	50-SS	-7.34	-14.63	C;N;micrite and matrix
96-CAT-TR5-A	49-TT	-7.16	-13.31	C;N;micrite,microspar, and matrix
96-CAT-TR5-A	48-UU	-7.27	-13.09	C;N;micospar
96-CAT-TR5-B2	47-VV	-8.05	-12.65	C;B;dense micrite
96-CAT-TR5-B2	47-WW	-7.99	-12.44	C;B;dense micrite
96-CAT-TR5-B3	46-YY-1	-7.68	-14.22	C;B;dense micrite
96-CAT-TR5-B2	45-YY-2	-7.32	-12.21	C;B;dense micrite and some spar
96-CAT-TR5-B2	43-ZZ	-7.38	-11.17	C;B;very dense micrite
96-CAT-TR5-B3	43-AB	-6.79	-12.13	C;B;dense micrite and spar

APPENDIX B (continued)

Paleosol Locality Trout Run (1992) Sample Number	Carbonate Sample Number	$\delta^{13}C$ ‰	$\delta^{18}O$ ‰	Carbonate Mineralogy & Morphology
Channel Sandstone	C3-1-1	-9.74	-12.49	C;---;clast
Channel Sandstone	C3-1-2	-9.85	-12.10	C;---;clast
Channel Sandstone	C3-1-4	-10.03	-12.77	C;---;clast
Channel Sandstone	C3-1-3	-10.79	-13.09	C;C;
Paleosol	C5-1-E	-5.59	-9.92	C;N;
Paleosol	C-5-90	-10.07	-11.93	C;N;
Paleosol	C-5-90	-10.28	-12.09	C;N;
Paleosol	C-5-90	-10.21	-11.86	C;N;
Paleosol	C-5-90	-10.21	-11.93	C;N;
Paleosol	C5-LCS-D	-7.24	-11.11	C;R;
Paleosol	C5-LCS-1-C	-7.21	-10.87	C;---;spar
Paleosol	C5-1-A	-8.78	-11.38	C;---;spar
Paleosol	C5-1-B	-7.65	-10.83	C;---;spar
Paleosol	C5-LCS-1-A	-7.62	-11.76	C;---;spar
Paleosol	C5-1-F	-7.92	-12.68	C;M;
Paleosol	C5-1-F	-7.90	-12.23	C;M;
Paleosol	C5-1-F	-7.06	-11.12	C;M;
Newport (1993)				
Paleosol	C1-3.58-A1	-8.27	-12.29	C;N;
Paleosol	C1-3.65-B1	-8.96	-12.77	C;N;
Paleosol	C1-3.65-B2	-9.20	-12.37	C;N;
Paleosol	C1-3.77-C1	-9.57	-13.47	C;N;
Paleosol	C1-3.58-A2	-9.73	-13.58	C;R;
Paleosol	C1-3.82-D1	-9.76	-12.72	C;R;
Paleosol	C1-3.82-D2	-9.39	-11.41	C;R;
Paleosol	C1-3.91-E1	-9.32	-12.10	C;R;
Paleosol	C1-3.91-E2	-9.72	-11.83	C;R;
Paleosol	C1-3.97-F1	-10.40	-12.35	C;R;
Paleosol	C1-4.00-G1	-9.85	-12.10	C;R;
Paleosol	C1-4.08-H1	-10.11	-12.81	C;R;
Paleosol	C1-3.65-B3	-9.40	-11.36	C;N;spar
Liverpool				
96-CAT-LIV-A	41-AC	-7.74	-15.37	C;N;spar and matrix

VITA

David C. King was born in Rochester, New York to Donald and Carolyn King on October 25, 1973. He attended Webster High School where his initial fascination in the Earth Sciences was established with inspiration from his Uncle Hank and 9th grade Earth Science teacher, Mr. Moriarty. After graduation in 1991, he enrolled as an undergraduate at the State University of New York at Geneseo, where his interests included geophysics and mathematics. After meeting the cast of characters in the Geology Department at SUNY Geneseo (collectively known as the staff) and an introductory class later, he knew that Geology was the correct choice. With the encouragement and guidance from the professors at Geneseo and friends, he earned his Bachelor of Arts degree in Geology by the Spring of 1995 with a minor in mathematics. That fall, he ventured outside state lines to begin his tenure as a geology graduate student at the University of Tennessee, Knoxville. With specific interests lying in the field of isotope geochemistry, he joined the paleopedology research group at UTK and after overcoming an obstacle or two, here or there, he graduated with his Master of Science degree by the Fall of 1998.

David initially plans to take some time off from his 20th consecutive year in academia, to catch up on three years of movies and being away from his family, who have patiently awaited his return in Rochester.